ADDIS ABABA UNIVERSITY
ADDIS ABABA INSTITUTE OF TECHNOLOGY
SCHOOL OF GRADUATE STUDIES
SCHOOL OF MECHANICAL AND INDUSTRIAL ENGINEERING

SYNTHESIS OF CRYSTALLINE NANOCELLULOSE ITS EFFECT ON THE MECHANICAL PROPERTIES OF E-GLASS FIBER-EPOXY COMPOSITE FOR PROSTHETIC SHANK APPLICATIONS

A Thesis submitted to the Graduate School of Addis Ababa University in partial fulfillment of the requirement for the Degree of Masters of Science In

Mechanical Engineering (Manufacturing Engineering)

By: Betselot Tesfaye

Advisor: Dr Desalegn Wogaso

Co-Advisor: Dr Eyobel Mulugeta

Addis Ababa, Ethiopia

March, 2023

ACKNOWLEDGEMENT

It has been a though experience to deal with this research work having a bit wide scope and was a great pleasure to come up with a happy ending. Thus, I would like to put God first for all positive things that has happened.

I would like to acknowledge and give my warmest thanks to my advisor Dr. Desalegn Wogaso who made this work possible. His guidance and advice carried me through all the stages of my thesis work. I would also like to thank my co-advisor Dr. Eyobel Mulugeta for being there when I am in need of support and guidance throughout the thesis work.

I also give special credit to Ms. Bethelhem Haile for her guidance and backing me whenever I was in need. Furthermore, my appreciation goes to Dr. Daniel, Dr. Alemayehu Dubale, Dr. Tekalign Tikish and Dr Kebede Gamo for their support and advise.

Finally, I would like to acknowledge Bio and Emerging Technology Institute for being supportive in the laboratory experimental work.

ABSTRACT

Prosthetic shank is one of the prominent parts of prosthetic leg that transfers load from prosthetic socket to the foot section. Nowadays, it is common to use composite materials for prosthetics and orthotics applications. This research focuses on the synthesis and characterization of properties of crystalline nanocellulose (CNC) powder and investigating its effect on the mechanical and physical properties of E-glass fiber - epoxy composite for prosthetic shank applications. Different properties including tensile, impact, flexural, water absorption, thermographic, density and surface morphology of a hybrid composite are investigated. The research further targets to test the suitability of developed composite material for prosthetic shank applications. Extraction of CNC powder is performed using chemical extraction technique which involves alkali treatment, delignification, bleaching and acid hydrolysis. Crystallinity of CNC particles are determined at 2θ values of 19.89^0, 44.04^0, 64.34^0 and 77.51^0. Crystallite size of these powders is found to be approximately 13 nm by x'pert high score software from the XRD analysis. FT-IR was conducted to determine fiber-fiber and fiber-epoxy chemical bonding interaction. Thermal properties of CNCs are examined using thermographic analysis (TGA) approch and the result reveals a three-stage decomposition of CNC powders in temperature ranges of 62-240 ^oC, 240-360 ^oC, and 360-625 ^oC, respectively. Hand layup method with light load compression is employed to fabricate hybrid composite specimens with different % CNC powder. Mechanical and physical tests are carried out to determine the composite's performance according to ASTM standards. The results reveal addition of CNC powder enhances the overall performance of the composite, and composite specimen with 8wt% CNC powder shows superior mechanical and physical properties. The numerical values obtained was tensile strength of 127.8Mpa, compression strength of 91.1Mpa, flexural strength of 251Mpa, and impact energy of 6.83J. Further, selected composite is modeled for the prosthetic shank application using finite element software, ANSYS 2022, and maximum equivalent von Mise's stress of 0.82598 MPa and deformation of 0.054065 mm are obtained. Based on the overall findings and analysis, it is highly recommended to develop and use hybrid E-glass fiber – CNC - epoxy composite as a substitute material for prosthetic shank applications.

Keywords: Crystalline nanocellulose, prosthetic shank, hybrid composite E-glass fiber, epoxy resin

Table of Contents

List of Figures

List of Tables

List of Abbreviation

CNC	Crystalline nanocellulose
MPa	Mega pascal
NC	Nanocellulose
NaOH	Sodium Hydroxide
H_2SO_4	Sulphuric Acid
SEM	Scanning electron microscopy
XRD	x-ray diffractometry
UTS	Ultimate tensile strength
UTM	Universal testing machine
APTMS	Aminopropyltrimethoxysilane
STF	Shear thickening fluid
ASTM	American standard testing method
Wt%	Weight Percentage
Composite 1	GF, Epoxy resin and with no CNC
Composite 2	GF with 2% CNC and epoxy resin
Composite 3	GF with 4% CNC and epoxy resin
Composite 4	GF with 6% CNC and epoxy resin
Composite 5	GF with 8% CNC and epoxy resin

ISO	International Organization for Standardization
FEA	Finite Element Analysis

CHAPTER ONE

1. INTRODUCTION

1.1 Background of the study

Materials have been a milestone for the development of various modes of technological aspects, this has been observed through time specially in Engineering materials. Composite materials which are currently used in a wide range applications like energy sectors, automobile, marine aerospace structures and various building blocks are of those Engineering materials currently in use [1]. The sectors stated above demand a material which is agile that result in less energy consumption of the whole system being in action. To meet the technological requirement new materials, need to be developed with lighter and stronger properties than the conventional one.

Having in mind about developing a new material with a better strength and light weight it is important to incorporate this concept with composite materials since these materials are being used in a wide range of applications.

Beside the strength and weight of materials being used in day-to-day activities there are also environmental issues that are most likely affecting nature. As technology is evolving through time some environmental issues have to be taken into consideration at the same time for the desire of ease of lifestyle of a community and most importantly safety. Of those technological contribution information technology, biotechnology and nanotechnology are the most important ones. However, future developments on these areas of studies should have to be designed considering our living environment and harmonize with it, which can secure a sustainable technological enhancement through time [2].

Because of their properties like flexibility, ease of fabrication, light weight and lower cost composite materials are widely used in orthotics and prosthetic applications [3]. A prosthesis can be understood as a convenient replacement for a lost body part, most regularly that of arm and leg, and have major components like, Socket, Extension (Shank) and Hand/ Foot [4].

Synthetic composites with a constituent carbon and glass fibers and thermoplastics are being widely employed in prosthetic fabrication industry. Owing the likes of better mechanical performances these synthetic composites possess some drawbacks at the same time. High cost and

weight are the major drawbacks beside being environmentally unfriendly emitting bunch of toxic substances in the process of fabrication and while damping after their service time ends [5].

The drawbacks of synthetic fibers have initiated lots of researches on improvement and replacement of those synthetic fibers with alternative natural fibers and their derivatives. In particular the prosthetic industry became attracted to natural fibers due to their ease of fabrication, low cost and better strength to weight ratio [6].

Glass fibers have been the ideal reinforcement for prosthetic applications, but still have some limitations as compared to other synthetic fibers like carbon and kevlar, thus hybridizing with natural fiber would result in a better performance of the composite material. Therefore, individual drawbacks of reinforcements will be reduced as the desire of hybridizing is to do so [7].

Consequently, this thesis research studied the effect of CNC hybridized with glass fiber with different weight percentage. Thus, based on the mechanical properties the best wt% addition of CNC was selected.

1.2 Problem statement

Most prosthetic shank is made from thermoplastics and synthetic fibers like glass and carbon fibers. The synthetic fiber reinforcement materials recently used in prosthetic industry exhibit limited mechanical property due to ineffective wettability with the matrix material. Glass fibers in particular exhibits lower mechanical properties than other synthetic fibers like carbon fibers, however they are affordable. Apart from poor wettability, porous regions in between the fiber and matrix due to fabrication technique and nature of the fiber is also the major cause for poor mechanical performance of the composite material. Thus, to enhance the mechanical and physical properties of glass fiber reinforced epoxy composite, a filler material CNC which is a derivative of natural fiber can be used. Furthermore, the light weighted CNC can be also a major in-put to be utilized as a hybridizing reinforcement alongside with the glass fiber [8].

In addition, the increasing interest of renewable materials has been the reason for various research works since synthetic fibers are affecting the environment while getting damped. Thus, preparing those renewable materials from waste resources can be an additional input in some particular

research work. Thus, from cellulosic biomass the byproduct of sugarcane factory which is bagasse can be used to extract CNC [3].

Thus, this research came up with the alternative material for prosthetic shank that is hybridizing CNC with glass fiber.

1.3 Objectives of the research

1.3.1 General Objective

To develop and characterize the properties of hybrid nanocellulose and E-glass fiber reinforced epoxy composite with various compositions then analyze effect of loads on simulated prosthetic pylon.

1.3.2 Specific Objectives

- ✓ To extract nanocellulose by alkali treatment, delignification, bleaching and followed by acid hydrolysis and characterize grain size (whether it is amorphous or crystalline using XRD) and morphology (using SEM) of nanocellulose.
- ✓ To fabricate E-glass fiber reinforced epoxy composite and its hybrid form with 2%, 4%, 6% and 8% wt% of crystalline nanocellulose by hand lay-up fabrication technique. (Note: E-glass fiber was 30% and that of epoxy resin 70% of the total composite wt% crystalline nanocellulose was added in the epoxy resin)
- ✓ To test and analyze mechanical properties like tensile, flexural, compression and Impact strength, and physical properties like density, void content, water absorption, Fourier-transform infrared spectroscopy (FT-IR) and thermographic analysis (TGA) of the fabricated hybrid E-glass/CNC epoxy composite with varying CNC concentration.
- ✓ To compare the nanocellulose enhanced composite with E-glass reinforced epoxy composite.
- ✓ To simulate and analyze the suggested material for prosthetic shank model using ANSYS 2022 software.

1.4 Scope of the study

The research covered the extraction and characterization of nanocellulose from sugarcane bagasse. Then fabricating the composite with hand layup process and testing for mechanical and physical properties of hybrid E glass/CNC epoxy composite material with 2%, 4%, 6%, and 8wt % of CNC and one control sample without CNC. The mechanical tests were performed according to ASTM. Dispersion of CNC into epoxy resin was studied with SEM that shows the morphology of the composite material.

1.5 Significance of the study

This thesis research will ease the effort to extract CNC for future works. Since bagasse is a headache for sugar industries as it occupies large area thus, utilizing bagasse for CNC extraction can reduce this.

1.6. Research questions

- ✓ How effective extraction of CNC from sugarcane bagasse can be made (Crystallinity of cellulose)?
- ✓ What was the effect of natural fibers hybridized with a synthetic fiber?
- ✓ To what extent could CNC improve the physical and mechanical properties of the composite and which composition of CNC showed a better performance of the composite material?

1.7 Limitations of the study

Finding chemicals, better fabricating technique like VARTM, testing devices like SEM and TGA here in Ethiopia was the major limitation that got stuck the research work.

1.8 Motivation of the study

War, disease and car accident are frequently causing amputation specially in developing countries, and most of the victims cannot afford to buy prosthetic limbs with highest quality that can last for long. Thus, hybridizing the existing conventional prosthetic limb with a cheap but less expensive reinforcement can ease life for the amputees. Recently sugar factories are struggling with by product management, thus converting this by product (bagasse) into a useful item can bring an imminent solution for the sector.

1.9 Organization of the thesis

The study has five sections each having different objective, The first section briefs the overall background of the topic and the purpose in performing the study. In the second section scientific approach were followed to introduce CNC and its hybrid composites with synthetic fibers thus, related literatures were reviewed. The third section covers about the materials utilized, experimentation techniques, testing machine setups and specimen preparation techniques. Fourth section describes and discussed the experimental results obtained and from the results a model of prosthetic shank was simulated with ANSYS. The final section of the study provides the conclusion of what has been done and recommendations were added based on the results obtained.

CHAPTER TWO

2. LITERATURE REVIEW

2.1 Composite Materials

A composite material is the combination of two or more materials having different property from the either side of the constituting parts. The formation process is performed without mixing or blending of the two materials, that is within the composite the materials can be detected apart. The two constituting parts of a composite are reinforcement which is the main load bearing part and matrix material which holds the reinforcing materials together and transferring loads in between them. In concrete, the cement and aggregate play a role of the matrix and reinforcement respectively [9].

Composite materials have become to be widely used in different application areas replacing many conventional materials due to their advantage in flexibility, non-corrosiveness, high strength to weight ratio, better stiffness, low cost, better dumping effect and low electric conductivity. Despite being chosen owing those advantages composites also have some limitations compared with other materials: composites are less ductile, demand long time to be formed or made, not ideal in moist environment and can be affected by high temperature [10].

Reinforcement: reinforcement materials are the major constituent of a composite material to which anchoring the whole structure and determines the strength and stiffness of the composite material [11]. Composite materials can be classified based on the type of reinforcement being used:

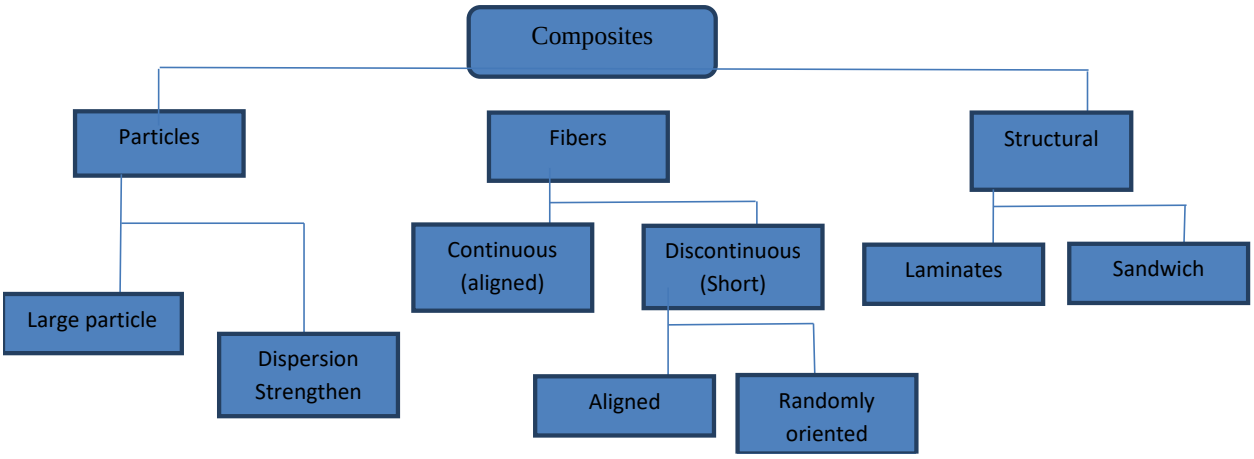

Figure 2.1Classification of composites based on reinforcement materials [10]

Particulate reinforced composite: A dispersed particle form of reinforcement in the matrix material. How the particles are arranged, their shape, and type is the key to determine the physical and mechanical properties of the composite material. Portland cement is example if particle reinforced composite material [12].

Whiskers reinforced composites: A short form of fibers which are oriented randomly throughout the matrix material. They have a crystalline structure with high length to diameter ratio. They can be made from materials like aluminum oxide, graphite and silicon nitride [11].

Structural composites: this type of composite is classified based on the arrangement of the reinforcement layers having two types that are laminar and sandwich.

Laminar composites: two dimensional panels arranged in a preferred direction which gives high strength to the composite material. Plywood is atypical example in which the layers are arranged in such orientation that each successive layer owe varying strength [13].

Sandwich composites: two thin but stiff skins attached to a thick and light weighted core forming a special kind of composite material [14].

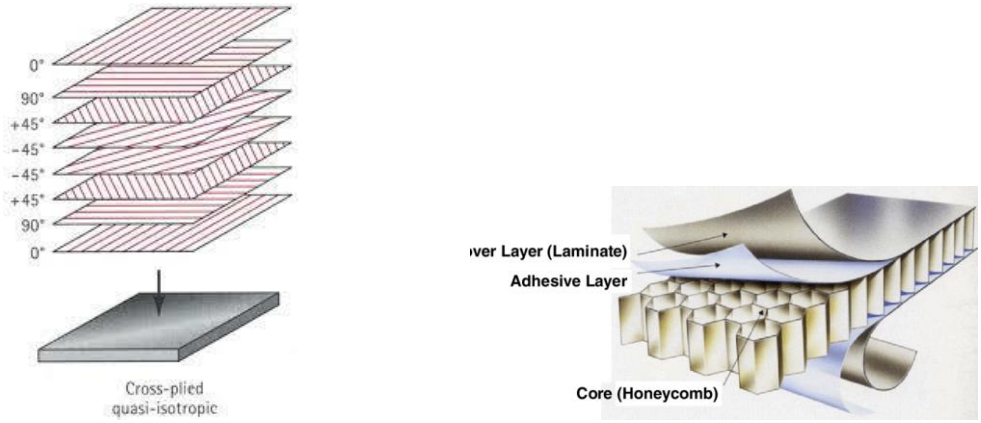

a) Laminar composites b) sandwich composites

Figure 2.2 Structural composites
[15], [16]

Fiber reinforced composites: fiber reinforcements might be found in various forms like discontinuous, woven, unidirectional, and bi-directional. Materials used for fibers include aramid, carbon, glass, and other than this wood or asbestos have been also be used. In comparison of the other types of reinforcements fiber reinforced composite composites are being used in a wide range of application areas and this is because of orientation, distribution and arrangement of single fiber strands in the matrix material can be made depending up on the desired application area [17].

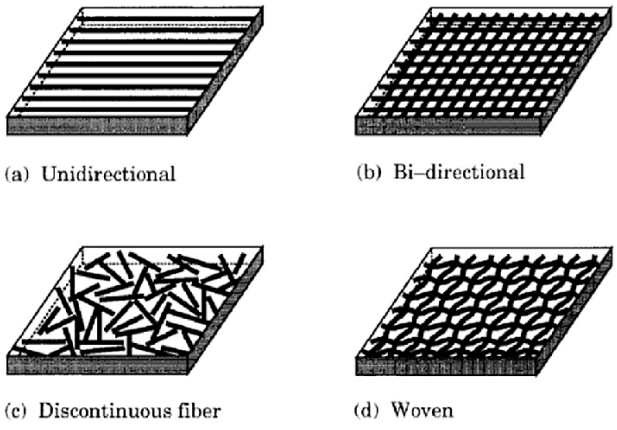

Figure 2.3 Fiber-reinforced composite lamina and arrangement of its fibers

(a) a lamina with unidirectional fiber arrangement (b) meshing bi-directional fibers (c) discontinuous fibers with random arrangement (d) A woven fibers interlocking each other [18]

Matrix: A monolithic material which keeps the reinforcing material to stick together and gives the composite material a definite shape and plays a vital role altering the characteristics of the material to meet the intended requirements [19]. A composite material can be classified based on the matrix material being used.

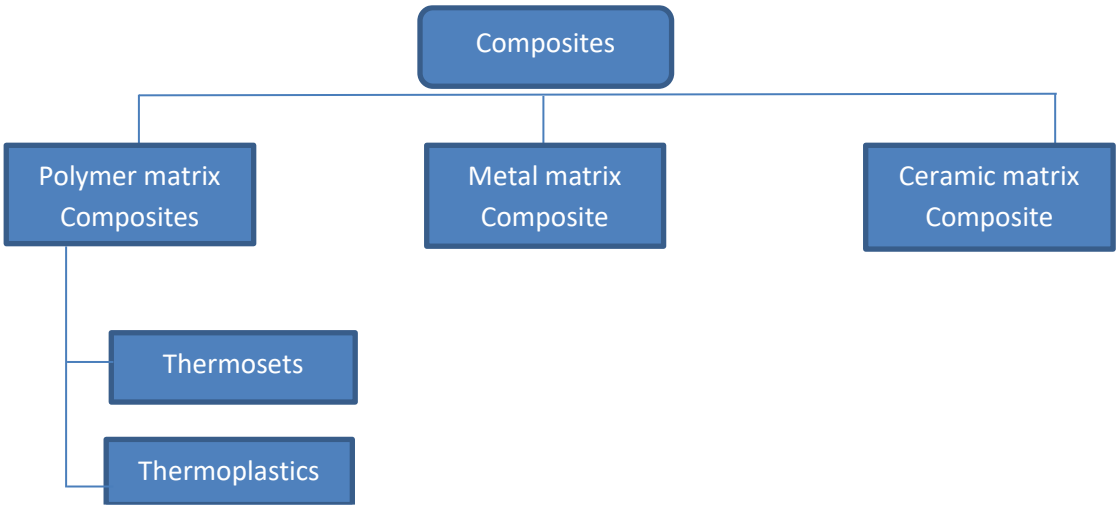

Figure 2.4 Classification of composites based on matrix materials [19]

2.2 Fibers

2.2.1 Natural fibers

Cotton, flax, hemp, bamboo, sisal, jute and sugarcane bagasse are of the most common natural fibers which are obtained from plants having a major component of cellulose. Beside the benefits for the consumer, natural fibers can be renewed and are nonhazardous to the environment while their derivatives being processed synthetically act in an opposite way to the environment. Synthetic/artificial fibers are most widely oil based products which is a nonrenewable extract, and the exploration and drilling process of the oil have its own impact to the environment [20].

Cellulose can be extracted from the likes of plants stated above and even from animals and microorganisms like bacteria. This well-known natural polymer can exhibit in an advanced way when utilized in its nano scale which is nanocellulose [21].

Plant stems which are natural fibers consists of various layers that made it stand firmly, of these layers' lignin separates fibrils thus its crucial to remove this layer with a process known delignification. Other than lignin hemicellulose and cellulose can be obtained stepwise in a plant stem. The removal may be mechanical or chemical, thus kraft pulping is the most common method known to remove lignin keeping the plant in a digester with sodium hydroxide and sodium sulfide [22]. But this method of extraction will only give us the micro crystalline cellulose (MCC) removing only the two layers of hemicellulose and lignin. But this extraction can indicate further surface removal of the pulp can result in a final product with a better particle size [23]. Thus, acid hydrolysis can be proposed as an effective process to obtain cellulose in a size below the microscale [24].

Cellulose can be obtained and processed from various plants, wood, bacteria and algae in addition further extraction can be undergone with various methodologies. Sugarcane bagasse with 40-50% cellulose content can yield much amount of cellulose and it is common to have crystal and amorphous part of cellulose located sequentially in longitudinal direction of the fiber, meanwhile crystalline structure of the cellulose cannot be easily broken due to an intensified hydrogen bond in between hydroxyl groups with in cellulose while that of amorphous parts can be easily broken [22]. As sugarcane bagasse is categorized in lignocellulosic biomass it mainly consists of three major polymers, cellulose hemicellulose and lignin.

2.2.1.1 Sugarcane bagasse

Innovative ideas are exploding in advanced materials development sector due to the growth in demand for novel fibers. Sugar is extracted from the stalk of sugarcane, after extraction the leftover sugarcane fiber pulp is known to be bagasse. Up until recently, bagasse was burned often as a waste product, which polluted the air. One of the reasons for increasing attention to bagasse is the disposal of agricultural residues and the need for boosting the sugarcane industry's profits [25].

Sugar factories and alcohol producing industries are sectors with a large scale of bagasse byproducts, and still the sector is facing a problem on how to manage this waste material despite

it is being utilized in the factory itself as a power source to run the sugar mill. Figure 2.5 shows sugarcane bagasse collected from Wonji sugar factory. Thus, the necessity to dispose of agricultural waste and increase the sugarcane industry's revenues are two factors contributing to the increased interest in bagasse. [26]. Worldwide annual production of bagasse is estimated to be more than 100 million tons. Various products and part of ingredients have been utilizing bagasse as a main source, products like paper, products derived by fermentation and most widely electricity generating plants utilizes bagasse as a major source [27]. even though it is being utilized in some production baselines it is still a headache for sugar and alcohol industries to dump the rest because of the enormous amount of bagasse per annum.

Figure 2.5 Waste sugarcane bagasse collected from Wonji sugar factory

As bagasse is biodegradable and cellulose rich pulp it is suitable to be utilized for composite production solving the waste management problem faced with the sectors having it as a byproduct. In particular extracting the cellulose from sugarcane bagasse to get microcrystalline and nano cellulose can be a crucial approach to efficiently utilize bagasse in engineering applications. It is known that of the total weight of sugarcane bagasse half of it is cellulose, a detailed ratio of bagasse constituents is listed in table 2.1.

Table 2.1: sugarcane bagasse constituents [28]

Sugarcane bagasse constituents	Weight percentage
Cellulose (in crystalline structure)	40-50%
Hemicellulose (amorphous structure)	25-35%
Lignin	18-24%

2.2.1.2 Sugarcane bagasse in Ethiopia

In Ethiopia, sugarcane is cultivated on about 33,777 ha of the country's land, located around the Wonji-Shoa, Metahara and Finchaa sugar factories. These factories currently produce an average of 893,270 tons of Ethiopian sugarcane bagasse (ESCB) annually [29].

2.2.1.3 Lignin

In plants, lignin is the main component to bind and hold intermediately and around hemicellulose and cellulose. These binding effects of lignin give it to enhance the plant cell wall to have compressive strength, better stiffness, to be resistant to decay and water impermeable. Phenylpropane monomers, p-coumaryl, coniferyl and sinapyl alcohols gives lignin the cross-linked amorphous copolymeric structure. The ratio of the stated monomers as a constituent of lignin depends on the source and species to which we get the lignin from [23].

2.2.1.4 Hemicellulose

Hemicellulose can be categorized as a heteropolymer composing branched, short, and linear chains of various monomers like hexoses and pentoses. Xylans and glucomannans are the most widely available hemicellulose type in which that we can get from hard wood and softwoods respectively. Because of Van der Waal's interactions and hydrogen bonds hemicellulose is kept attached to cellulose surfaces and cross-links with lignin at the same time, meanwhile this bonding can only be hydrolyzed by acid, alkali, enzymes [30].

2.2.1.5 Cellulose

Cellulose, which composes the major part of a lignocellulosic biomass is a composition of three hydroxyl groups (linear homopolysaccharide of b-1, 4-linked anhydro-D-glucose units with the repeating unit of cellobiose) which are the cause for the strong hydrogen bonding with the glucose

unit intramolecularly and with different chain intermolecularly. The networks formed due to the hydrogen bonding formed inter and intramolecularly are the major reason for the strong, and closely packed crystalline sections of cellulose that in turn result in strong, toughened, resistant to various organic solvents and making the cellulose insoluble in water [31].

2.2.1.6 Nanocellulose

Extracting nanocellulose involve pretreating the plant to break the amorphous structure of the cellulose so as to get the crystalline form of it which is crystalline nanocellulose (CNC) and crystalline nanofiber (CNF). These materials exhibit a better performance compared to other materials on similar application area, table 1 shows the comparison of materials properties of cellulose with other materials [21].

Table 2.2 Comparison of material properties [13]

Materials	Tensile Strength (GPa)	Young's Modulus (GPa)	Density (g/cm3)	Tensile/ density	Modulus/ density	Thermal Exp. Coe. (ppm/K)
CNC	7.5	145	1.6	4.7	90.6	3-22
Glass fiber	4.8	86	2.5	1.9	34.4	13
Steel wire	4.1	207	7.8	0.5	26.5	15
Kevlar	3.8	130	1.4	2.7	92.9	-4
Graphite	21	410	2.2	9.5	186	2-6
CNT	11-73	270-970	1	11-73	270-970	-

2.2.2 Glass fibers

Glass fibers are being used widely in the polymer composite producing industries this is due to its versatility and being cheap than that of Kevlar and carbon. Glass fibers are known for their light weight, extremely strong, less stiff and less brittle properties having 50% of silica content with different mineral oxides [32].

Thereby some of the mechanical properties like stiffness of a composite is determined with that of the fiber volume content, typically borosilicate glass (E-glass i.e electrical glass) are used as a major reinforcing constituent of a composite [33]. The volume content of a fiber determines the stiffness, tensile and compression of a composite material but a fiber content beyond 65% might cause too much dry areas in the composite since the volume of the resin might not be enough to wet the fiber which will reduce the fatigue strength of the composite.

Glass fibers are classified based on their desired properties in which they are made for, this is determined by the composition they attained with respect to their intended application. S-glass, R-glass and carbon fibers can be stated, 'S' means strength here which stands for the high strength property of the fiber in particular. S-glass fiber developed in 1960s, shows 40% higher flexural and tensile strengths, and 10 – 20 % higher compressive and flexural modulus compared to E-glass; however, S-glass is too expensive compared to that of the E-glass. However various studies suggests that the gap in mechanical performance of E-glass and S-glass fibers can be filled with modifications employed to E-glass fibers. On the other hand, carbon fibers are also other promising fibers which can be used alternatively, where they have lower density and higher stiffness than the glass fiber, making it possible to make thinner, lighter and stiffer composite materials. However, they have some limitations on some mechanical properties like low compressive strength and low damage tolerance.

In most of prosthetic limb manufacturing sectors E glass fiber is used as a reinforcing constituent, this is mainly due to its low cost compared to that of carbon fibers. Carbon fibers owe high specific strength and specific modulus but more expensive and are vulnerable to be corroded easily while making contact with metals. [34].

2.3 Prosthetic Limbs

Many reasons like chronic disease (diabetes and cancer), deformity, war and accidents could lead lower limbs to amputation. Thus, for those stated reasons lower amputation can occur at the knee, ankle, hip or at the extension parts in between the joints. Amputation on the femoral bone that can leave some portion of residual limb can be termed as below knee (BK) amputation. BK amputation may cause the patient to be limited in normal daily activities due to the loss of joints, tenons, ligaments and muscles [35]. Thus, an ideal replacement that is prosthetic limbs should match the mechanical movements of the residual limb with equivalent load bearing capacity [36].

A customized artificial limb can be employed to enhance residual limbs with amputation which can ease daily activities of the amputees. Prosthetic limbs have four major types depending on where it is to be fitted. Transtibial (below the knee), transfemoral (above the knee), trans-humeral (above the elbow) and trans-radial (below the elbow) are the major classifications. The prosthetic toe fitted to an Egyptian woman back in to 950 to 710 BC was the first artificial limb [37]. A

microprocessor-controlled C-leg which was introduced in 1999 was the first prosthetic knee and is considered as a milestone for the advancement in the prosthesis industry [36]. Components of a prosthetic limb can be wide enough to be dealt in this thesis research but in accordance with the scope of the thesis a few parts can be discussed.

Socket liners / Interface materials: prosthetics used to be applied directly to the skin of a human being before the introduction of socket liners. Earlier to the socket liner introduction amputees were suffering with over sweating, compliance and abrasion. Materials like silicone-gel, and foams are used to make these liners. Socket liners can ease the challenges that the patient could face while walking and make the prosthesis to last longer [38].

Prosthetic socket: This part needs to be designed in accordance with the residual limb of the amputee and is the important part of the prosthesis and the amputee activities. The suction valve provided with in the socket part keeps and the residual limb with the prosthesis.

Prosthetic knee joints: Knee joints are required while transfemoral, hip and knee disarticulation amputations. Swing and stance control are the two main moving mechanisms to be controlled. The control mechanisms of the knee joint are responsible for keeping safety of the amputee while swinging the knee foot segment and standing respectively.

Prosthetic shank/pylon: A component that connects the socket with the ankle-foot system and transfers the body weight of the amputee to the floor.

Prosthetic foot: At heel strike, the feet absorb shocks, support the prosthesis during the stance phase of gait, and then roll over smoothly to propel the body forward by pushing the ground behind them [39].

A prosthesis cannot be used if the residual limb length is less than 5 cm in transfemoral or transtibial. In consultation with a competent prosthetist, the choice to go to the next higher amputation level should be taken. For example, a transtibial residual limb with a length of less than 5 cm is considered short, although it is favored over a transfemoral amputation if acceptable range of motion (ROM) is available at the knee. Another point to consider is that the longest feasible time may not always be the best option.

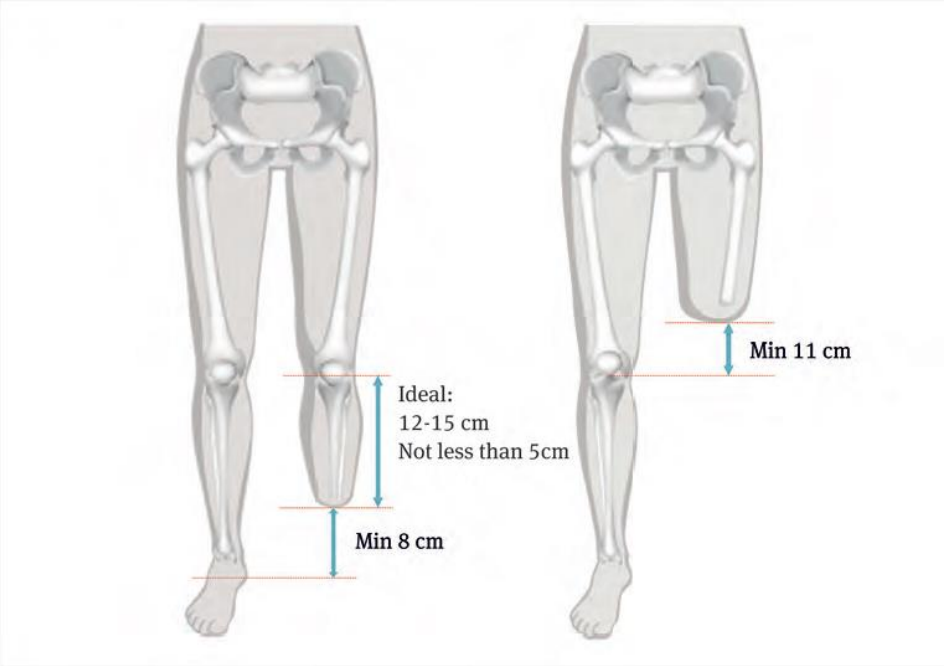

Figure 2.6: Ideal residual limb lengths
[39]

Prosthetic appliances have two major divisions depending on how they suspend load and their aesthetical looks, these divisions are exoskeletal and endoskeletal prosthesis.

Exoskeletal prosthesis: The exoskeletal prosthesis, also known as the traditional or crustacean prosthesis, is often made of wood or plastic.

Endo-skeletal prosthesis: The endoskeletal prosthesis is covered in aesthetic foam and features a tubular construction that connects the components [38].

2.4 Method of extraction of CNC

A. Moslemi et al. [30] employed a chemo-mechanical method to extract nanofibers from rice straw. This procedure included swelling, acid hydrolysis, alkali treatment, bleaching, and sonication. First, rice straws with the length of around 4–5 cm were soaked in 17.5 wt % sodium hydroxide solution for 2 h. Then, the swollen straws were washed with abundant distilled water and mixed by a blender for 30 min before being air dried at room temperature. The fiber obtained being washed and dried out was hydrolyzed with a diluted HCL solution so as to be able to remove the amorphous sections of the cellulose. Thus, to adjust the pH value of the fiber a thorough

washing was followed with hot water. The lignin, pectin and hemicellulose were removed by treating the hydrolyzed pulp with sodium hydroxide (NaOH, 2wt%) for about 2hr at 8 ± 5 ^{o} C. Bleaching was followed by treating the pulp with sodium chlorite solution (20 wt% w/v) at 50 ^{o} C for one hour then washed with hot distilled water then dried with air. A suspension of the fiber being chemically treated was made to be sonicated at 400 W and 20 KHz for about 30 minutes. Water / ice bath was used to control the temperature.

S. Mehanny et al [40] studied the extraction of nanocellulose from Different palm plant residues like coir, fronds and leaves. The process of extraction was begun by chopping the collected palm and then grinding into powder form. Alkali treatment was followed containing 1L of 10% NaOH (wt/wt), with 100 gm at 160 ^{0}C for about two hours. As an intervention the pulp was washed and air dried. Acid hydrolysis taken place by mixing 200 ml of 20% H_2SO_4 (v/v) being heated at 120 ^{0}C stirring with constant speed of the stirrer for 30 minutes. Quenching was undergone by adding 1500 ml ice cube of distilled water. A Millipore filter with 0.22 µm was used to filter the pulp suspension, the neutralization was kept by adding 5% w/v $NaHCO_3$ til a pH of 7-8 is attained. Then after, centrifugation at 6000 rpm for 15 min was followed. Finally, the sedimented section of the suspension being centrifuged was left and the supernatant poured into 50 ml tube with a distilled water added on and then shaken. Repeating the last two steps a till a pH of 7 is attained was important. Thus SEM, TEM, particle size distribution, FTIR and XRD analysis were performed on the final product of nanocellulose.

A. Mandal and D. J. C. P. Chakrabarty [41] carried out extraction of nanocellulose from bagasse. The collected bagasse was grinded and dried in an oven followed by delignification. Delignification was employed by mixing 0.7% (w/v) of sodium chlorite solution with fiber to liquid ratio 1:50 having controlled the pH of the system by adding 5 % acetic acid and boiling the mixture for 5 hours. The residue will be then treated by boiling 250 ml 5% (w/v) sodium sulfite for 5 h. Isolation of cellulose was undergone by boiling 250 ml 17.5% (w/v) sodium hydroxide for 5 h tto remove hemicellulose. Acid hydrolysis was followed with 60% (w/v) sulfuric acid at 50 ^{o} C for 5 hours with fiber to liquor ratio of 1:20 having a constant stirring mechanism for a better dispersion of the solution. Quenching, centrifugation and repetitive washing by distilled water

were employed. XRD and SEM analysis were employed to detect the particle size and surface morphology of the sample prepared respectively.

S. Rashid, H. J. I. C. Dutta [42] investigated extraction of nanocellulose from rice husk. Dewaxing of powdered rice husk through Soxhlet extraction (i.e 2:1, v/v of methanol and benzene) at a temperature of 75 ^{o} C for 9h. Evaporating the solvent alkali treatment was followed by treating the pulp with 3% (w/v) of sodium hydroxide (with solution to sample having a ratio of 1:1) for about 8h at a temperature of 45^{o} C with constant stirring. The alkali treated husks were steam exploded by subjecting to triple autoclaving under 15 psi (121 °C ± 2 °C) for 8 h this step is considered as part of delignification. To remove any remaining hemicellulose, lignin and pigment, the fibers were bleached 4 times using peracetic acid (6.5:2.0, acetic acid: hydrogen peroxide, v/v) at 45 °C for 7 h under mechanical stirring. A measured amount of cellulose was treated with 65 % sulfuric acid (1:20, cellulose to acid ratio) at 45 °C for 90 min with continuous mechanical agitation (1500 rpm). After ceasing the hydrolysis by adding chilled distilled water then centrifugation was followed at 12,000rpm for 10 min. The centrifugation was undergone 6 times to obtain a neutral suspension. The resulting suspension was then sonicated (300 W) for 15 min and frozen at -40 °C and freeze dried for 84 h to obtain dry nanocellulose powder.

2.5 Natural fiber reinforced polymer composite

M. Boopalan et al. [43] performed a comparative study on the mechanical properties of sisal and jute fiber reinforced polymer composites with and without 20% NaOH treatment. The fibers were treated with 20% NaOH for 2 hours and treated with acetic acid to neutralize the alkaline then followed by washing with water and dried in an oven at 110^{o} C. Hand layup fabrication technique was performed to embed both treated and untreated fibers separately using epoxy resin with HY951hardener on a mold having a size of 210×210×40 mm3. Mechanical property investigation was performed with Universal Testing Machine (TNUM-5900), Surface morphology was tested with DXS-10ACKT Scanning electronic microscope. Water absorption was tested by drying sample composites in an oven then all the samples was weighted before getting immersed in a water for 24 hours then weighting it to compare with the dried samples to check how much water it absorbs.

R.Badrinath and T.Senthilvelan [44] performed a comparative study on physical and mechanical properties of sisal and banana reinforced polymer composite. Mechanical extraction was employed on banana fiber prior to alkali treatment with 5% NaOH solution for about four hours. The alkali was cleaned with tap water and dried in an oven at 105^{o}C for 24 hours. Leaves of sisal was collected and submerged in a benzene- ethanol having a ratio of 2:1 by volume. Then sisal leaves were treated with NaOH solution for 90 minutes at 80^{o}C, and was washed with distilled water and dried in an oven at 60^{o}C. Hand layup fabrication technique was used and 12 wt% of fibers were applied for both sisal and banana, both with unidirectional and bidirectional fiber orientations that is (sisal at 90^{o}, sisal at 0^{o},90^{o},0^{o} and banana at 90^{o}, banana at 0^{o},90^{o},0^{o}).

2.6 CNC reinforced polymer composite

Sami Boufi [45] have studied both cellulose nanocrystal (CNC) and nanofibrilated cellulose (NFC) from that of rachis and alfa of date palm tree. The raw powdered pulp was first treated with tolune-ethanol (62:38) % for 24 hours followed by alkali treatment of 2 % NaOH at 80^{o}C for 2h (this treatment was repeated) followed by bleaching process with $NaOCL_2$. TEMPO-oxidation/ high pressure homogenization and acid hydrolysis (with 65% H_2SO_4) for 45 minutes were employed for NFC and CNCs respectively. Nanocomposite films were prepared with latex having each of CNC and NFC content of about 0 to 15 wt.% by stirring for 1hr, then the mixture was casted in a mold then dried at 40^{o}C. The effect of nanocellulose was observed in ranging thickness of 300-400 µm exhibiting from transparent to translucent film as a factor of nanofiller content. Dynamic mechanical properties were examined and cellulosic nanoparticle aspect ratio was found to be determinant for rubbery modulus indicating an increase in aspect ratio in higher reinforcing capability.

K R Srivastava [46] studied the effect of nanocellulose as a filler material on a PVA film which was extracted from Banana pseudostem fiber undergoing a green synthesis process. Solvent casting was used as a fabrication technique with varying weight percentage of nanocellulose to study the effect. Mechanical properties like flexural and tensile strength and physical properties like water barrier properties were improved with increasing amount of nanocellulose. The nano-filled film exhibits higher stiffness showing a lower transparency of the film. A film with 3 wt% nanocellulose showed a reduction in percent elongation by 9.1 % and 14.3% improvement in tensile strength. Having immersed the film in a water for 24 hours it was observed 29.7%

improvement in water permeability. The film with no nanocellulose gained 67.4% weight and that of nanocellulose added film gained 16.8%.

Gangesh Kumar Rai and V.P. Singh [47] studied on method of extraction of nanocellulose and fabrication of nanocellulose reinforced polymer composite. A lignocellulosic biomass needs to be treated by chemicals like alkali so as to remove lignin, pectin, waxes, hemicellulose, and other impurities. Post alkali treatment would be either chemical methods like acid treatment or enzymatic hydrolysis, or mechanical actions like applying high pressure and velocity to obtain nanofibers. The authors identified that ultrasonication, high pressure homogenization, planetary ball milling and ball milling as a mechanical method of nanocellulose extraction. According to the study alkali treatments with varying concentration and duration can result in various mechanical property improvement. It was studied that natural fiber being treated in 10% of NaOH for 24 hours exhibits better flexural modulus and strength by 60% and while treating the fiber for 48 hours with the same concentration a stiffer and brittle material was obtained. Therefore, after extracting nanocellulose the fabrication technique can be selected according to the resin matrix in used and the desired application area of the composite material.

Anish Khan et al. [48] studied on research to identify the effect of nano-clays (montmorillonite (MMT) and organoclay (OMMT)) and cellulose nanofibers (CNFs) on kenaf-epoxy composites at 0.75wt%. Hand layup fabrication technique was employed to prepare sample composites with 40 wt% of kenaf fiber. Thus, various physical and mechanical tests were performed for each sample composites with three nanofillers to compare their effect. Thus, compared to montmorillonite cellulose nanofibers and organoclay contributed for the enhancement of mechanical properties particularly stiffness was improved due to uniform distribution of the particles as a filler material. Apart from mechanical properties physical properties of sample composite with OMMT and CNFs showed significant improvement and surface adhesion with kenaf was also improved. Therefore, it was recommended that kenaf reinforced epoxy composite materials with OMMT and CNFs are ideal for construction application.

2.6.4 Hybrid E-glass and natural fiber or CNC reinforced polymer composite

Mark Miller [49] depicted that addition of CNC can enhance the mechanical properties of a composite material decreasing its weight at the same time. The reduction in weight was attained by replacing the glass fiber with that of CNC without affecting mechanical properties of the

composite material. CNC was added either on the glass fibers directly or mixed to the resin, SMC manufacturing line with a fiber coating bath was used for fabrication. As a result, adding CNC in epoxy resin have shown an improvement in flexural and tensile strength while impact strength and density doesn't showed improvement.

Infanta Mary Priya and BK Vinayagam [1] studied the effect of graphene platelet nano powder (GPN) on a bi-axial type glass fiber reinforced epoxy composite. Two control samples with a thickness of 2 and 3 mm were prepared both with and without GPN, 0.1 wt% GPN was added to epoxy resin. Compressive strength was improved by 26.4% and 24.6% for the samples with 2 and 3mm thickness and for similar two samples there was also improvement in tensile strength by 11.18% and 33.4% respectively. High velocity gas gun was used to perform impact test and energy absorption of samples with GPN showed was higher than that of the control samples that is 9.2% and 8.2% for the sample's composites having 2 and 3mm thickness respectively.

K. Ansal Muhammed et al. [50] performed Experimental investigation on AW 106 Epoxy/E-Glass fiber/nano clay composite for wind turbine blade. Hand layup fabrication technique was used to fabricate four samples one with no nanomaterial, and the other three sample composites with 1wt%, 2wt% and, 3wt% of montmorillonite. Result for mechanical and morphological tests indicated a sample composite with 1% montmorillonite showed better tensile strength as compared to other samples and 4.4% higher than that of neat sample. However, adding more than 1% of nanomaterial showed a reduction in tensile strength, affects nano particle distribution causing agglomeration and a linear increment in hardness of the composite material. Thus, it was concluded that 1% montmorillonite is an optimized weight for hardness and maximum for tensile strength.

Arun prakash V.R. and Rajadurai A. [51] studied on Thermo-mechanical characterization of siliconized E-glass fiber/hematite particles reinforced epoxy resin hybrid composite. The surface of E-glass was modified for a better adhesion with epoxy and iron (III) oxide particles with a size of 200nm (formed by ball milling) to 100nm (prepared by sol-gel process). Surface modification was performed with 3-Aminopropyltrimethoxysilane (APTMS). Hand lay-up was used to fabricate the composite, 15% treated E-glass fiber and 0.5% and 1% vol% iron (III) oxide particle added into epoxy resin, where siliconization was performed to enhance adhesion. Therefore, mechanical properties showed improvements, impact strength was improved by 23.9%, flexural strength

showed 9.7% improvement and 55.4% enhancement in tensile strength. A maximum increase in thermal conductivity by 36% was found for composites made with hematite. Morphology with SEM showed a better adhesion of fiber-filler and epoxy interaction.

R. Prem chand et al. [52] performed an investigation and analysis for mechanical properties of banana and E glass fiber reinforced hybrid epoxy composites. Adhesion properties of E glass and banana fibers were improved by treating with 5% of NaOH, Na-Cl solution and was further treated in a hardener of HY951. Banana fiber was used with different volume fraction that is 10%, 20% and 30% yielding different young's modulus which affects the stiffness of the material. Mechanical tests were performed on specimens made according to ASTM with UTM with a maximum capacity of 100KN. Tensile and flexural strength of the hybrid composite showed an improvement by 57.09% and 76.5% respectively. While hardness was decreased from 39.65 to 37.44Mpa with banana fiber volume fraction of 10% to 30%. Thus, it was concluded that the hybrid banana E glass epoxy composite showed a better mechanical property than the composite material with only banana fiber.

Abhishek M R et al. [53] evaluated mechanical properties of jute/E-glass epoxy hybrid composites by varying fiber loading with and without shear thickening fluid. Hand layup fabrication technique was used along with different orientation of fibers in which E glass and jute were placed at 0 ^{o} and 90 ^{o} respectively. Four different compositions of jute and E glass were performed, that is 20 to 20, 25 to 15, 30 to 10, and 35 to 5 wt% having a fixed weight percentage of epoxy resin which is 60%. Thus prior to mechanical property investigation the same number of sample composites were prepared by adding a shear thickening fluid into epoxy resin to compare with the previous samples. Sample composites with higher E glass fiber composition and STF showed higher UTS and young's modulus while having lower % elongation. In particular sample composites with 25% and 30 wt% E glass showed better results.

Sivasaravanan.S et al. [54] investigated the effect of nanoclay (Cloisite 20A) on E glass reinforced epoxy composite. Bi directional E glass fiber having orientation of fiber at 45^{o}, cloisite 20A which is natural montmorillonite treated with quatermary ammonium salt and epoxy resin (LY 556) with a hardener (HY 951) were used as reinforcement, filler material and matrix respectively. Nanoclay powder was added to epoxy resin and was sonicated using ultrasonicator

to keep uniform dispersion of particles. Hand layup was used to fabricate the samples with 1 wt%, 2wt%, 3wt%, 4 wt% and 5 wt% of nanoclay and specimens were prepared as per ASTM. Izod testing machine was used to test impact strength to which better performance was observed at 5 wt% of nanoclay which is 10.75 J/m, and was recommended using above this percentage would result a brittle composite material.

MD Nadeem M. et al. [55] performed research on the effect of multi walled carbon nano tubes (MWCNT) and glass fibers with other particulate reinforcing materials at higher working temperature. It was investigated that how particulate reinforcements affect the composite both in micro (Aluminium Oxide (Al2O3), Barium Sulphate (BaSO4) and Activated Carbon Powder (ACP)) size and nano-size (Multi-Walled Carbon Nanotubes (MWCNTs) and Nano Silica Powder (NSP)). The composite material was fabricated with hand lay-up and pressed for 24 hours at room temperature and kept in an oven at 100^{o}C for 12 hours. The compositions of chopped E glass fiber and MWCNT was fixed to a total combined 10 vol%. Mechanical properties of the composite material were investigated at different temperatures, thus a composition of 8.5 vol% EGF and 1.5 vol% MWCNT exhibits a better hardness value, impact strength and tensile strength at 25^{o}C.

2.7 Prosthetic limb

Muhammad Safa Al-Din Tahir and Fahad M Kadhim [56] have studied on a new prosthetic shank made of PLA carbon fiber material which was created and fabricated to generate a pylon that is lighter in weight and less expensive than regular shanks while yet bearing the patient's weight without mechanical failure. The testing and numerical results revealed that the novel prosthetic shank weighs 42%, 50%, and 60% less than Titanium, Aluminum and Stainless-steel pylons. In other hands the costs were found to be less by 96%, 97.5% and 98% for that of Aluminum, Stainless-steel and Titanium respectively. It was generalized that the new design is less expensive, lighter, and can handle heavier patient.

Jawad Kadhim Oleiwi [57] performed experimental and numerical investigation on composite prosthetic pylon materials compare to the conventional ones (Aluminum, Titanium, or Stainless steel). Specimens were fabricated utilizing Vacuum bagging technique from Poly methyl methacrylate (PMMA) as matrix with constant Perlon layers and various numbers of Hybrid (Carbon + Glass) fiber layers as reinforcing materials at (45^{o}&0^{o}/90^{o}) orientation relative to

applied load. Additionally, finite element method (ANSYS-15) was used to generate a model of the prosthetic pylon and apply compressive load at the heel striking step throughout the gait cycle to determine the critical buckling stress. At ($0^o/90^o$) fibers orientation relative to tensile force, the percentage increase in tensile strength, modulus of elasticity, and critical buckling stress for specimens with three Hybrid (Carbon + Glass) layers and Perlon layers in PMMA resin compared to pure PMMA specimens was 302.7 percent, 300 percent, and 257.22 percent, respectively.

E Stenvall et. al. [58] aimed at combining bio-composites made from forestry-based derivatives with additive manufacturing processes to create systematic solutions for prosthetic products and services. Polypropylene (PP) composite materials reinforced with microfibrillated cellulose (MFC) were created. The MFC concentrations (20,30, and 40 wt percent) were evenly disseminated in the polymer PP matrix, and the MFC addition greatly improved the materials' mechanical performance. When injection molding was done with 30 wt percent MFC, the tensile strength and Young's modulus was about double that of PP.

M. Saquib Hasnain [59] focused on studies about nanocomposite materials for prostheses applications. It was also studied that nanocomposites, are newer nanomaterials that are made up of numerous nanoscale materials or a nanoscale material embedded in a bulk material. It was also studied that nanotechnology is a multidisciplinary field that includes physics, chemistry, biology, materials science, and engineering. In the disciplines of materials, metals, plastics, ceramics, biomaterials, electronic materials, and so on, a variety of nanocomposites have already been researched and used. These nanocomposites are employed in orthopedics, dentistry, tissue engineering, antibacterial characteristics, wound dressings, drug delivery, cancer therapy, stem cell therapy, and biosensors in biomedical applications. Orthopedic prosthetics, dental prosthetics, maxillofacial prosthetics, and cardiac prosthetics, among other uses in relation to prosthetic applications. It was concluded that prosthetic appliances made of nanocomposite have shown better prospects than the conventional.

Harsimran Jeet Singh Sidhu et. al [60] studied to develop a prosthetic leg that could bridge the gap between imported and traditional legs. The research was conducted such that the limb should be lighter in weight than a traditional leg and far less expensive than a leg purchased from another

country. The employment of the new limb was accomplished by assessing the drawbacks of the traditional leg and proposing changes that result in less weight. Following that, the ideal material for lowering weight was identified to be E-Glass Epoxy, based on the characteristics of numerous polymer matrix composites materials. The prosthetic leg's socket and shin were designed in SOLIDWORKS using the material properties of this composite, and stress analysis was carried out using simulation simulations.

Nazik Abdulwahid Jebur et al. [61] studied the mechanical properties of a composite material with different reinforcing layers. Three layers prosthetic socket (3pyrlon,3carbon,3pyrlon) was fabricated. A case study was conducted on a man weighing 85 kg and 23 years old thus, the F-Socket test uses a pressure sensor to evaluate the interface pressure between the below-knee prosthetic socket and the residual lower limb. The tensile test determined the elasticity modules (1.109 GPa), yield stress (34 MPa), and ultimate stress (1.109 GPa) (38 MPa). BK prosthesis was simulated with ANSYS software, thus the results demonstrated that the highest equivalent Von-Mises stress to be (18.5 e7 Pa) and that the maximum deflection 0.00604 mm.

H. N. Shasmin et al. [62] studied to replace the commercial pylon with a bamboo. The initial stage in this research is to figure out which bamboo species can be used to make pylons. The data from bamboos examined by the Forest Research Institute of Malaysia (FRIM) was crucial in selecting a strong and long-lasting bamboo. Second, the mechanical properties of the chosen bamboo were assessed, including stiffness, tensile strength, deformation, and wear resistance. The FRIM mechanical testing on a number of bamboo species led to the selection of Gigantocloa Ligulata and Bambusa Heterostachya. Furthermore, both species have 30-34mm diameters, which is similar to the commercial pylon. The bamboos have a high tensile strength of 341-530 MPa, which is suitable for pylon applications. Natural bamboo, on the other hand, cannot last more than three years owing to distortion. Heat treatment process and laminating the bamboo was suggested to increase the bamboo durability. It was concluded that bamboo can be used as a pylon to construct a prosthesis with good tensile qualities for a low-cost artificial leg.

S Hanie Nadia [63] studied and compared a treated bamboo fiber with fiber reinforced plastic and aluminum. Bambusa Heterostachya was harvested and dried for 72 hours at 200 ^{o}C in an oven,

then pre-treated with V-Sawit oil at around 120°C for 30 to 90 minutes before lamination. Vinyl urethane adhesive and polyvinyl acetate were utilized to laminate the bamboo pylon with at least three layers. The flexural, compressive, and tensile properties of bamboo pylon were examined. A computer simulation of the person walking with a bamboo pylon was also carried out. Gait comparisons were performed on six transtibial amputees while walking with bamboo and stainless-steel pylon prosthetic legs. The results showed that bamboo pylon was three times stronger than fiber reinforced plastic and two times stronger than aluminum, with yield compressive stress and Young's modulus of 132.6 MPa (SD 3.3 MPa) and 30.7 GPa (SD 4.7 GPa) respectively. There was no significant difference found in vertical and antero-posterior ground reaction forces.

Ameer A. Kadhim et al. [64] investigated a favorable material to manufacture a prosthetic pylon and modeling it on a 3D printer. To achieve excellent load distribution on the shank's walls, the shank was developed and analyzed using solid work software before being manufactured using a 3D printer. The new shank material was intended to be fabricated with Acrylonitrile butadiene styrene (ABS) and Polylactic acid (PLA). A sample pylon made with PLA exhibits better mechanical performance than that of ABS. Gait cycle test was performed with two phases of, one of which is the swing phase and the other is the stance phase, in which the ground reaction force is generated, the amount of which is 1.3 of the amputee's weight at the heel and toe, and then design a special device to examine the life of the new shank by alternating load. It was concluded that in addition to its reduced weight, the new shank is simple to make and inexpensive.

2.8 Summary of literature review

- ✓ Chemical extraction method of CNC is observed to be effective while that of mechanical method denatures the structure of cellulose.
- ✓ Alkali treatment at prior stage of the extraction process was understood to have superior outcome than the other methods.
- ✓ Acid hydrolysis was found to be the critical stage so as to attain CNC
- ✓ Hybridizing natural fibers with synthetic was suggested to bring better physical and mechanical performances.
- ✓ Hand layup composite fabrication technique was used in most of the papers as it can be found employed easily.

- ✓ Most widely synthetic fibers are employed for prosthetic applications thus having toxicity both on the amputee and to the environment while getting damped.
- ✓ Optimization on chemical extraction was understood to be a key step
- ✓ Hybridizing particulate at its finest size could bring a better property of a prosthetic limb

2.9 Gaps Identified in literatures

From the literatures reviewed various techniques of CNC extraction were employed, some affecting the nature of the cellulose material and some failing to obtain crystalline form of it. Agglomeration which is the major characteristic to be resolved while extracting cellulose which determines the dispersion rate of CNC in a matrix material should be taken into consideration while extracting CNC from its plant derivative. It was understood most of the papers concluded their work stating agglomeration as a drawback of their work. Limited weight percentage trials of CNC to hybridize the composite material were employed in most of the papers reviewed. Application of CNC as a filler material for prosthetic pylon is limited. Most of the research found were on nanofibers while crystalline form of cellulose has advantage to be employed as a filler material that will enhance the mechanical property of the composite material.

CHAPTER THREE

3. MATERIALS AND METHOD

3.1 Methodology

In this thesis work various methodologies were followed from identifying the problem to the testing of different mechanical and physical properties.

Various journals and articles were reviewed so as to be able to clearly identify and understand the stated problem and meet the general and specific objectives regarding natural fibers and the hybrid one. Various plant resources were examined and studied to be a source for the extraction of CNC, thus the selection was based on abundance of the source plant and yielding. A chemical method of extraction was taken to extract CNC from the source plant, and a commercial E-glass fiber and epoxy resin with its hardener were used. Thus, based on different literatures the wt% of E-glass to CNC and epoxy resin was determined. Based on the desired application area of the composite being fabricated and the type of reinforcing material used different techniques of fabrication can be applied, in this thesis research hand layup technique was used because of its ease of fabrication and availability.

In the fabrication section of the research CNC power, E-glass fiber, epoxy resin, mold, plastic sheet, releasing agent, roller and clamp were utilized. Onwards a control sample composite of neat E-glass fiber with epoxy and four sample composite materials each with varying wt% of CNC were prepared. Having completed the fabrication process specimens were prepared into size that is according to the ASTM standards to be tested for tensile strength, compression strength, impact strength, flexural strength, water absorption, density, void content and TGA. Overall methodology followed is described in Figure 3.1

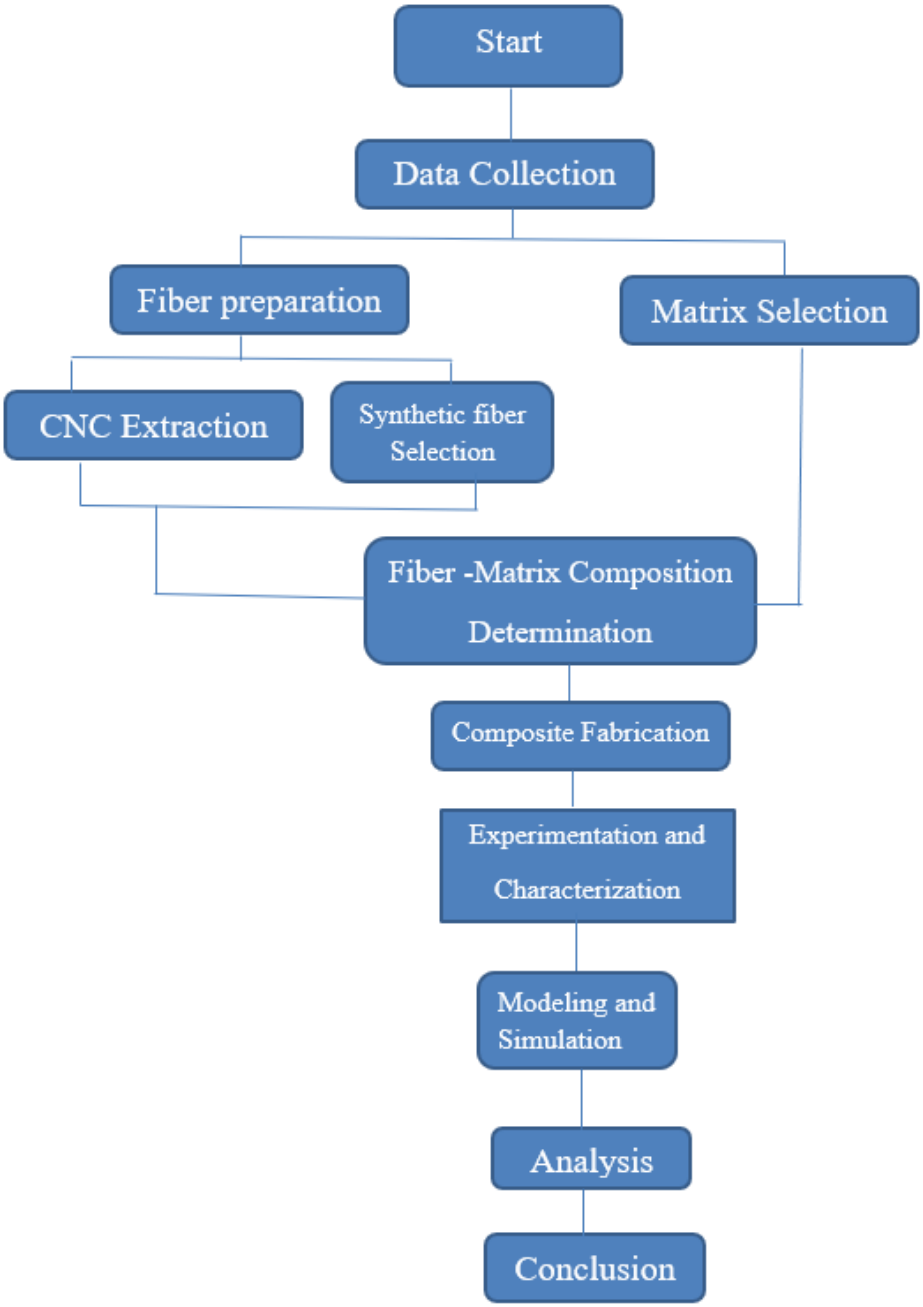

Figure 3.1 Methodology of the study

3.2 Materials

In this experimental work section of the study sugarcane bagasse which is the byproduct of sugar production is used as a raw material for the extraction of nanocellulose. Thus, to extract the desired crystalline nanocellulose from a given bagasse various chemicals like sodium hydroxide (NaOH), formic acid, acetic acid, hydrogen peroxide (H_2O_2) and sulfuric acid (H_2SO_4) are used for various stages of the extraction process.

Other than chemicals different laboratory equipment like grinding machine, water bath, falcon tube, centrifuge machine, funnel, petri dish, measuring cylinder, beaker, oven, electronic pH meter and ultra-sonicator were used. To fabricate the composite material the following materials in Table 3.1 was used.

Table 3.1 Materials to fabricate the composite material

S/N	Materials
1	Glass fiber
2	CNC
3	Epoxy resin
4	Hardener
5	Releasing agent
6	Meta mold
7	Plastic sheet
8	Roller
9	Jig saw

3.2.1 Fiber materials used

Various studies implied the use of natural fibers in the application areas that demand to be compatible and be environmentally friendly is being understood to be important. In particular natural fibers at lower scales of their structure could result in mechanically and physically unique property owing material. In addition, unlike the synthetic fibers natural fibers cannot be a threat to the environment in both cases while being in used and when dumping.

In the case of this thesis research two types of fibers were used as a reinforcement and epoxy resin as a matrix material. The composite material was fabricated varying weight percentage of the two fibers.

3.2.1.1 E-glass fiber

A glass fiber having randomly distributed fibers is chosen for this research, since E-glass is the cheapest one of those available on the market but comparable properties. Figure 3.2 shows E-glass fiber prepared into size of the designed mold and weighted according to the calculated mass fraction of the composite material.

Figure 3.2 Commercial E-glass fiber

Several fine fibers of glass made a reinforcing glass fiber material and is known for its versatile industrial application. Due to its thickness, weight, and strength, fiberglass has certain distinct advantages over other materials and has mechanical properties comparable to many other fibers like carbon fiber [65]. Glass fiber at a lower weight exhibits better tensile strength than a steel wire of similar diameter. Its dimensional stability makes it to be favorable in most mechanical application of composite materials. Its low coefficient of linear expansion contributed to its dimensional stability, and GF is not sensitive to variations in temperature. Glass fibers are highly heat and chemical resistant and thermal insulator due to its high ratio of surface area to weight [66].

3.2.1.2 CNC particulate from sugarcane

Sugar cane which is the primary source for bagasse is suited in a tropical climate zone in a temperature ranging between 32.2^{o}C to 37.78^{o}C. Sugarcane bagasse, an agro-industrial waste (Saccharum officinarum) is a by-product of the sugarcane industry. It is a lignocellulosic fiber byproduct derived from sugarcane culm following the milling and juice extraction of the culm. Figure 3.3 shows a stalk of sugar cane and bagasse after the extraction of sugar. Sugar cane typically contains 65 - 75 % water, 11 - 18 % sugars, 8 - 14 % fiber, and 12 - 23 % soluble solids. The fiber that is left over after the sugars have been removed is known as sugarcane bagasse as shown in Figure 3.4. [67].

Figure 3.3 Sugarcane plant, stalk and bagasse [68]

As shown in Figure 3.4 bagasse is a fibrous material having low-density with a huge range of particle sizes and a lot of moisture. Characterizing properties of bagasse is not performed in usual ways like determining drag coefficient, particle size and density [69]. Two distinct methods are used to separate the bagasse fibers from the sugarcane rind: chemical extraction and mechanical separation. Numerous variables are taken into account, including reaction time and sodium hydroxide solutions with various concentrations [25].

Figure 3.4 Bagasse fiber[25]

3.2.1.3 Extraction of Crystalline nanocellulose (CNC)

Cellulose in its crystalline form can play a major role in composite fabrication due to its significant role in enhancing mechanical and physical properties of the material which it is being used to make. Thus, cellulose needs to be treated with different chemicals to reduce its size so as to obtain it in nanoscale.

Various method of extraction is available in the case of CNC like mechanical and chemical extraction in this thesis work chemical method of extraction was selected. Chemical extraction is selected because of the tendency to obtain cellulose in the desired size by optimizing the procedures and concentrations of the chemicals being in use.

3.2.1.3.1 Alkali treatment

As shown in Figure 3.5 (a) the collected bagasse was grinded and prepared to be treated with the alkali, thus with 1:9 pulp to alkali (sodium hydroxide (NaOH)) ratio of 10 % NaOH solution was made and heated in a water bath for one and half hour at 90^{o} C as shown in Figure 3.5 (b) [70].

After heating the solution, it will be filtered and repeatedly washed with distilled water to remove the alkali from the surface of the bagasse and dried at 60^{o}C till the moisture in the pulp is removed, this will ease the surface of the bagasse to be exposed for the next process which is delignification.

3.2.1.3.2 Delignification and bleaching

The alkali treated and filtered pulp powder was further treated with 20% formic acid, 20% acetic acid and 7.5 % H_2O_2 (2:1:2) solution (1:10 solid to liquid ratio) in a water bath at 90 ^oC for one and half hour, as illustrated in Figure 3.5 (c). Here as an intervention the cellulose material separated from lignin and hemicellulose by filtration was properly washed several times with hot distilled water.

Having performed the delignification process bleaching was carried out by treating the pulp with 7.5% H_2O_2 in 4% NaOH solution (with 1:9 fiber to liquid ratio) first at room temperature for 30 minutes followed by in a water bath at 70 ^{o} C for 30 minutes as shown in Figure 3.5 (d). The cellulose chain contains strong intermolecular hydrogen bonding and hydrophilic interactions, that can result to agglomeration form of CNC that is why acid hydrolysis followed [71].

3.2.1.3.3 Acid hydrolysis

Acid can easily infiltrate in the amorphous section of cellulose fibers during the first step of acid hydrolysis. The glycosidic linkages were easily accessible after hydrolysis. At the reduction end and on the surface of the residual crystal section, the reaction time is added considerably more slowly [72].

Figure 3.5 (e) shows that the bleached pulp powder of sugarcane bagasse was slowly added into H_2SO_4 solution (60% w/v) with 1:12 solid to liquid ratio under vigorous stirring at room temperature on a hot plate with a magnetic stirrer for 15 minutes. Thus, a jelly product was obtained which indicates the formation of CNC and followed by adding an ice cube to quench the hydrolysis.

As the process of acid hydrolysis ends quenching was followed by adding an ice cube to stop the hydrolysis process forming a gel like material as shown in

Figure 3.5 (f). At the end of quenching process, the ice water was decanted and the pulp was washed with hot distilled water.

Then after having quenched. As shown in Figure 3.5 (g) the mixture was centrifuged with a TGL-16/18/20/22/24M Benchtop High-speed refrigerated centrifuge first at 1000rpm for 10 minutes

and then to obtain CNC [centrifuge at 6000rpm for 15 minutes] with six sample holder of falcon tube having a capacity of 50ml each at room temperature.

Then the resulting CNC suspension was sonicated with ultrasonic cleaner device model 8848 COLE PARMER for 30 minutes to keep homogeneity and remove the concentrated sulfuric acid easily as illustrated in Figure 3.5 (h). Long cellulose from microfiber was broken into cellulose nanocrystals using a combination of acid hydrolysis and ultrasonication, resulting in a size reduction from micron to nano scale [73]. Thus, as shown in Figure 3.5 (i) the sonicated suspension was thoroughly washed with hot distilled water till a pH of 7.5 attained and was filtered with a filter paper, finally it will be dried in an oven at 60^{o}C. Finally, the dried CNC was grinded in to a powder form as indicated in figure 3.2 (j).

Figure 3.5 Extraction of CNC

3.2.2 Matrix material

3.2.2.1 Epoxy resin

Figure 3.6 shows araldite (LY556) which was selected as a matrix material, which is a thermoset polymer having excellent adhesion, better mechanical and electrical properties, good chemical resistance, good performance at elevated temperature and low shrinkage. Table 3.2 shows the specification of Araldite (LY556) epoxy resin.

Table 3.2 Specification of Epoxy Resin LY556

Product type	Epoxies – Bisphenol-A based
Chemical composition	Bisphenol -A-based epoxy resin

Aspect (visual)	Clear, pale-yellow liquid
Viscosity at 25^{o}C	10,000 – 12,000 MPa S
Density at 25 ^{o}C	1.15 – 1.20g/cm3
Curing time	10-20min
Shelf time	2 years

Figure 3.6 Araldite (LY556) epoxy resin

3.2.2.2 Hardener

Catalysis is required to get the epoxy resin dried up within a desired timeline, thus catalysts can take this role by initiating chemical reaction. Proper amount of hardener should be added thus, as recommended by the supplier 10:1 (epoxy to hardener) ratio was applied. Figure 3.7 shows a hardener material HY951 from the same supplier Herenba from India was used, thus the hardener lets the epoxy resin to be cured in a lesser time.

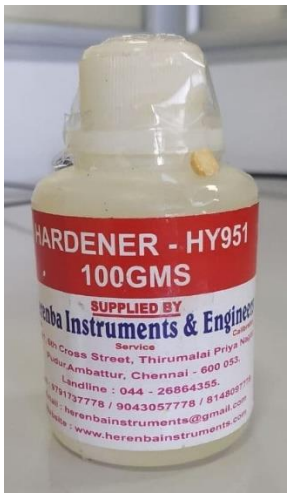

Figure 3.7 HY954 Hardener

3.2.3 Additional materials

3.2.3.1 Release agent and plastic sheet

A release agent in a form of honey wax was used for a better surface finish and ease of detachment of the fabricated composite material from the mold. Figure 3.8 (a) shows a product branded with HONEY WAX 250 (Mold release agent) was used. Plastic sheets which are illustrated in Figure 3.8 (b) are used to ease the removal of sample composite from the mold and prevents it from various impurities while performing the fabrication process.

(a)

(b)

Figure 3.8 (a) Release agent (b) Plastic sheet

3.2.3.2 Roller

Figure 3.9 illustrates an equipment having cylindrical rolling section on the leading tip of it and a handler on the trailing end. This material is used to make homogenous distribution of epoxy resin and ensure the wettability of fiber and remove air bubbles by squeezing the composite material while performing hand lay-up process of fabrication.

Figure 3.9 A roller

3.3 Fabrication and sample preparation of hybrid E-glass CNC composite

Epoxy resin was purchased and utilized as a matrix for sample preparation of the hybrid CNC/E-glass fiber polymer composite. The produced CNC was mixed with the commercial epoxy resin with respect to its weight with various percentage that is (2% wt., 4% wt., 6% wt., and 8% wt.). A control sample of neat E-glass reinforced epoxy composite was also fabricated so as to compare the hybridized one with it.

Hand layup technique of fabrication was used; thus, a release agent was applied on the bottom of the mold so as to remove the composite easily from the mold. Then a commercial mat type E-glass fiber was used as a reinforcement and followed by applying epoxy resin on it with adequate ratio.

3.3.1 Mold preparation

As shown in Figure 3.10 the mold was formed according to the dimensions of the specimens required to perform mechanical and physical tests; thus 250 mm *140mm *4 mm is the dimension of the mold and from this the volume is calculated.

Volume of mold (V) = 25×14×0.4

= 140 cm^3

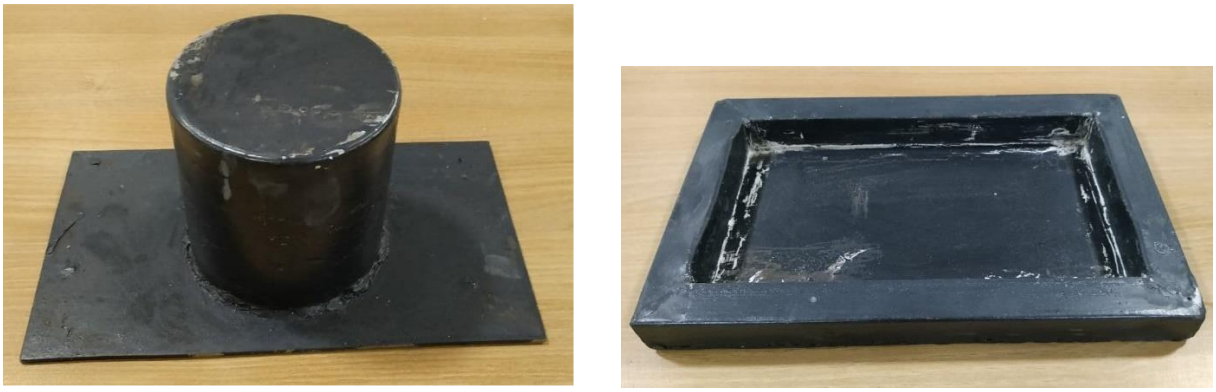

Figure 3.10 A mold material

3.3.2 Fiber and Matrix volume and mass fraction calculation

The amount of E-glass fiber and that of the CNC mass which is required to form the weight percentage with respect to the total mass of the epoxy resin is determined as follows:

3.3.2.1 Volume Fraction of Matrix

Volume fraction of a matrix is the ratio of volume of the matrix to volume of the composite:

$Vm = \frac{vm}{vc}$……...……eqn. 3.1

Where: *Vm = volume fraction of matrix*

vm = volume of matrix

vc = volume of composite

3.3.2.2 Mass Fraction of Matrix

$Mm = \frac{\mathrm{mm}}{mc}$……..……...eqn. 3.2

Where: *Mm* = mass fractions of matrix.

m_m = mass of the matrix

m_c = mass of the composite

3.3.2.3 Volume Fraction of Fiber

Volume fraction of fiber in a composite material is volume of the fiber to volume of the composite:

$$Vf = \frac{vf}{vc} \quad \text{.....eqn. 3.3}$$

Where: V_f = volume fraction of fiber

v_f = volume of fiber

v_c = volume of composite

3.3.2.4 Mass Fraction of Fiber

$$Mf = \frac{mf}{mc} \quad \text{.....eqn. 3.4}$$

Where: Mf = mass fractions of fiber

mf = mass of fiber

mc = mass of composite

And from composite theory,

For the volume fraction

$$Vm + Vf = 1 \quad \text{..... eqn.3.5}$$

$$vc = vm + vf \quad \text{.....eqn.3.6}$$

For the mass fraction

$$Mf + Mm = 1 \quad \text{.....eqn. 3.7}$$

$$mc = mf + mm \quad \text{..... eqn. 3.8}$$

3.3.2.5 Density of composite

The density of the composite can be determined as the ratio of mass of the composite material to the volume of the composite material.

$$\rho c = \frac{mc}{vc} \quad \text{.....eqn. 3.9}$$

Where, ρc = density of the composite material

mc = mass of the composite material

vc = volume of the composite material

Since, $vc = vf + vm$ and $v = \frac{m}{\rho}$

Where: ρ = density
m = mass
v = volume

Therefore, equation 3.6 can be rewritten as,

$$\frac{mc}{\rho c} = \frac{mf}{\rho f} + \frac{mm}{\rho m} \quad \text{.....eqn.3.10}$$

To find the density of the composite multiply both sides of equation 3.6 by $\frac{1}{mc}$

$$\frac{Mc}{\rho c} \times \frac{1}{mc} = \frac{mf}{\rho f} \times \frac{1}{mc} + \frac{mm}{\rho m} \times \frac{1}{mc}$$

$$\frac{1}{\rho c} = \frac{1}{\rho f} \times \frac{mf}{mc} + \frac{1}{\rho m} \times \frac{mm}{mc}$$

Since, $\frac{mm}{mc} = Mm$ and $\frac{mf}{mc} = Mf$

Thus, $\frac{1}{\rho c} = \frac{Mf}{\rho f} + \frac{Mm}{\rho m}$ ……..eqn. 3.11

$Mf = 30\% = 0.3$

$Mm = 70\% = 0.7$

$\rho\, f\ (E - glass\ fiber) = 2.54\ \mathrm{g/cm3}$

$\rho\, m\ (epoxy) = 1.2\ g/cm3$

$\rho\, CNC = 1.6\ \mathrm{g/cm3}$

Where: $\rho_{f\ (E\text{-}glass\ fiber)}$ = Density of E-glass fiber

$\rho_{m\ (epoxy)}$ = Density of epoxy resin

ρ_{CNC} = Density of crystalline nanocellulose

3.3.2.6 Mass of composite one (without CNC)

Composite one is a control sample to compare it with the hybrid one and is formed with E-glass fiber and epoxy resin. The mass required to form the sample can be calculated as follows but prior to that density has to be determined:

From equation 3.11 density can be calculated

$$\frac{1}{\rho c} = \frac{Mf}{\rho f} + \frac{Mm}{\rho m}$$

$$\frac{0.3}{2.54} + \frac{0.7}{1.2}$$

$\rho c = 1.4\ g/cm3$

$m1 = \rho \times v$ ……eqn. 3.12

$$= 1.4\ g/cm3 \times 140 cm3$$

$$m1 = 196g$$

Therefore, the mass required for glass fiber and epoxy resin can be calculated according to the mass fraction of each:

m_{GF} =0.3×196 $m_{epoxy(Neat)}$ = 0.7×196

= 58.8g = 137.2g

3.3.2.7 Mass of composite two (with 2wt% CNC)

Prior to calculation of mass required for hybrid composite its density considering that of CNC has to be identified:

$$\frac{1}{\rho c} = \frac{Mf}{\rho f} + \frac{Mm}{\rho m} + \frac{\text{m CNC}}{\rho \text{CNC}}$$

$$= \frac{0.28}{2.54} + \frac{0.7}{1.2} + \frac{0.03}{1.6}$$

$$= 1.42$$

$\mathrm{m2} = \rho \times \mathrm{v}$ $\quad \mathrm{m}\,GF = \mathrm{M}GF \times \mathrm{m2}$ $\quad \mathrm{m\ CNC} = \mathrm{M}CNC \times \mathrm{m2}$

$= 1.42\ \mathrm{g/cm3} \times 140\ \mathrm{cm3}$ $\quad = 0.3 \times 198.8$ $\quad = 0.02 \times 198.8$

$= 198.8\mathrm{g}$ $\quad = 59.6\mathrm{g}$ $\quad = 4\mathrm{g}$

$\mathrm{m_{Epoxy}} = \mathrm{M_{Epoxy}} \times \mathrm{m_2}$

$= 0.68 \times 198.8$

$= 135.2\mathrm{g}$

3.3.2.7 Mass of composite three (with 4wt % CNC)

$\mathrm{m\ Epoxy} = \mathrm{M}Epoxy \times \mathrm{m2}$ $\quad \mathrm{m\ CNC} = \mathrm{M}CNC \times \mathrm{m2}$

$= 0.66 \times 198.8$ $\quad = 0.04 \times 198.8$

$= 131.2\mathrm{g}$ $\quad = 8g$

3.3.2.8 Mass of composite four (with 6wt% CNC)

$\mathrm{m\ Epoxy} = \mathrm{M}Epoxy \times \mathrm{m2}$ $\quad \mathrm{m_{CNC}} = \mathrm{M}_{CNC} \times \mathrm{m_2}$

$= 0.64 \times 198.8$ $\quad = 0.06 \times 198.8$

$= 127.2g$ $\quad = 11.93g$

3.3.2.9 Mass of composite five (with 8wt% CNC)

$\mathrm{m\ Epoxy} = \mathrm{M}Epoxy \times \mathrm{m2}$ $\quad \mathrm{m_{CNC}} = \mathrm{M}_{CNC} \times \mathrm{m_2}$

$= 0.62 \times 198.8$ $\quad = 0.08 \times 198.8$

$= 123.3g$ $\quad = 15.9g$

Overall weight percent and mass fraction of the sample composite materials was summarized in table 3.3.

Table 3.3 : E-glass fiber/CNC and epoxy matrix weight fraction formulation

	Weight percent of Epoxy (wt%)	Weight percent of E-glass fiber (wt%)	Weight percent of CNC (wt%)	Mass of epoxy (gram)	Mass of E-glass fiber (gram)	Mass of CNC (gram)
Neat	70	30	0	137.2	58.8	0
Composite 1	68	30	2	135.2	59.6	4
Composite 2	66	30	4	131.2	59.6	8
Composite 3	64	30	6	127.2	59.6	11.9
Composite 4	62	30	8	123.3	59.6	15.9
TOTAL				654.1	297.2	39.8

3.4 Fabrication of hybrid E-glass/CNC epoxy composite

Hand layup fabrication technique was used as it can be easily applied and is the simplest as compared with other fabrication techniques. prior to fabrication materials required for the procedure should be prepared as shown in Figure 3.11.

Figure 3.11 Materials required to fabricate sample composites

Thus, the fabrication process begins by preparing a plastic sheet into size which can cover the mold which will ease the extraction of composite. Then, release agent was applied on the plastic sheet as shown in Figure 3.12 (a). The bottom part of mold cavity was cleaned to get smooth surface finish and the plastic sheet was placed gently.

Then E-glass fiber was prepared into size of the mold which is 25cm ×14cm and weighted for each sample composites according to the calculated weight ratio. For the four sample composites with varying wt % of CNC two steps were followed to add and mix CNC. The hardener was used as a dispersion medium because of its low viscosity compared to that of epoxy. A measured amount of CNC power was added and stirred in to appropriate amount of hardener and then sonicated to keep uniform dispersion for 7-18 minutes depending on the dispersion rate of CNC, this was detected by visualization of the mixture [74].

Epoxy-hardener was mixed with 10:1 ratio according to the supplier and measured for each sample as shown in Figure 3.12 (b). Thus, a portion of measured epoxy resin was poured on the mold basement and using a roller it was spread on the required surface and then a layer of E-glass fiber was applied then with the help of a roller the glass fiber was impregnated with epoxy resin as illustrated in Figure 3.12 (c), (d) and (e), this process continues until the whole mass of glass fiber was embedded. Having completed laying up the top cover plastic sheet with a releasing agent of

honey wax was applied as a top cover for a better surface finish and ease of detachment. Finally, as shown in Figure 3.12 (f) the top cover of the mold with a cylindrical mass of 7.2 kg was applied for ease of extraction of the composite from the mold. For compression and curing the composite was placed under hydraulic pressing machine applying a pressure of 4.5Mpa for 24 hours as illustrated in Figure 3.12 (g) [75]. This made the composite fabricated to have uniform load distribution and excess epoxy get removed while uniform thickness was kept on top of that uniform impregnation of fibers with the epoxy resin was achieved. Figure 3.14 shows a final product of the composite materials.

(a) Applying wax on plastic sheet

(b) Epoxy-hardener mixing

(c) placing E-glass fiber

(d) Applying epoxy resin

(e) impregnating epoxy resin with roller

(f) Applying mold cover

(g) Compression under pressing machine

Figure 3.12 Fabrication process of composite

Thus, similar procedures were followed to fabricate the whole sample with different crystalline nanocellulose weight percentage that is 2wt%, 4wt%, 6wt%, and 8wt%. The amount of CNC added

is given in table 2, in this study the maximum amount of CNC to be added in the epoxy resin was taken to be 8wt%. The reason for this stated maximum amount of CNC is that agglomeration could be problem if the volume was taken beyond this value, due to the nature of CNC bonding to its neighboring CNC particle. Thus, more dispersion techniques might be required to reduce agglomeration that would in turn cause stress concentration. The addition of CNC to the resin was performed with simple mechanical stirring of the CNC powder added into the hardener. Adding to the epoxy directly might cause uneven distribution and agglomeration of CNC particles since epoxy resin is highly viscous. Therefore, after stirring the measured amount of CNC powder in the hardener, it was sonicated on ultra sonicator for 3 minutes to keep uniform particle dispersion of CNC as shown in Figure 3.13. Finally, the hardener-CNC powder mixture will be mixed gently with epoxy resin ensuring that air bubbles are not formed.

Figure 3.13 Mixing of CNC with a hardener on a sonicator

Figure 3.14 Hybrid E-glass fiber / CNC composite final product

3.5 Specimen preparation for testing

According to American Society for Testing Materials (ASTM) specification the specimens for each testing samples that is tensile, flexural, hardness, water absorption and morphology were prepared as shown in Table 3.4. A hand jig saw of model JS6508 from a company of INGCO tools with a cutting sped of 800-2800 mm/min and blade length of 100mm was utilized as show in figure 3.15.

Figure 3.15 Cutting specimens into size with a jig saw

Table 3.4 Experimental test standards

Test	Standard	Specimen dimension (mm)
Tensile test	ASTM D 3039	250 × 25 × 3
Compression test	ASTM D 3410	80 × 20 × 3
Flexural test	ASTM D790	125× 13 × 3
Impact test	ASTM D265	64 ×13× 3

Water absorption	ASTM D570	25 × 25 × 3
Density	ASTM D792	50×20×3
Thermographic analysis	For decomposition kinetics, ASTM E164	-

3.6 Experimental testing procedures and conditions

The hybrid composite specimens being prepared according to the standards, then various tests were performed with different testing procedures with respect to test types. Mechanical and physical tests were performed at different laboratories, Tensile and flexural strength were conducted at Bishoftu Defense Engineering College, Ethiopia where a testing machine with a maximum capacity of 50KN as shown in Figure 3.16 was used. Hardness was conducted at Adama Science and Technology University. Three specimens were tested for each of mechanical and physical tests with different CNC composition at room temperature.

Figure 3.16 Gunt Hamburg WP 310 hydraulic material testing machine

3.6.1 Flexural Testing:

Three-point bending according to ASTM D790 was executed to perform flexural strength test, thus specimens with a size 125mm× 13mm ×3mm was placed on 125mm span on two-point support bed as shown in Figure 3.17. After setting up the specimen a vertical one-point jaw exerts load at

the middle of the specimen at a speed of 6mm/min under room temperature until the specimen fractured at maximum applied load as illustrated in Figure 3.18.

Figure 3.17 Flexural strength test specimens

Figure 3.18 Flexural strength test set up

Figure 3.19 Fractured flexural strength testing specimens

3.6.2 Tensile Strength Test

Specimens were prepared according to ASTM D 3039 as shown in Figure 3.20 and placed into the UTM jaws with vertical orientation as shown in Figure 3.21 (a) so as the movable upper jaw applied the given load and the lower being kept fixed, thus at maximum loading the specimen fractures as illustrated in Figure 3.21 (b). The testing machine have a speed of 6mm/min and the test was conducted at room temperature.

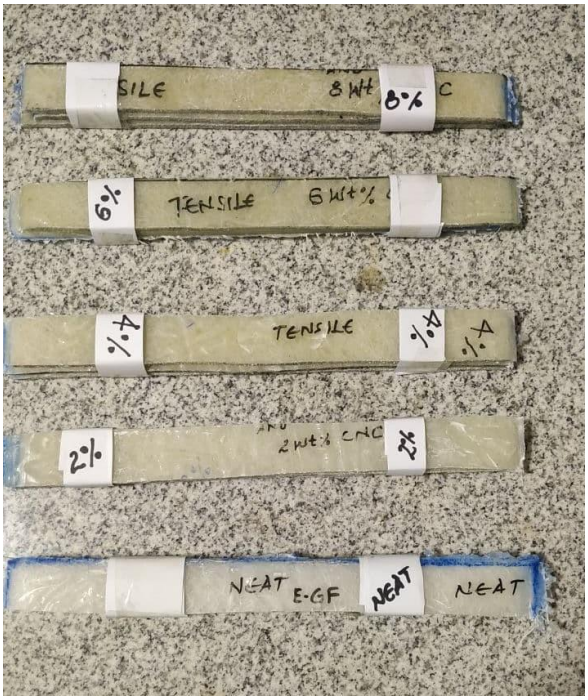

Figure 3.20 Tensile test specimens


(a)

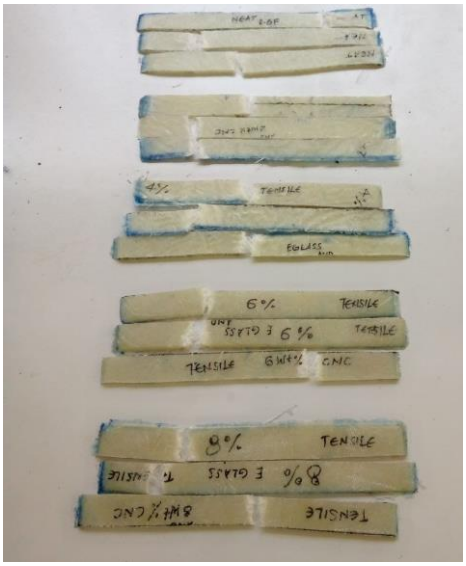
(b)

Figure 3.21 Tensile test set up (a) deformed specimen (b) Fractured specimens of tensile test (b)

3.6.3 Compression Strength

As shown in Figure 3.22 for compression test specimens were prepared as per ASTM D 3410 and placed in between the upper and lower jaws of the UTM then an axial compressive load was applied as illustrated in Figure 3.23. The compression load just before fracture as shown in Figure 3.24 was recorded as the ultimate compression load of the composite material.

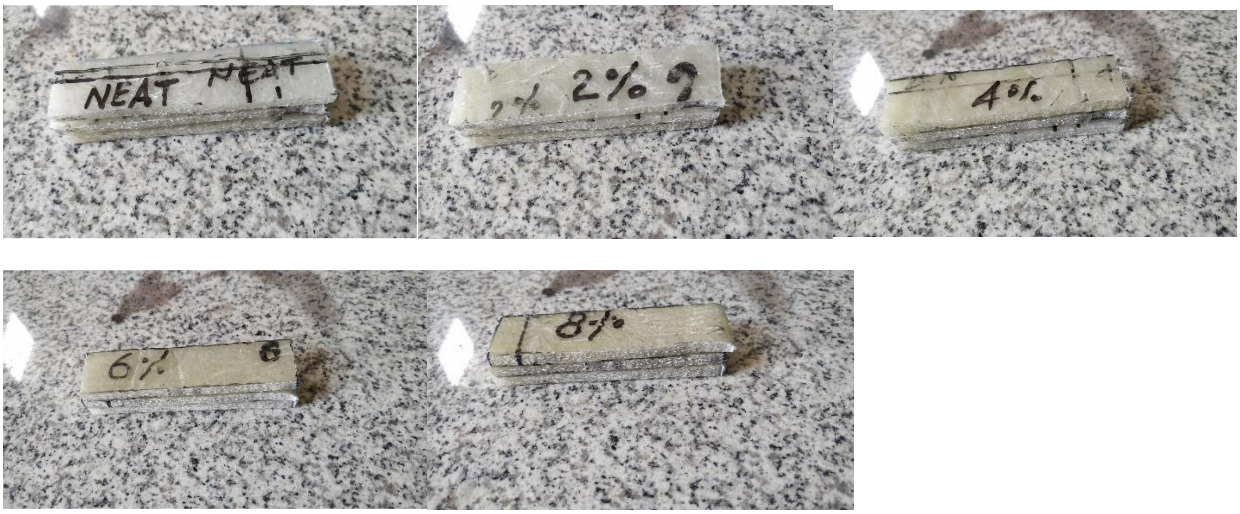

Figure 3.22 Compression test specimens

Figure 3.23 Compression test setup

Figure 3.24 Compression test specimen at fracture

3.6.4 Impact Strength Test

Charpy impact was utilized to perform the impact strength (fracture toughness) test of the neat specimen and the other four specimens with different wt% CNC. As shown in Figure 3.25 the specimens were prepared as per ASTM D265 and set to be clamped into a bed of the tester (specimen holder). The specimen holders have two nodes at the ending of both sides, so as to be able to support the specimen two edges while the load is released. The load was applied through a pendulum at 45^{o}. The dial indicator attached to the pendulum can display the amount of energy absorbed by the specimen until the specimen fractures as shown in Figure 3. 26. A fractured specimens are shown in Figure 3.27.

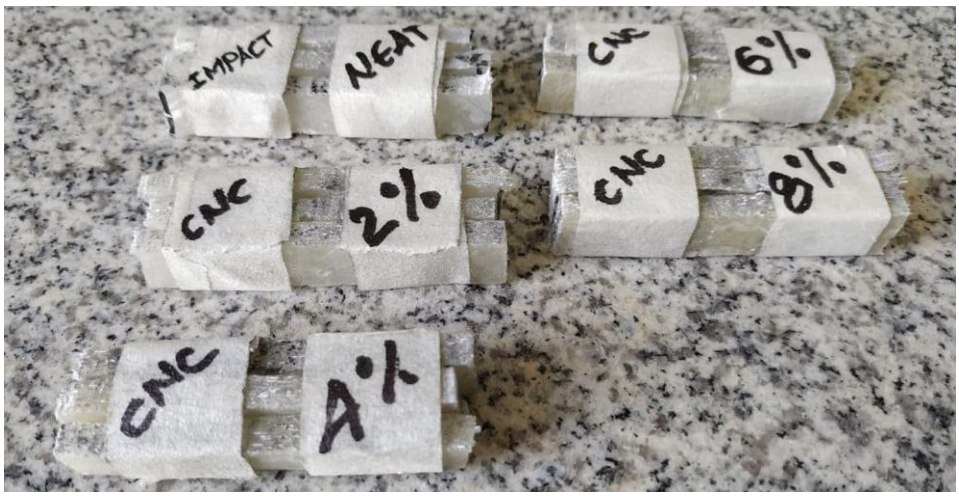

Figure 3.25 Impact test specimen

Figure 3.26 Impact test setup

Figure 3.27 Fractured specimens of impact test

3.6.5 Water Absorption Test

Water absorption was conducted as per ASTM D570 by making specimens into size as shown in Figure 3.28 and weighing the specimens prior to immersing into water and the values were registered. The specimens were then kept in water for 24 hours at room temperature as shown in Figure 3.29, then were removed and excess water was cleaned from the specimen's surface to get the actual weight of water absorbed. After cleaning the surface, the specimens were weighed with

electronic balance then finally the weight gained or the water absorbed can be identified from the weight difference as follows:

$$water\ asorption\ \% = \frac{Final\ weight - Initial\ weight}{Initial\ weight} \times 100 \quad \text{..... eqn 3.13}$$

Where:

Initial weight: The weight prior to immersion of the specimens

Final weight: weight measured after immersing the specimens for 24 hours

Figure 3.28 Water absorption test specimens

Figure 3.29 Specimens soaked in water under water absorption test

3.6.6 Density measurement

Archimedes principle was employed to measure the density of the composite materials that employ the buoyancy measurement technique. Where Archimedes' principle stated that "a body immersed partially or fully in fluid experiences a buoyant force acting upwards on it. The magnitude of this force is equivalent to the weight of the fluid displaced by the body." Thus, all composite samples were prepared in size according to ASTM D792 and weighted in air m_{air}, on an electronic balance pan and in water m_{water} as shown in Figure 3.30, then density of the composite material can be calculated as follows:

$$\rho c = \frac{\text{mair}}{\text{mair}-\text{mwate}} \times (\rho w - \rho a) + \rho a \quad \text{.....eqn 3.14}$$

Where:

ρc: Density of the composite material

ρw: Density of water

ρa: Density of air

$m_{air::}$ Mass in air

m_{water}: Mass in water

Specimens were first weighted on the pan of electronic balance, then specimens were tied with a tiny rope with negligible weight to measure the weight of the sample in air and water using the same electronic balance.

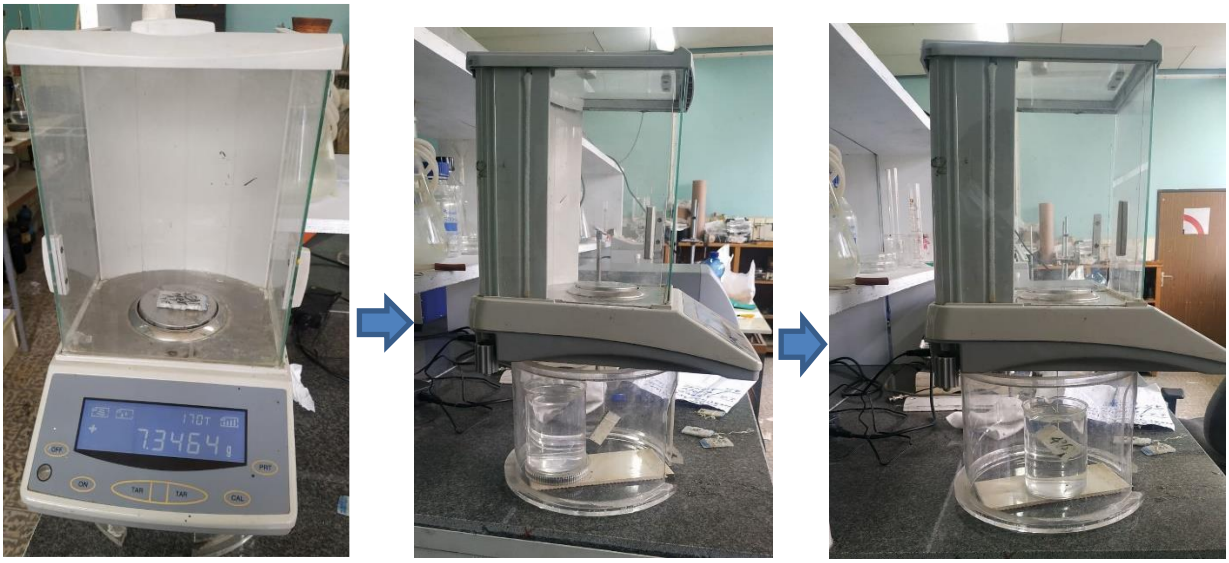

Figure 3.30 Archimedes' density measurement procedure

Void content

The void content of the hybrid and neat composite was calculated using the experimental and theoretical densities according to Equation 3.15 following ASTM-D-2734-94. Theoretical density of the composite materials was calculated based on the density and weight fraction of each constituent and fillers.

$$void\ content = \frac{\rho theory - \rho exp}{\rho theory} \times 100\% \quad \text{.....eqn 3.15}$$

Where:

ρ_{theory} = Theoretical density of the composite material

ρ_{exp} = Experimental density of the composite material

3.6.7 Thermo gravimetric analysis (TGA)

Thermal analysis was performed to study how stable the crystalline nanocellulose and the composite material with CNC as a constituent is under various temperature ranges. Thermal gravimetric analysis determines the change in temperature decomposition of CNC powder and its

composite material. TGA in particular measures the weight of a sample specimen as a function of time. A sample of 40.272 mg powder of CNC was prepared and conducted with heating range of 10^{o}C per minute from room temperature to 700^{o}C. STA 409 PC Luxx Simultaneous thermal analyzer was used to analyze the thermal property of CNC.

3.6.8 Surface morphology analysis

Surface morphology or texture of the crystalline nanocellulose, the particle's dispersion and tendency of agglomeration was investigated and determined using scanning electron microscope (SEM). The surface morphology test was performed on field emission scanning electron microscope 6500F (FESEM), JOEL 6500F at National Taiwan University of Science and Technology (NTUST). For both tests that is CNC and the composite materials, before observation, the samples were sputter-coated with platinum to prevent charging. SEM images are used to demonstrate details such as the degree of adhesion between the fiber and the resin, internal failures, interfacial bonding, voids, and fiber pullout.

Energy-dispersive X-ray spectroscopy (EDX) is a method used for identifying the chemical elements present in a sample. Both quantitative and qualitative data of a chemical element in a sample ca be determined. The peak heights in the EDX analysis show the quantity of elements while the peak positions of the chemical elements in the sample shows the position of chemical elements.

3.6.9 Particle size determination

XRD patterns provide information on the particle size and defects, while the peak relative intensities provide insight into the atomic distribution in the unit cell. XRD analysis, by way of the study of the crystal structure, is used to identify the crystalline phases present in a material and thereby reveal chemical composition information.

Crystalline materials are characterized by the long-range orderly periodic arrangements of atoms or structure. The crystal structure describes the atomic arrangement of a material and the atom types and positions determine the diffraction peak intensities.

A measurement condition at a current of 30mA and 40 kV was employed by the x-ray diffractometer machine with a model XRD-7000 x-ray diffractometer, Shimadzu Corporation,

Japan at Adama Science and Technology University (ASTU). The scattering angles (2θ) were taken in the range of intensity 5^o to 90^o and with a speed of 10^o /minute. Crystal size was determined by Scherrer equation and with the data obtained from the XRD analysis [76].

$$L = \frac{K\lambda}{\beta.cos\theta} \quad \text{.....eqn 3.15}$$

Where:

λ (nm): wavelength

K: Shape factor (can be 0.62 - 2.08 and is usually taken as about 0.89)

β: Full width at half maximum of peaks in radian located at any 2θ in the pattern

X'pert highscore plus software was used to analyzes the raw data obtained from XRD analysis and determine almost all the information that is required about the size of CNC. Full width at half maximum of peaks in radian located at any 2θ in the pattern (β), 2 theta values and high crystallinity peaks at 2θ can also be determined.

Crystalline index and crystalline size of sample composites is determined with x-ray diffraction analysis. Sample composites with 0 wt% and 8 wt% CNC are determined using XRD -7000 X-ray diffractometer with settings of 30 mA of current, temperature of 25°C. The signals were recorded for 2θ in the range of 10° to 90°. The monochromatic radiation source used for the analysis is Cu Kα with a wavelength of 0.514 nm. The percentage of the crystallinity index and crystallinity index (CI) of the fabricated samples are calculated with equations 3.16 and 3.17.

$$\mathrm{CI} = (1 - \frac{I_{am}}{I_{200}}) \times 100 \quad \text{eqn3.16}$$

$$\%\ \text{of}\ \mathrm{CI} = (\frac{I_{(200)}}{I_{(200)} - I_{am}}) \times 100 \quad \text{eqn3.17}$$

$$L = \frac{K\lambda}{\beta.cos\theta} \quad \text{eqn3.18}$$

Where:

λ (nm): 0.1541 nm is the wavelength of the radiation

K: Shape factor (Sherrer's constant) (can be 0.62 - 2.08 and is usually taken as 0.89)

β: Full width at half maximum of peaks in radian located at any 2θ in the pattern

θ: is the Bragg angle.

CI: Crystallinity index

$I_{200:}$ Crystallinity Index at crystalline region

$I_{am:}$ Crystallinity Index at amorphous region

2.6.10 Fourier transform infrared spectroscopy

Various functional groups, bonds, structures and stretching of bonds within the fabricated composite samples were determined using Fourier transform infrared spectroscopy (FTIR). The analysis is conducted on all sample composites with 0, 2, 4, 6, and 8wt % CNC. The spectrum is recorded with wavenumbers stretching from 4000 to 400cm^{-1} with a resolution of 4cm^{-1}.

CHAPTER FOUR

4 RESULTS AND DISCUSSION

4.1 Introduction

A section of the previous chapter discussed the mechanical and physical testing procedure of the extracted CNC, fabricated control sample and hybrid GF and CNC reinforced epoxy resin composites. For every testing three specimen trials were employed, thus the testing result have been discussed as follows in this section.

4.1.1 Surface morphology result

Figure 4.1 shows SEM image of the extracted CNC with different magnification. The image obtained from the scanning electron microscope (SEM) analysis shown that the crystalline nanocellulose particles are highly ordered and are in a position that lower state of agglomeration. [77].

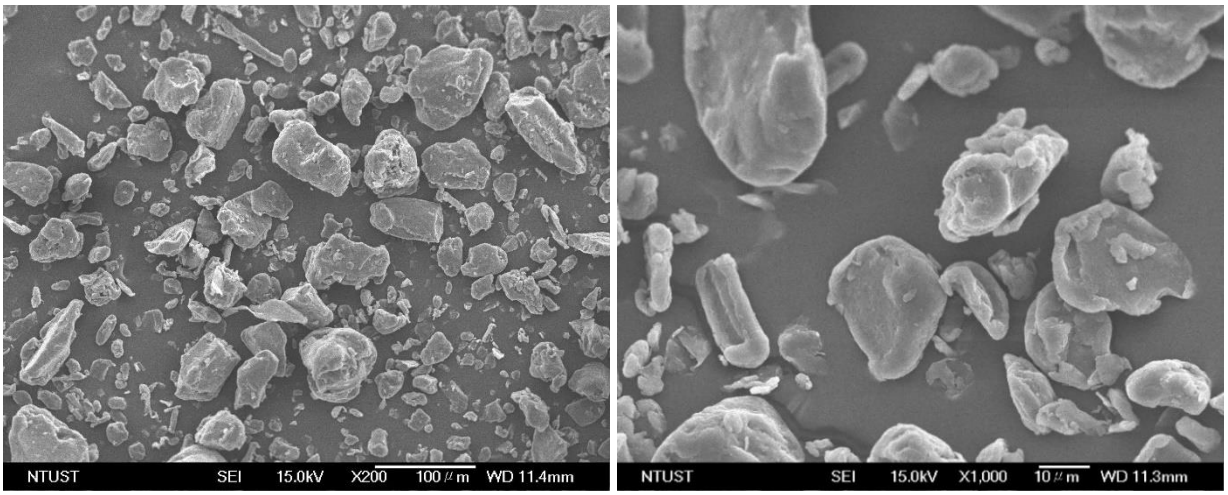

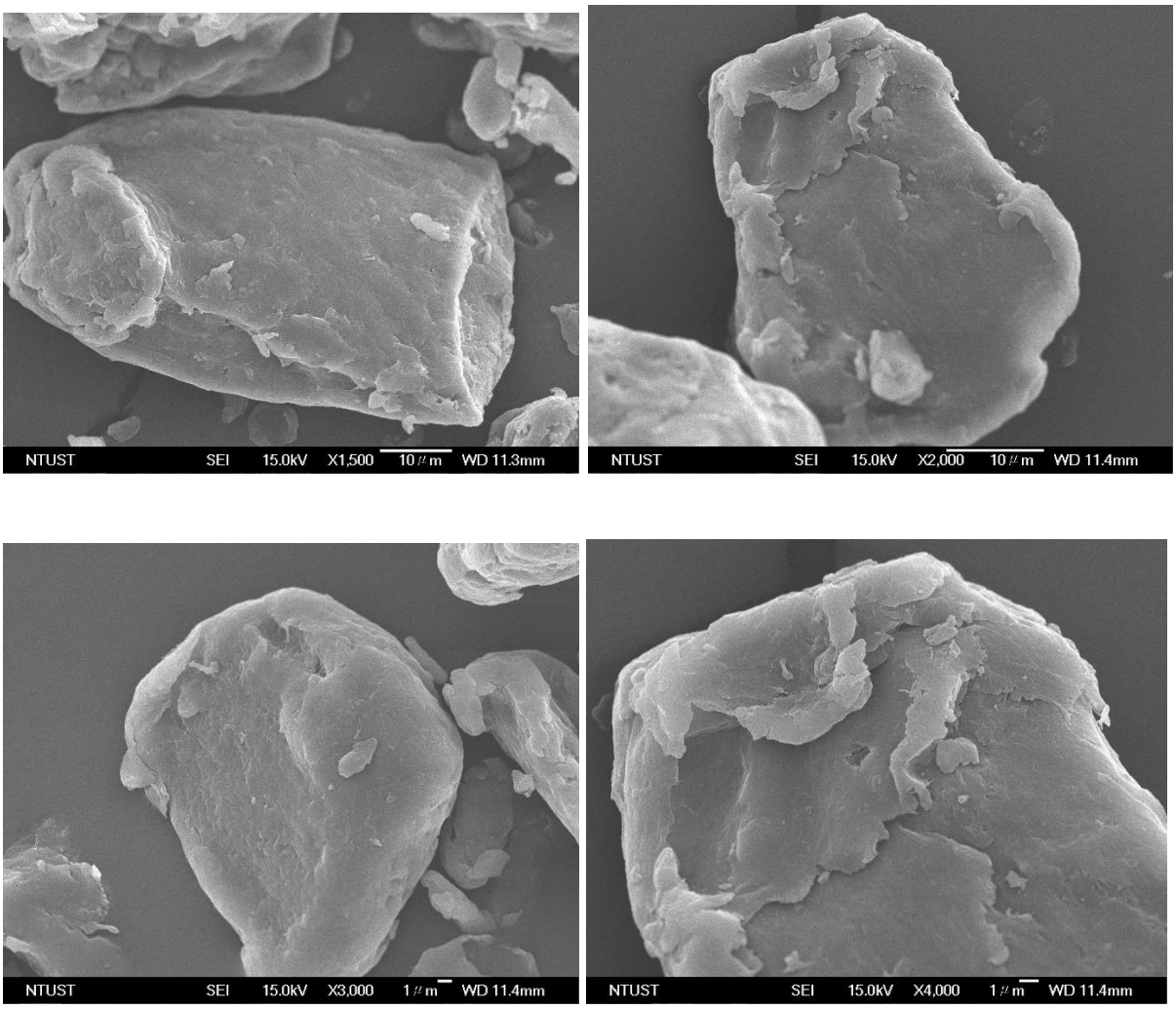

Figure 4.1 SEM image of crystalline nanocellulose with different magnification

4.1.2 Surface morphology discussion

The nanoparticles' deagglomeration is critical because it will enhance uniform dispersion while employing the particles as a reinforcement in the composite material. It was observed that the CNC has a particulate form, with approximately similar particle size. There was found crystal bundles of uniform nano dimension, as shown in the SEM image. The smooth surface observed can improve interfacial bonding of CNC particles with the matrix material of the composite material [77].

4.1.3 Energy dispersive x-ray spectroscopy (EDX)

FE-SEM is attached with energy dispersive x-ray diffraction (EDX) and it was used for elemental analysis of CNC.

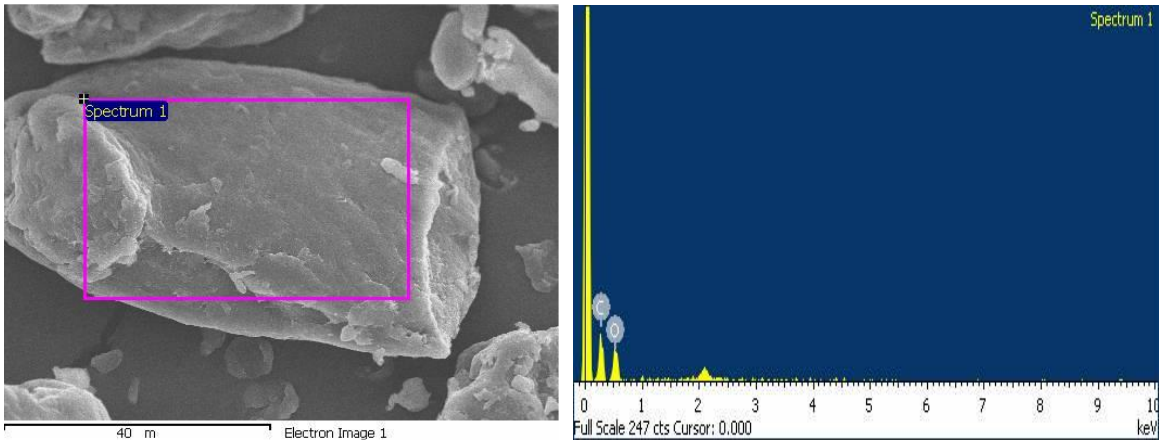

Figure 4.2 Energy dispersive x-ray (EDX) diffraction for elemental analysis of CNC

4.1.4 Energy dispersive x-ray spectroscopy (EDX)

Figure 4.2 shows the peaks obtained from the EDX spectrum analysis shows that the percentage of impurities is almost zero with carbon and oxygen having atomic percentage 77.01% and 22.99% respectively. Impurities like Sulphur from the acid hydrolysis, sodium which was employed for alkali treatment and other chemicals which was utilized for treatment of cellulose was not found on the surface of CNC. Thus, as shown in table 4.1 Oxygen and carbon are the two elements found at the end of the extraction. This is due to the interventions which involved frequent washing of the pulp with distilled water in between every treatment stage of cellulose.

Table 4.1 Elemental content and its weight percentage of CNC

Element	Weight	Atomic%
Carbon	71.55	77.01
Oxygen	28.45	22.99
Total	100	

4.1.5 X-ray diffractometry (XRD)

The XRD graph of CNC shown in Figure 4.3 is the result showing the crystallinity of the extracted nanocellulose. At 2θ values of 19.89, 44.04, 64.344 and 77.51 degrees, the crystalline section of CNC revealed three different peaks. [78].

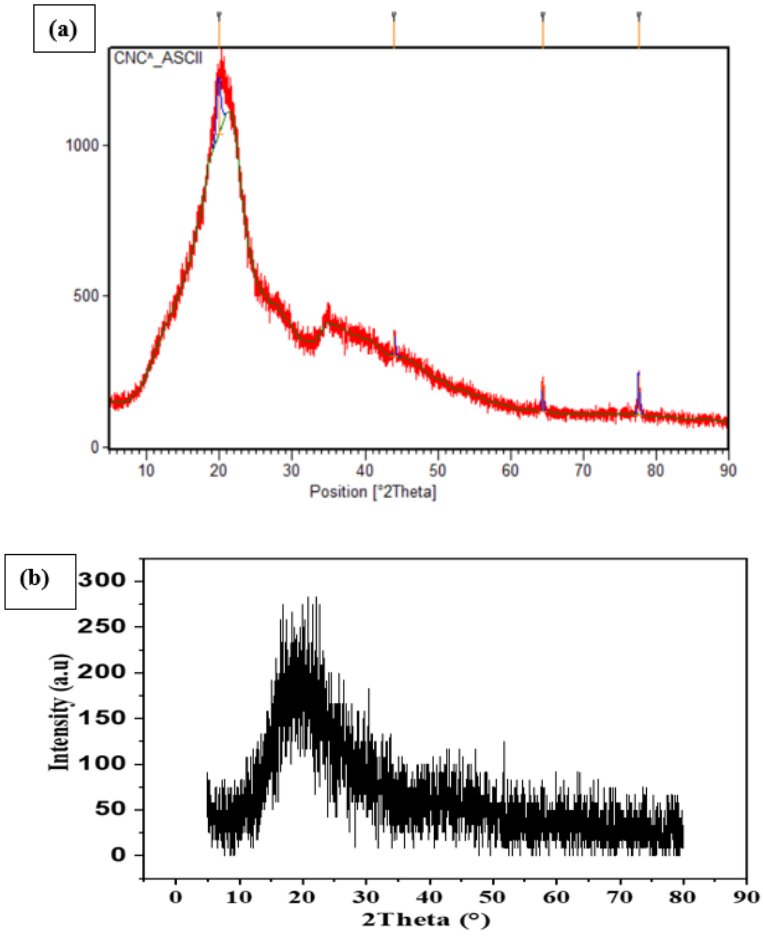

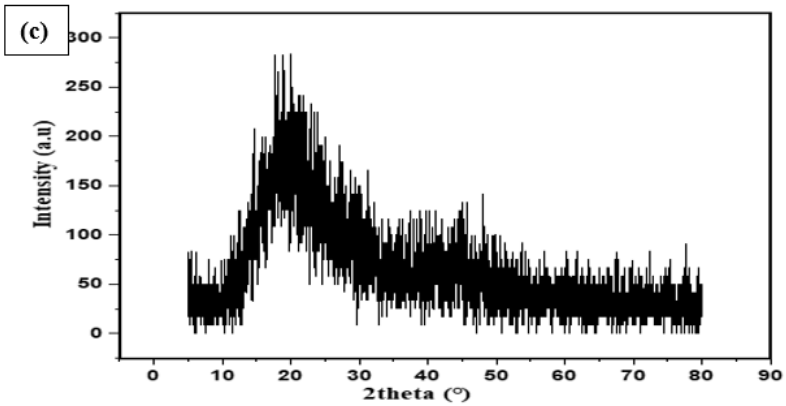

Figure 4.3 XRD image of (a) CNC powder (b) E-glass fiber epoxy composite (c) Hybrid E-glass fiber/CNC epoxy composite

Figure 4.3 (a) shows how peaks of cellulose varies at different particle size with x-ray diffractometer results represented by 2theta vs intensity graph. From the figure it is shown that peak of CNC is sharper than that of pulped and MCC.

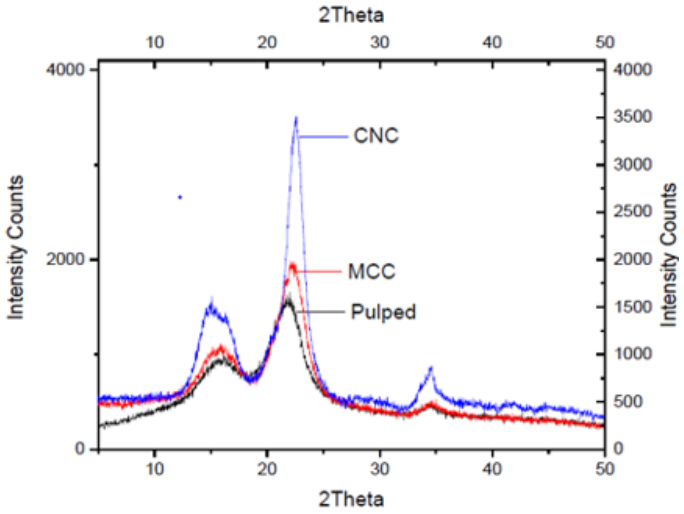

Figure 4.4 The combined XRD difractograms of CNC, MCC and pulped bagasse [79]

4.1.6 X-ray diffractometry (XRD) discussion

The peak values at 2 theta that is 19.89, 44.04, 64.344 and 77.51 degrees can tell us a detail information about the crystallinity that is the crystalline zone is represented by the high peaks, while the amorphous region is represented by the low peaks as indicated in figure 4.3[78].

Table 4.2 shows the particle size of CNC which is calculated with Scherrer's equation with the data obtained from X'pert highscore plus software [76]. Scherrer's equation can be employed only

for crystallite sizes of 200 nm and less. The calculated crystalline size is in angstrum so dividing the values by 10 the particle size was obtained in nanometer, thus for each four peak values 13nm, 37.6nm, 85.3nm and 55.4nm are the sizes of the CNC particle.

Table 4.2 Particle size of CNC determined with x'pert highscore plus

No	2 Theta	Crystalline size [Å]
1	19.898	130
2	44.04	376
3	64.344	853
4	77.51	554

The effect of CNC on glass fiber epoxy composite was also conducted using XRD analysis. A broad and noisy peak are observed since glass fiber and epoxy resin are amorphous in nature. The broad peaks are due to the broad matrix of the glass and the oscillations are an indication of noise. Crystalline structure is spotted but superimposed by the amorphous structure of glass fiber. The percentage of crystallinity, crystallinity index, and crystal sizes of the fabricated composite samples were calculated using Equations 3.16, 3.17, and 3.18 and the values are given in Table 4.3. Figure 4.4 (b) shows XRD analysis of a sample composite with 0wt % CNC. The figure represents a peak superimposed in the amorphous region of glass fiber at 20°. Figure 4.4 (c) shows the XRD analysis of a hybrid glass fiber/CNC epoxy composite. From the figure a slight indication of the presence of CNC was observed. In addition, a couple of superimposed peaks are observed at $2\theta = 20°$ and 44°.

Table 4.3 XRD analysis of fabricated composite samples

Samples	**Crystallinity index**	**Percentage of crystallinity**	**Crystallite size (nm)**
0 wt% CNC	0.17	22.1	2.01
8 wt% CNC	0.24	33.37	2.41

4.1.7 Water absorption

Table 4.3 shows the percentage of water absorption of each composite materials which was kept in water for 24 hours. The control sample without the addition of CNC didn't absorb water at all, composite 3 with 4wt% CNC is the least water absorbent, composite 5 with 8wt% CNC is the second least water absorbent. While composite 4 with 6wt% CNC is the highest water absorbent of all in comparison and that of composite 2 with 2wt% CNC the second highest water absorbent.

Table 4.3 Water Absorption percentage of all composites

	Composition of Composite	Sample	Water Absorption (%)
1	GF and Epoxy resin	1	0
		2	0
		3	0
		Average	**0**
2	GF, Epoxy resin and 2wt% CNC	1	0.46
		2	1
		3	0.46
		Average	**0.64**
3	GF, Epoxy resin and 4wt% CNC	1	0.24
		2	0.48
		3	0.73
		Average	**0.483**
4	GF, Epoxy resin and 6wt% CNC	1	1.24
		2	0.58
		3	0.9
		Average	**0.91**
5	GF, Epoxy resin and 8wt% CNC	1	0.52
		2	0.73
		3	0.24
		Average	**0.5**

4.1.8 Water absorption discussion

Cellulose is hydrophilic and tend to strongly interact with water that is water molecules interact easily with cellulose chains. This is because the surface of CNC has OH groups which make it easy to form hydrogen bond if there is no crosslinking formation with other nearby OH group. Thus, the increase in water absorption with increasing wt% of CNC is due to cellulose cavities having free water and water bonding at the amorphous region [80]. On the other hand, those of glass fiber and epoxy resin are hydrophobic, the result also shown this property of the composite materials fabricated. C1 that is a composite with no CNC have shown water absorption percentage of 0%. The highest water absorption was observed on C4 which is Glass fiber with 6 wt% of CNC having water absorption percentage of 0.91 and the second highest was C2 which is Glass fiber with 2wt % CNC and epoxy resin having water absorption percentage of 0.64.

The least water absorbent composite was **C3** which is a composite with Glass fiber, 4 wt % CNC and epoxy resin having water absorption percentage of 0.483. The composite with the second lowest water absorption percentage is C5 a composite with Glass fiber 8% CNC and epoxy resin having water absorption percentage of 0.5. Thus, the least water absorbent composite of the overall materials fabricated is composite 3 with 4wt % of CNC.

4.1.9 Surface morphology result of 8 wt% E-glass/ CNC epoxy composite.

Morphological examinations were carried out to study the effect on interfacial interactions and rate of dispersion of CNC on the neat and hybrid composites as illustrated in Figure 4. The dispersion of CNC particles as spotted with yellow arrows in Figure 5 (b) revealed homogenous dispersion of the particles and stronger interfacial interaction between the glass fiber and epoxy resin which will contribute for enhancement of tensile strength. Since flexural strength is particularly more sensitive to the fiber-matrix interface, addition of CNC particles results in a significant improvement over tensile strength. This occurs when CNCs are uniformly distributed in the fiber-matrix interfacial region. The "crack-tip bridging" effect makes it easier to redistribute the stresses around the surface cracks, which delays the crack propagation during loading.

The fiber pull-out on Figure 5 (c) was evident, which is characterized by a hole and a smooth fiber surface. This suggested that the glassfiber and epoxy matrix had weak interfacial adhesion. On the other hand, for the hybrid glassfiber/ 2wt % and 4wt % CNC epoxy samples, a small fragment of

fractured epoxy was examined on the glass fiber surface indicatinga slight increase in the interfacial adhesion between glass fibers and epoxy/CNC blednded matrix as indicated in Figure 5 (d) and (e). Contrarily as shown in Figure 5 (f), the failure surface for the hybride composite containing 6wt% CNC revealed a thin layer of tightly bonded epoxy covering a portion of the fiber surface. A small layer of epoxy that adhered closely to a section of the fiber surface on the failure surface was an indication of improved interfacial adhesion between the epoxy matrix, CNC, and glass fibers. The hydroxyl (–OH), carboxyl (–COO-), and –C-O-C groups of CNCs adhering to the glass fiber surface interacted tightly with the epoxide groups of the epoxy through the formation of hydrogen and covalent bonds, improving the wettability between the glass fibers and the epoxy/CNC resin. The FT-IR spectra, as previously described, revealed the chemical interactions via hydrogen bonding between the carboxyl/or hydroxyl groups of the CNCs and epoxy resin. This interaction causes a progressive change in the modulus along the interface, ensuring more efficient stress transmission and improving the mechanical properties. The local strengthening of the matrix around the fiber is a result of this interaction.

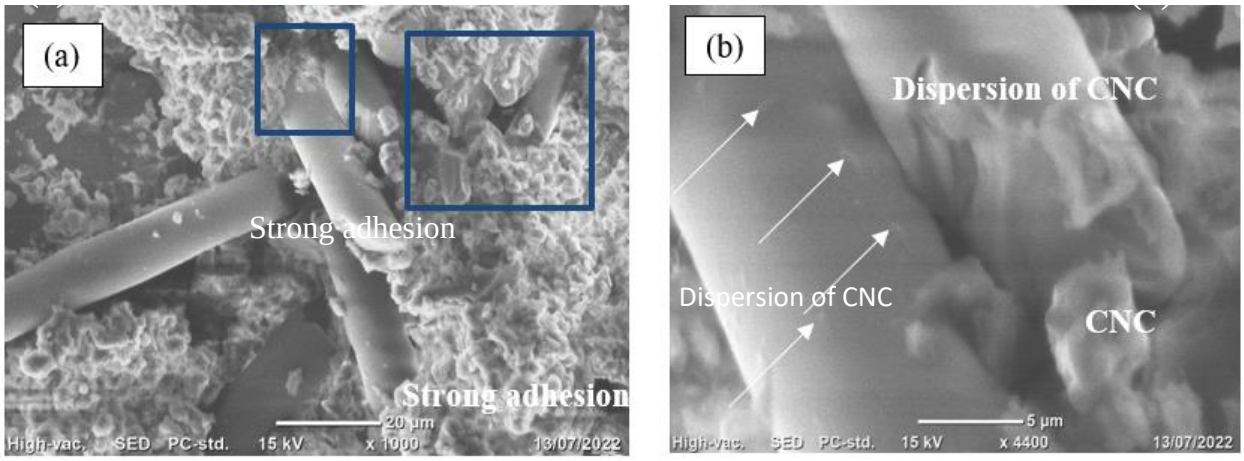

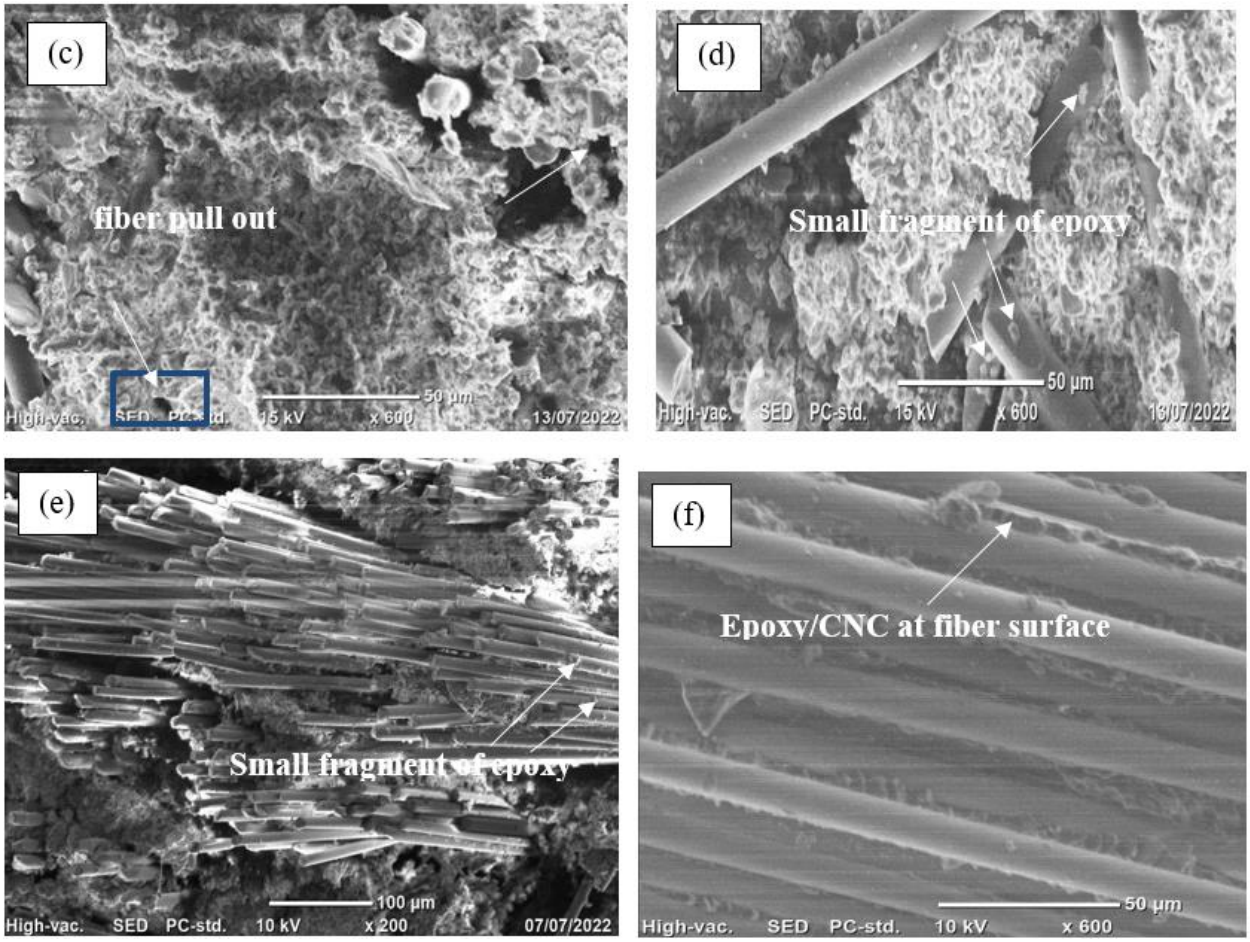

Figure 4.5 SEM images of neat and hybrid E-glass fiber-CNC-epoxy composite a) 8wt% CNC b) Dispersion of CNC particles c) 0wt% CNC d) 2wt% CNC e) 4wt% CNC f) 6wt% CNC

4.1.10 Surface morphology of 8 wt% E-glass/ CNC epoxy composite discussion

Figure 4.5 (b) revealed the dispersion of CNC particles as spotted with white arrows and stronger interfacial interaction between the glass fiber and epoxy resin. The faster diffusion of CNC particles in the hardener eases the particle's distribution in the viscous epoxy resin. The ultrasonication process also played a vital role for the dispersion on the particles in the composite material Figure 4.5 (b) shows the dispersion [81]. As described in section 4.1.2 of this study improvements in mechanical properties were achieved. Tensile strength improvement was due to better interfacial interaction between glass fibers and matrix which was attained by the addition of CNC that act as a nanofiller. The better interfacial adhesion will let better load transfer in between the fiber and matrix material enabling the composite material to bear more load [82]. The modulus of epoxy resin was enhanced with the addition of CNC that further resulted in tensile modulus of

the composite material. CNC particles contribute to the stiffening of the local interface of glass fiber and epoxy resin that can also contribute to the increase in modulus [83].

As many studies indicated addition of nanofillers like CNC showed more significant improvements in flexural strength than tensile strength. Flexural strength is particularly sensitive to the fiber/matrix interface, even though tensile and flexural performances depend on the intrinsic stiffness/modulus of individual parts [82]. The separation of individual CNCs within the epoxy coating the fiber surface, which provides an interface strengthening mechanism by bridging/suppressing the surface microcracks, is how high flexural strength is achieved in CNC/GFRP composites. When CNCs are uniformly distributed in the interfacial regions, the "crack-tip bridging" effect makes it easier to redistribute the stresses around the surface cracks, which delays the crack opening [84].

Aggregation of nanoparticles in the matrix or interfacial area causes stress concentration, which lowers the strength of the interface. Uniform dispersion of nanofillers has been observed to be extremely important for interfacial strength [85]. Hydroxyl groups on the surface of CNC interact with glass fiber forming hydrogen bonding then opening epoxy epoxide ring to form covalent bonding. The chemical bonding contributes for another additional interaction resulting in better interlaminar adhesion [86].

4.1.11 Thermal stability analysis

As shown in figure 4.6 thermogravimetric analysis of the CNC powder exhibited three phase decomposition at different temperature range.

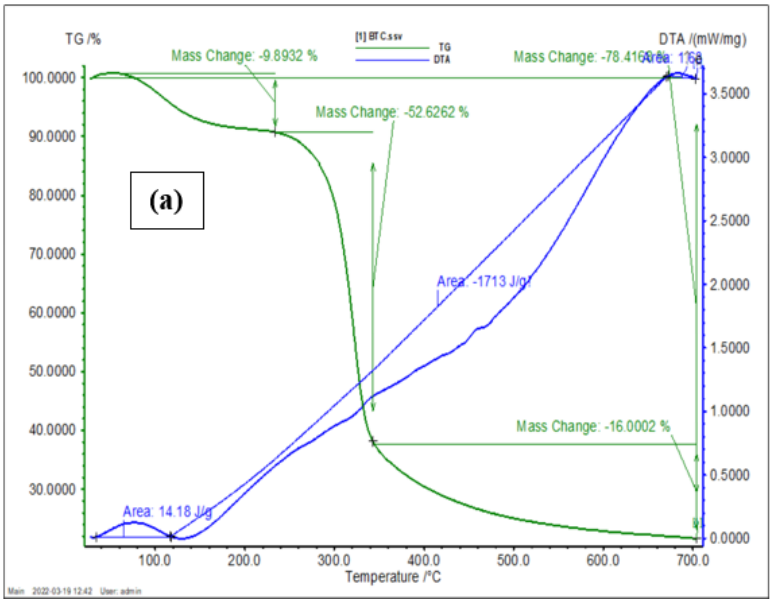
TG /%
DTA /(mW/mg)
[1] BTC.ssv
TG
DTA
Mass Change: -9.8932 %
Mass Change: -52.6262 %
Mass Change: -78.4168 %
Area: 1758
(a)
Area: -1713 J/g
Mass Change: -16.0002 %
Area: 14.18 J/g
Temperature /°C

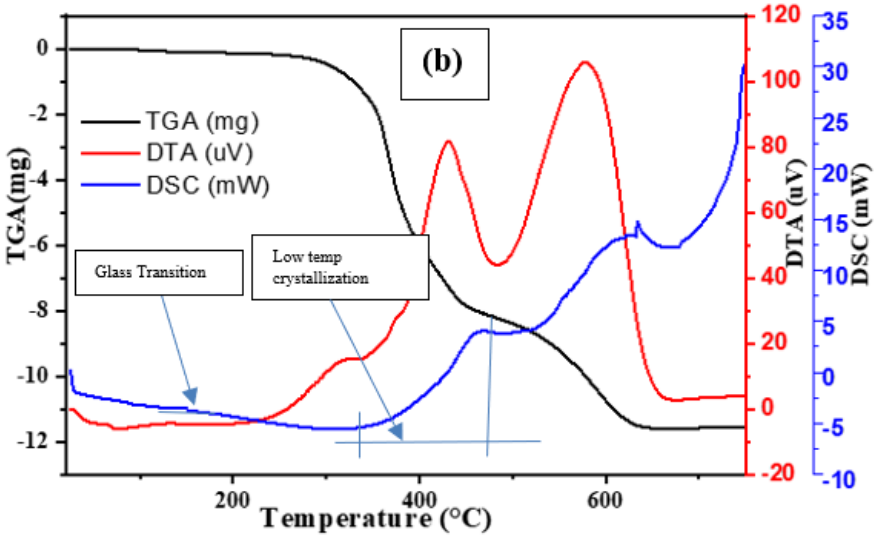
(b)
TGA (mg)
DTA (uV)
DSC (mW)
TGA(mg)
DTA (uV)
DSC (mW)
Glass Transition
Low temp crystallization
Temperature (°C)

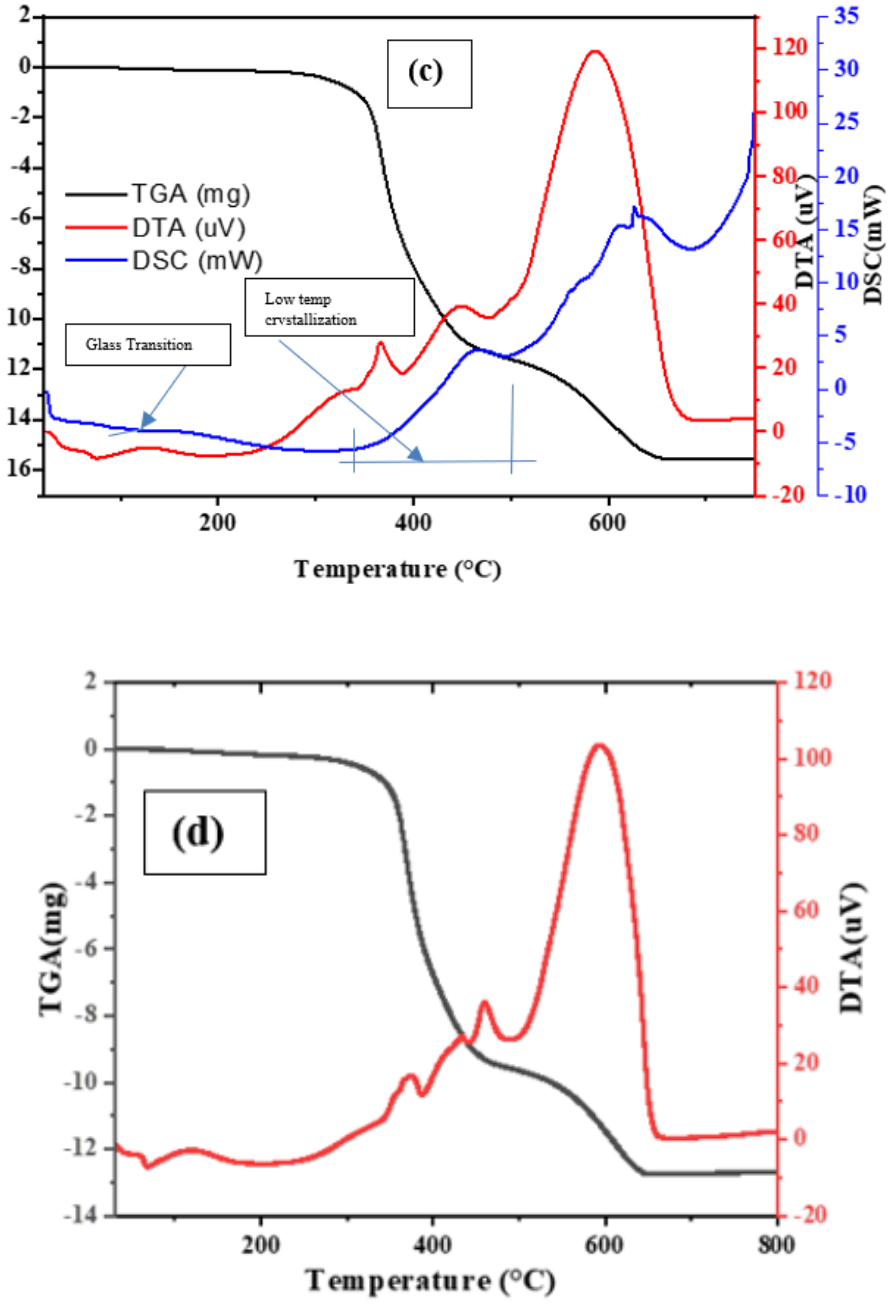

Figure 4.6 TGA and DTA curve of CNC particles, (b) TGA, DTA, and DSC of Hybrid E-glass fiber -CNC-epoxy composite, (c) TGA, DTA and DSC of E-glass fiber-epoxy composite (d) TGA and DTA of cured epoxy resin

Figure 4.6 shows the TGA and DTA curves of the epoxy resin, GF/Epoxy composite and hybrid GF/CNC/ Epoxy resin composite. Addition of CNC have shown a slight improvement in thermal property of the hybrid composite material.

4.1.12 Thermal stability analysis discussion

The first degradation which occurred at 62–240 ^{o}C was associated with the evaporation of moisture and absorbed water in CNC, thus causing a weight loss of the CNC sample around 9.8932 % in this range [87]. The second transition was occurred at a temperature ranging between 240–360 ^{o}C, and was attributed by structural deterioration of crystalline nanocellulose, with a total weight loss of 52.6262% which is the highest loss. The cleavage backbone of nanocellulose or the decomposition of carbonaceous materials caused the third zone to form above 360 ^{o}C. At 625 ^{o}C, the total weight loss in this range was more than 78.4168%.

While comparing thermal properties of CNC, epoxy resin, GF/Epoxy composite and GF/Epoxy/8wt% CNC a different thermal property was obtained. Due to the absence of water molecules unlike CNC, epoxy resin, epoxy/GF composites and GF/Epoxy/8wt% CNC composite did not lose weight at around 240 °C. The major degradation of the three samples almost occurred in the same regions of temperature at roughly 300–400 °C during the second degradation stage. Pyrolysis and degradation of epoxy molecules and CNCs (cleavage of glycosidic bonds) found in epoxy/glass fiber/CNC hybrid composites into carbon, hydrocarbons, and volatiles was attributed to this [88]. The third degradation stage occurred at 460–650 °C, which matched to the polyaminoamide curing agent's breakdown.

DSC (differential scanning calorimetry) analysis has been carried out on the samples with 0 wt% and 8 wt% CNC as shown in Figure 4.6 (b) and 4.6 (c). The dynamic measurements were taken when the heating rate constantly remained 10°C/min from 25° to 750°. The glass transition temperature of the hybrid composite with 0wt% and 8wt% CNC was found to be 115.5°C and 150°C respectively. DSC curves also showed the presence of two exothermic peaks that shows low temperature crystallization of the composite material. This indicate that an increase in chain stiffness of hybrid glass fiber 8wt% CNC epoxy composite as it increases along with glass transition temperature (T_g).

4.1.13 Density of the composite

The result obtained from density measurement of the composite materials with different composition of CNC employing Archimedes principle and void content is described as follows on table 4.4.

Table 4.4 Theoretical density, experimental density and void content of glass fiber/CNC hybrid composite

	Mass on pan (g)	Mass in air (g)	Mass in water (g)	Theoretical density (g/cm^3)	Experimental density (g/cm^3)	Void content (%)
Composite 5	6.4865	6.5301	1.7722	1.42	1.3633	4
Composite 4	6.5554	6.6016	1.7845	1.42	1.361	4.2
Composite 3	7.2974	7.342	1.8482	1.42	1.3283	6.3
Composite 2	6.8282	6.8714	1.6452	1.42	1.3065	8.5
Composite 1	7.3472	7.3895	1.686	1.4	1.2882	7.8

4.1.14 Density measurement discussion

From table 4.4 density of the composite materials showed that as the weight percentage of CNC increased the density of the composite material also increases. Thus, when compared to epoxy/glass fiber composites, the density of hybrid composites was higher. This was most likely due to the cellulose nanofibers filling the holes or air spaces between the glass fibers and epoxy matrix [89]. Chee et al. found that adding nanofillers like nanoclay and halloysite nanotube to epoxy/bamboo fibers/kenaf fibers hybrid composites increased density [90]. From table 4.4, it is observed all composites' experimental densities were found to be lower than their theoretical densities. This could be attributed to void creation during composite production. Two different reasons can be stated for the void formation. First, the fabrication process produces a lot of trapped air or other volatiles. Second, voids can arise when the matrix is unable to completely replace the air trapped in the glass fibers during impregnation [91].

The void content of all the hybrid composites was lower than that of the control sample. This suggests that the void content of the epoxy/glass fiber composite was reduced by including CNCs. This is most likely due to cellulose nanofibers' superior surface wetting capacity, which results in improved contact and adhesive bonding [92]. The E/GF/8%CNC sample has the lowest void content (4 %) of all the samples. This was due to greater CNC dispersion in the epoxy matrix, which resulted in a decreased void content in the hybrid composite containing 8 wt% CNF. In

comparison to the E/GF/8% CNC sample, the other composite samples with 2wt%, 4wt%, 6wt% of CNC had a larger void content of 8.5%, 6.3% and 4.2% respectively. The increased void content of the hybrid composite with 2, 4 and 6 wt% CNC could be attributed to inadequate CNC dispersion in the epoxy matrix, resulting in agglomeration of CNC particles, resulting in a larger void content [93].

4.1.2 Mechanical properties

4.1.2.1 Tensile strength Test Result

Composite 1: A sample composite to detect the effect of addition of CNC and is fabricated wit GF and epoxy resin without CNC and three specimens have been tested to which three graphs were plotted.

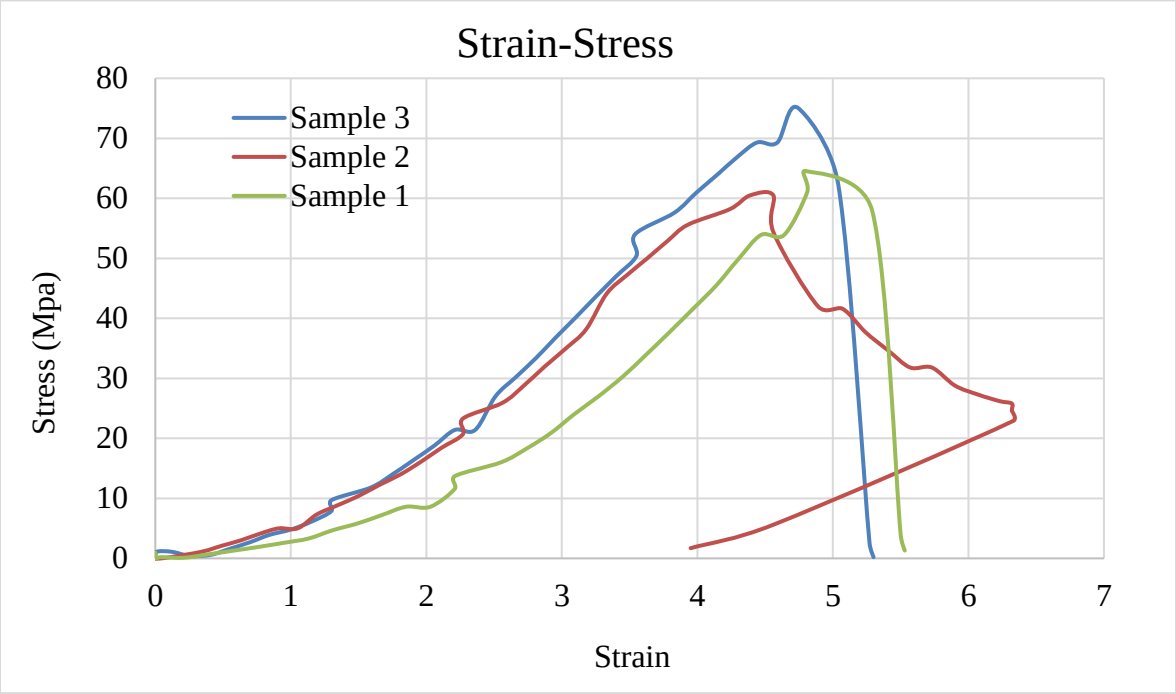

Figure 4.7 Tensile stress-strain curve for C1

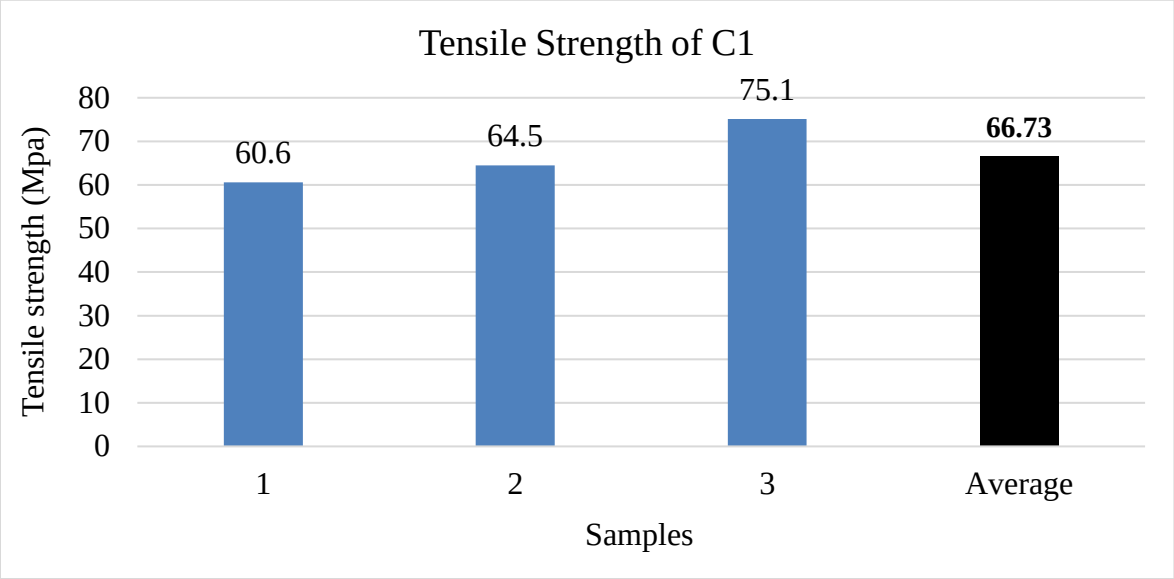

Figure 4.8 Comparison and average tensile strength of samples for C1

Composite 2: A sample composite with 2wt% CNC, GF and epoxy resin and three specimens have been tested to which three Stress-strain graphs were plotted.

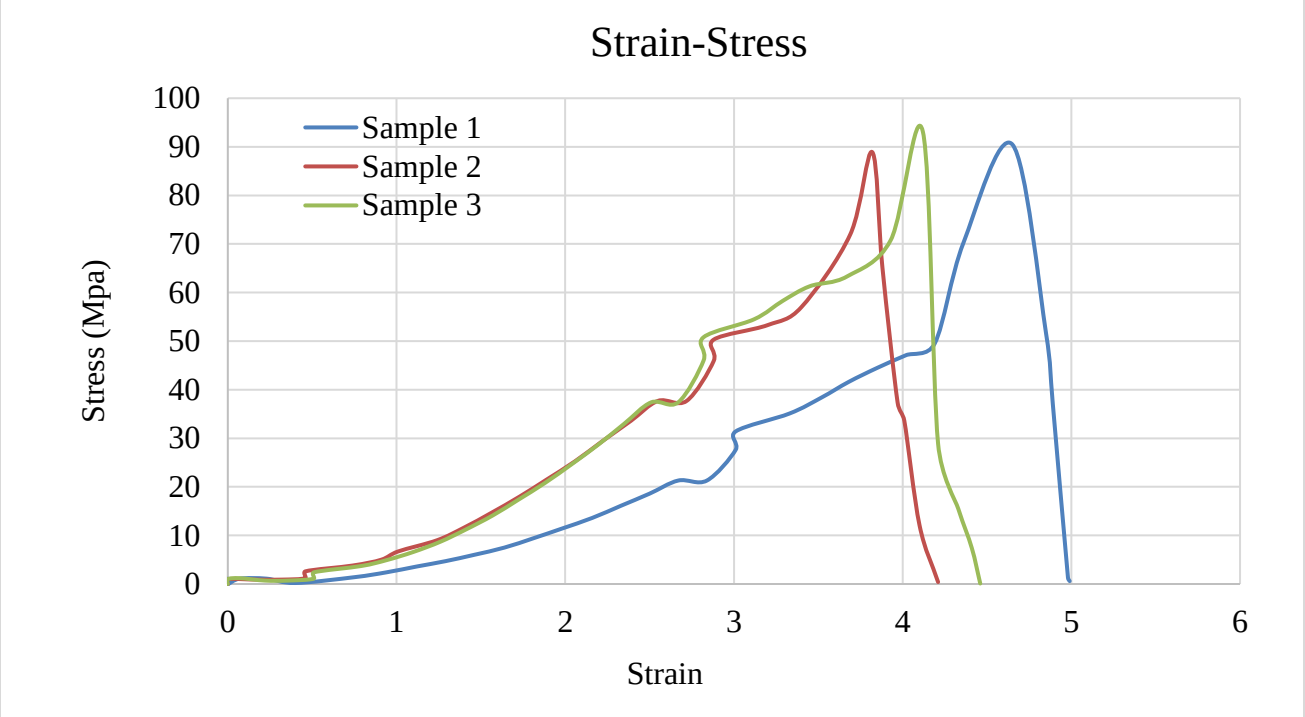

Figure 4.9 Tensile stress-strain curve for C2

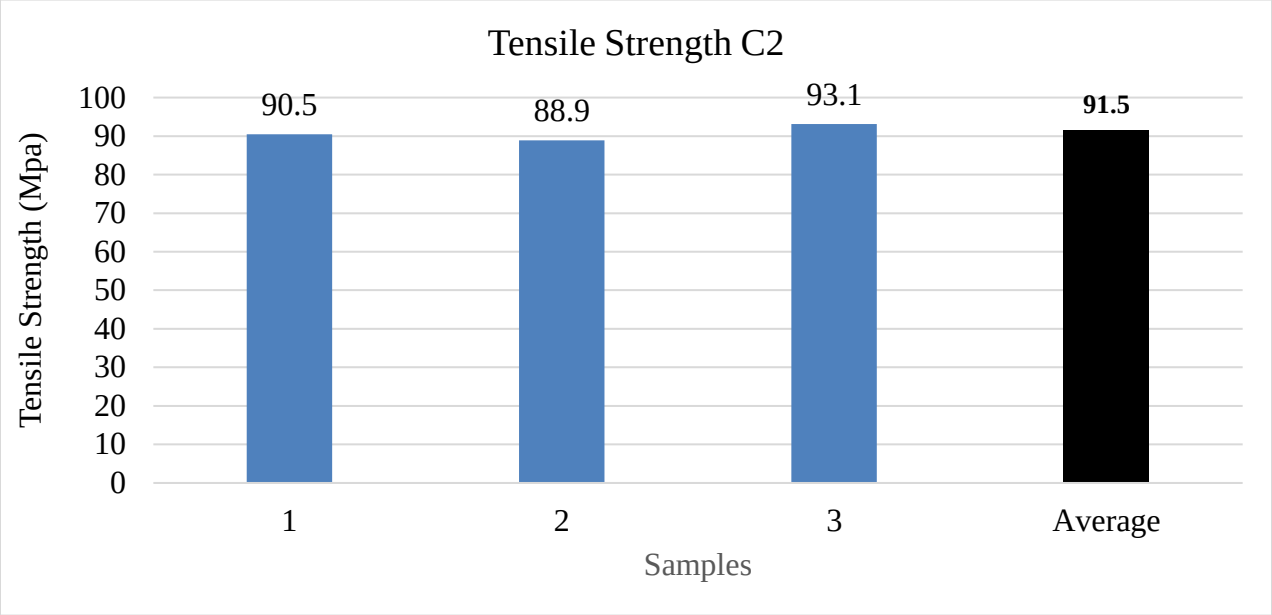

Figure 4.10 Comparison and average tensile strength of samples for C2

Composite 3: A sample composite with 4wt% CNC, GF and epoxy resin and three specimens have been tested to which three Stress-strain graphs were plotted.

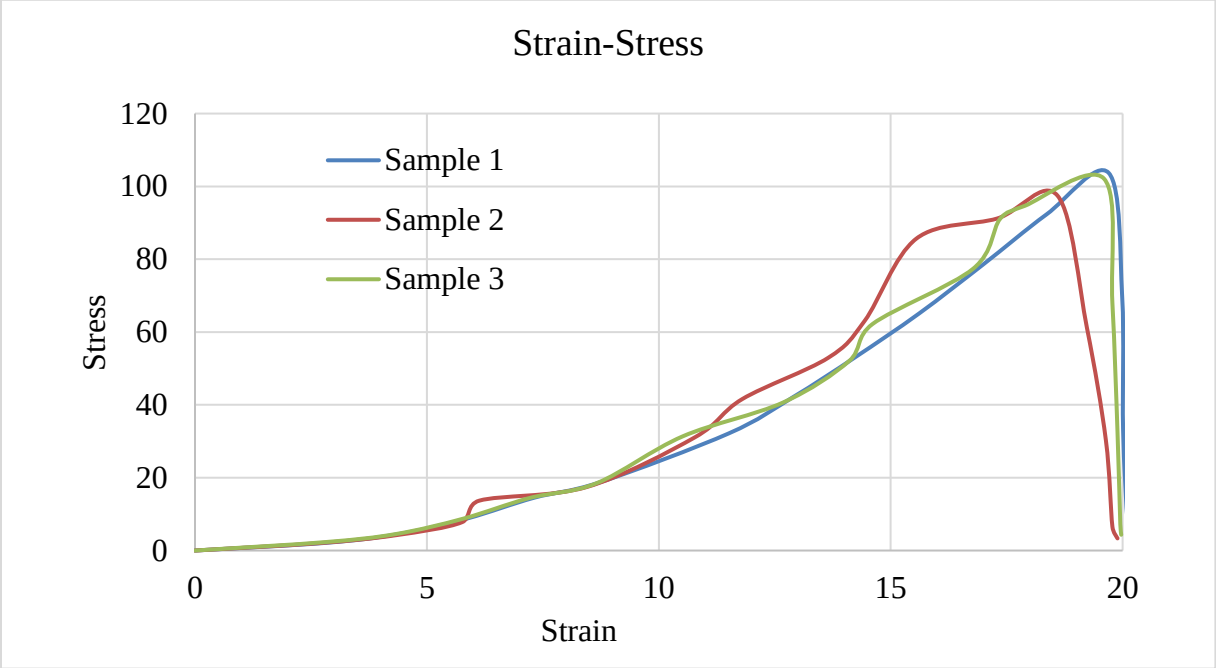

Figure 4.11 Tensile stress-strain curve for C3

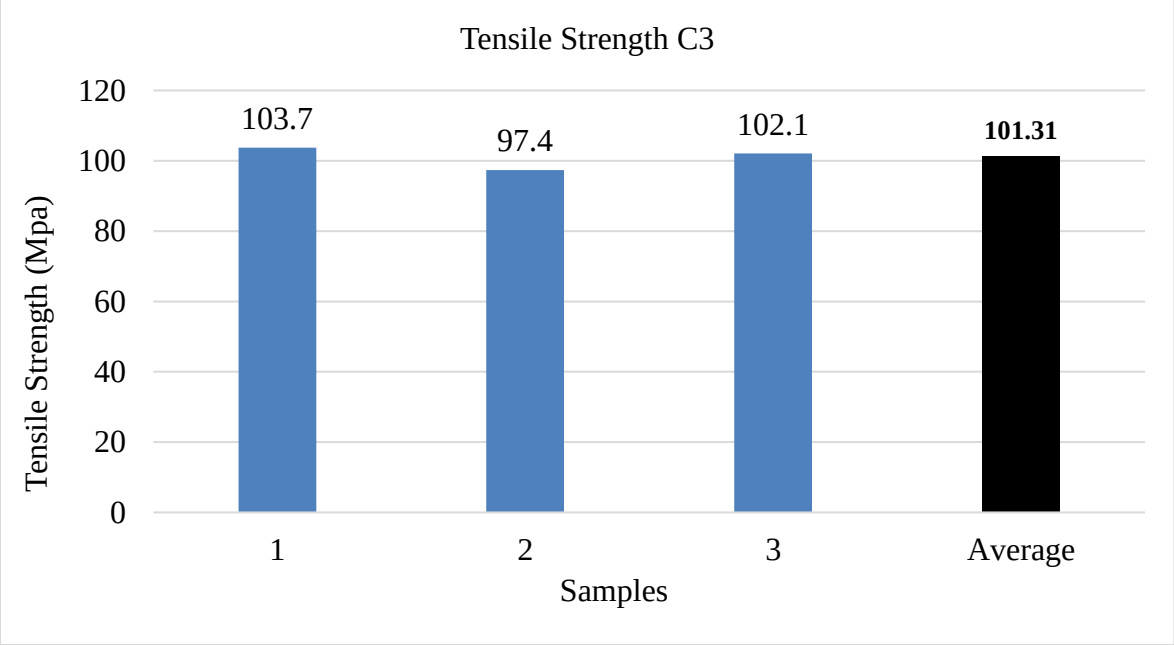

Figure 4.12 Comparison and average tensile strength of samples for C3

Composite 4: A sample composite with 6wt% CNC, GF and epoxy resin and three specimens have been tested to which three Stress-strain graphs were plotted.

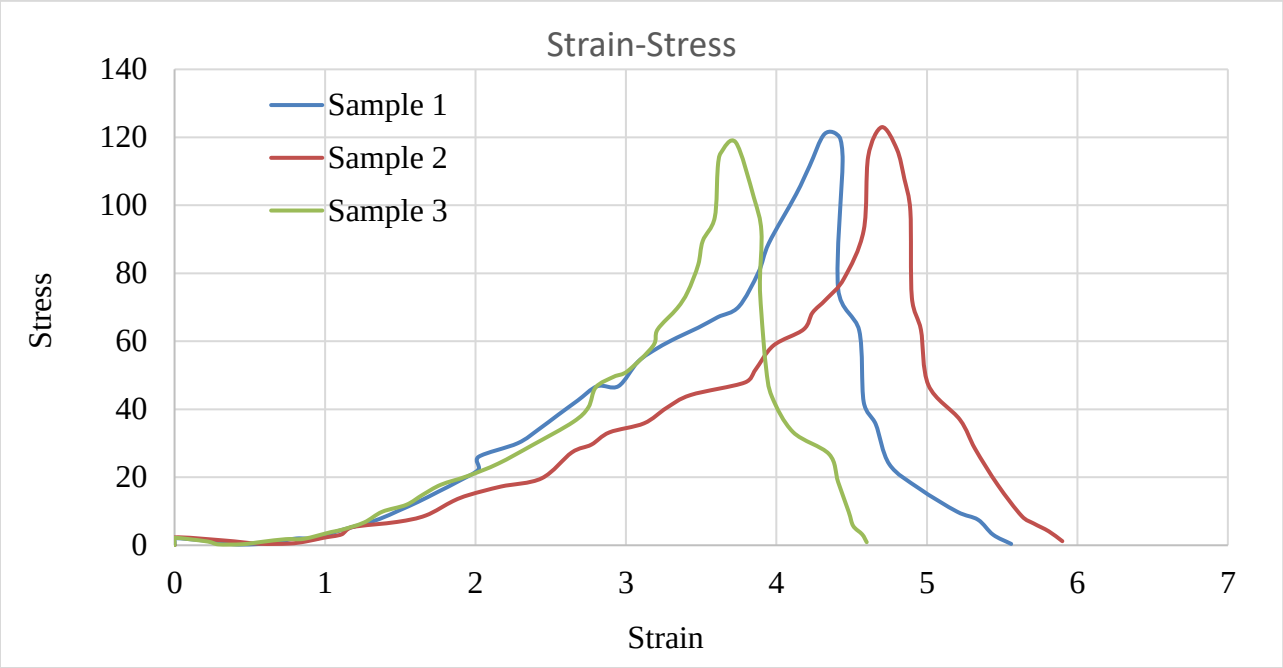

Figure 4.13 Tensile stress-strain curve for C4

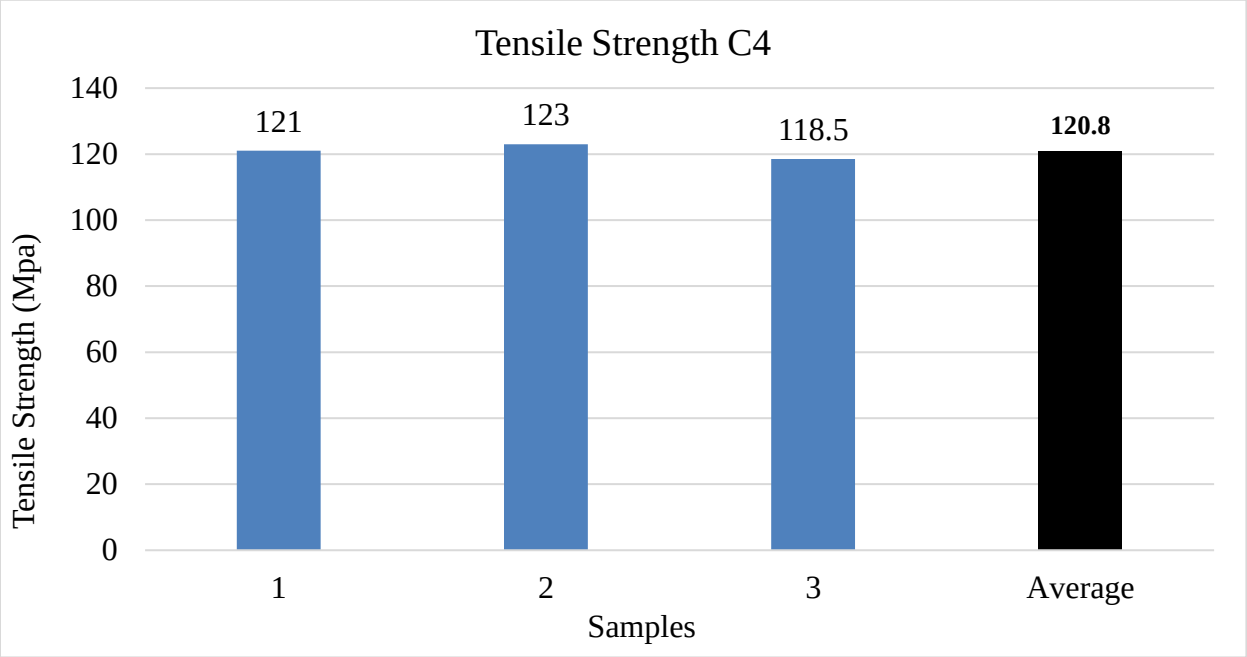

Figure 4.14 Comparison and average tensile strength of samples for C4

Composite 5: A sample composite with 8wt% CNC, GF and epoxy resin and three specimens have been tested to which three Stress-strain graphs were plotted.

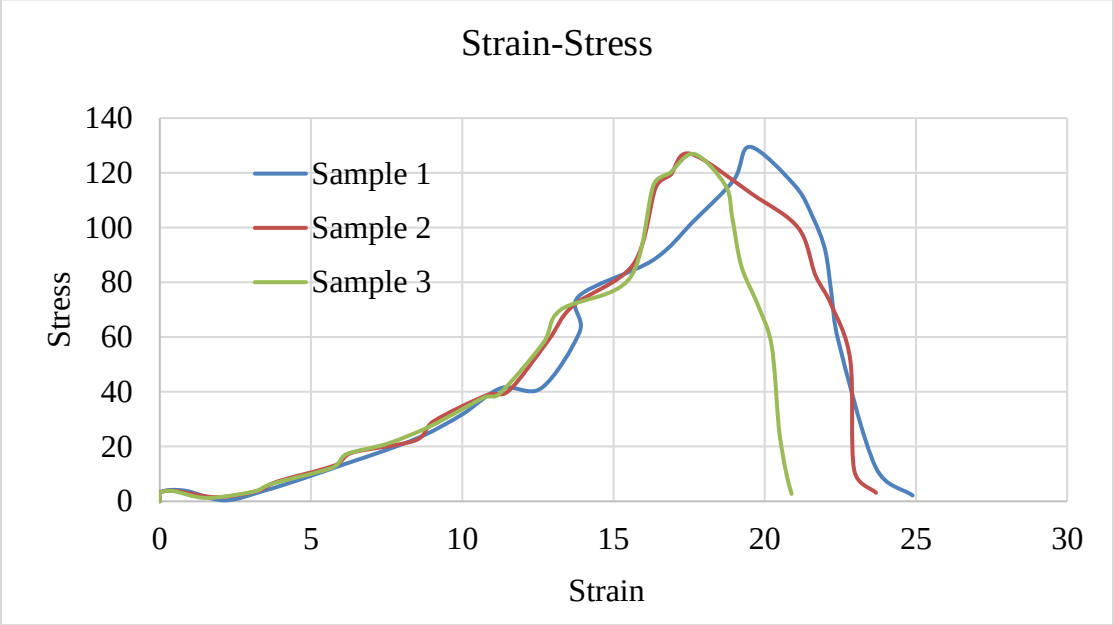

Figure 4.15 Tensile stress-strain curve for C5

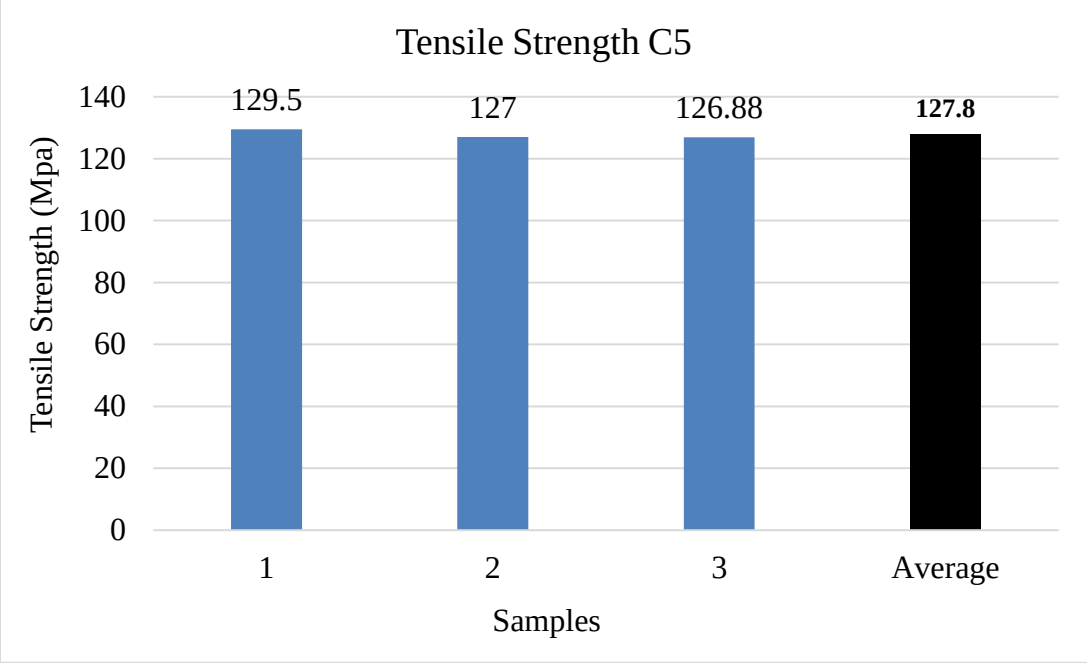

Figure 4.16 Comparison and average tensile strength of C5

The overall tensile strength comparison of the composite materials with varying weight percentage of CNC and without CNC is described in the graph plotted below.

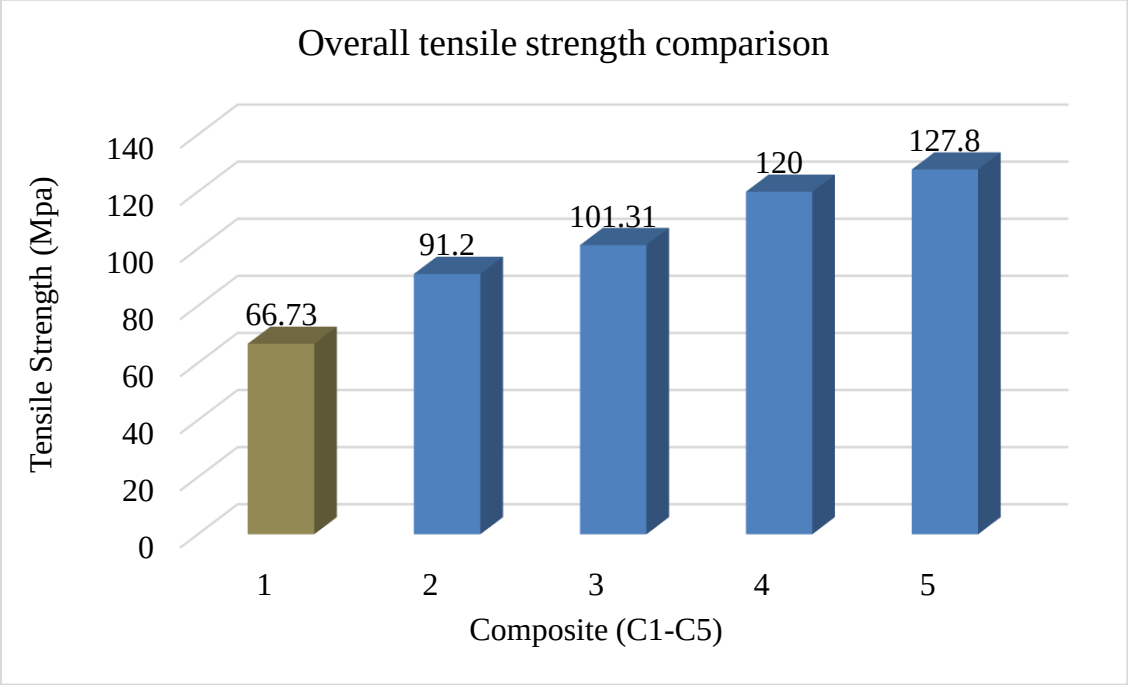

Figure 4.17 Overall tensile strength comparison

4.1.2.2 Tensile strength test discussion

Tensile strength was performed on three samples for each composition and average of each were taken as a final value. The highest value was observed on C5 with 8wt % of CNC having a value of 127.8Mpa. The second highest value was exhibited on C4 with CNC weight percentage of 6% with a tensile strength of 120Mpa. Composite 2 which have 2wt % CNC exhibits the least tensile strength which is 91.2Mpa of all, this could be due to the partial agglomeration of CNC and decreased contact with epoxy/glass fiber composites [94]. Furthermore, CNFs have a high aspect ratio, resulting in significant electrostatic interaction and van der Waals attraction, resulting in a high tendency to agglomerate which in turn could act as stress concentration and crack initiation, thus uniform dispersion of CNC particles by sonication can reduce this effect [95]. Composite 3 with 4wt % of CNC shows 101.31Mpa of tensile strength making it the third highest of all the compositions. Thus, the increase in weight percentage of CNC have shown an increase in tensile strength with the highest value obtained at 8wt %. A similar finding was made by Panchagnula and Kuppan, who found that adding 0.1–0.4 percent multi-wall carbon nanotubes (MWCNTs) to glass fiber-reinforced polymers enhanced their tensile strength (GFRPs)[96].

Tensile analysis for the neat and hybrid composites illustrate elastic and plastic deformation in nonlinear curve by depending on the rate at which the force is applied in test. The curves show linear and ultimately develop into nonlinear behavior. The linear region occurs due to the deformation of Hybrid fibers reinforcement. The nonlinear region is basically due to the deformation of epoxy matrix.

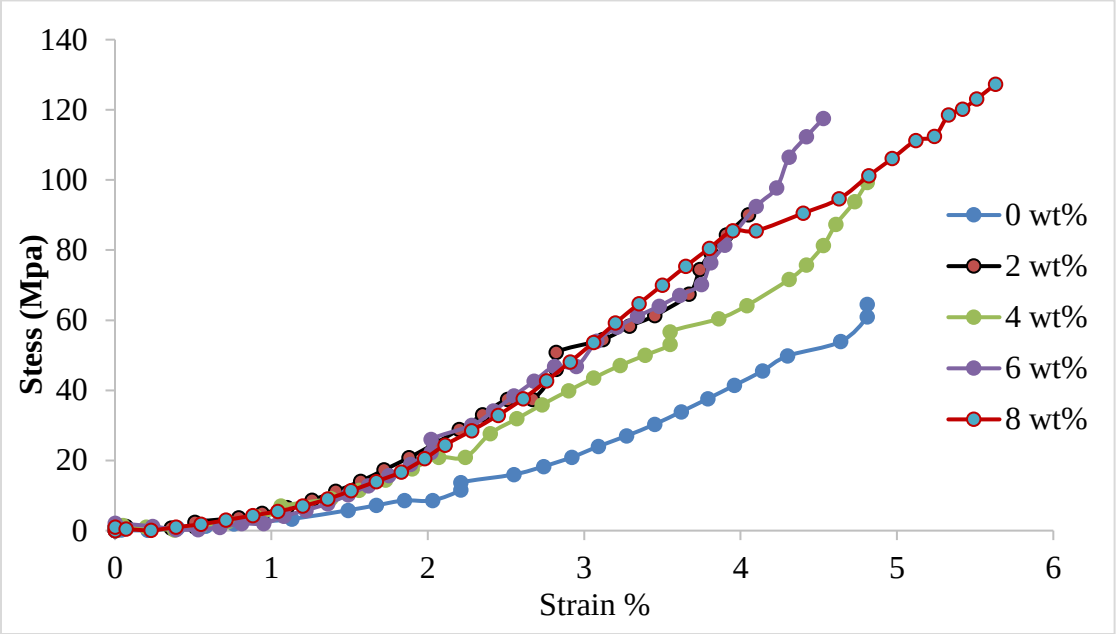

Figure 4.18 Stress-Strain curves for neat and hybrid composites

It can be observed from Figure 4.18 that, the tensile strength, modulus of elasticity (stiffness) increase with increase in the weight % of CNC. In addition, the hybrid composite with 8wt% CNC showed the highest failure strength. Besides the experimental results increasing the weight % of CNC increases the stiffness of the hybrid composite since cellulose have high stiffness as presented in Table 1.

4.1.2.3 Compression Strength results

Specimens that are prepared according to the ASTM specification were tested for each composite composition. Three trials were performed for each composition and an average value was taken.

Five compositions, four of which with varying wt % CNC and one without CNC were tested and compared. The maximum values of each trial with corresponding average value are presented as follows.

Composite 1: A control sample composite material with a composition of glass fiber and epoxy resin to detect the effect of addition of CNC was fabricated without CNC and three specimens have been tested to which three graphs were plotted as shown in figure 4.19 and average value of the three was taken as illustrated in figure 4.20.

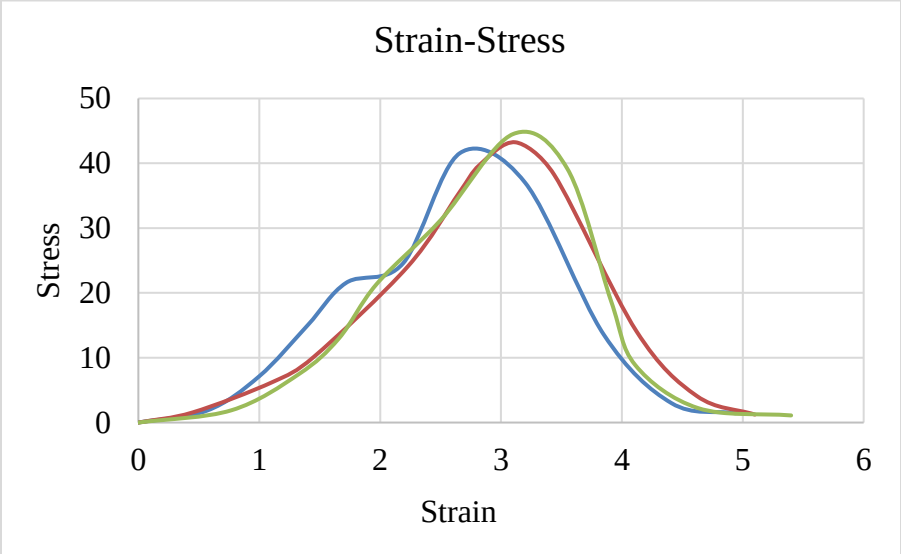

Figure 4.19 Stress-strain curve for compression strength test of C1

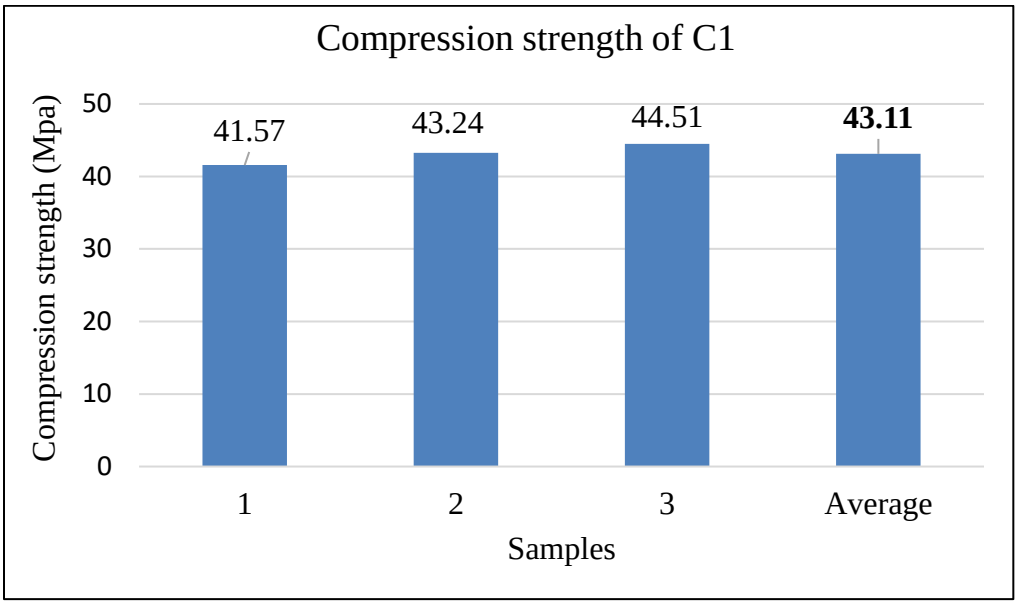

Figure 4.20 Comparison and average compression strength of C1

Composite 2: A sample composite with 2wt% CNC, GF and epoxy resin and three specimens have been tested for compression strength to which three Stress-strain graphs were plotted as shown in figure 4.21 and average value of the three were taken as plotted in figure 4.22.

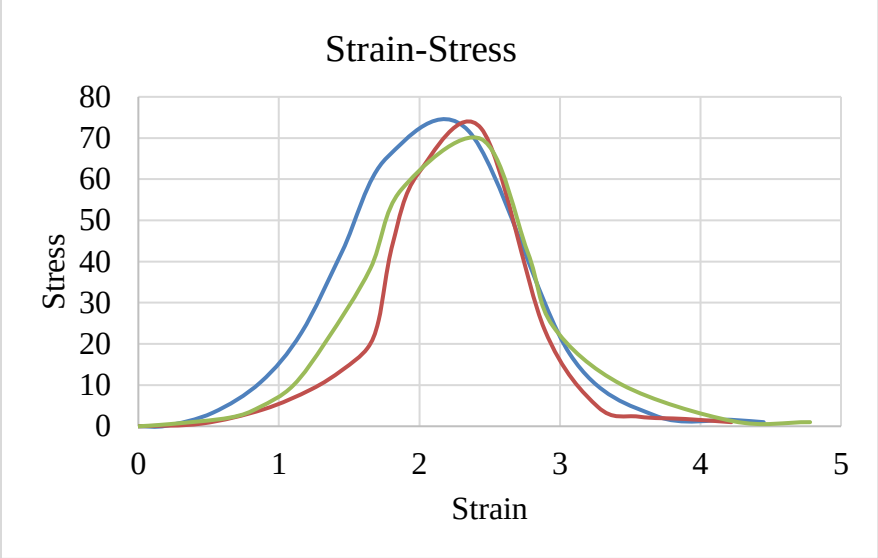

Figure 4.21 Stress-strain curve for compression test of C2

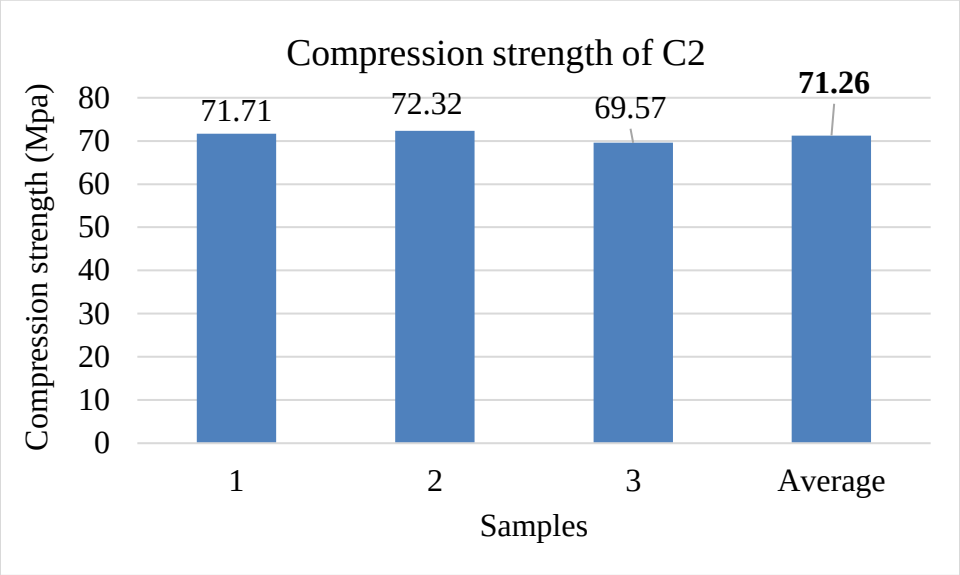

Figure 4.22 Comparison and average compression strength of C2

Composite 3: A sample composite with 4wt% CNC, GF and epoxy resin and three specimens have been tested for compression strength to which three Stress-strain graphs were plotted as shown in figure 4.23 and an average value of the three trials was taken as shown in figure 4.24.

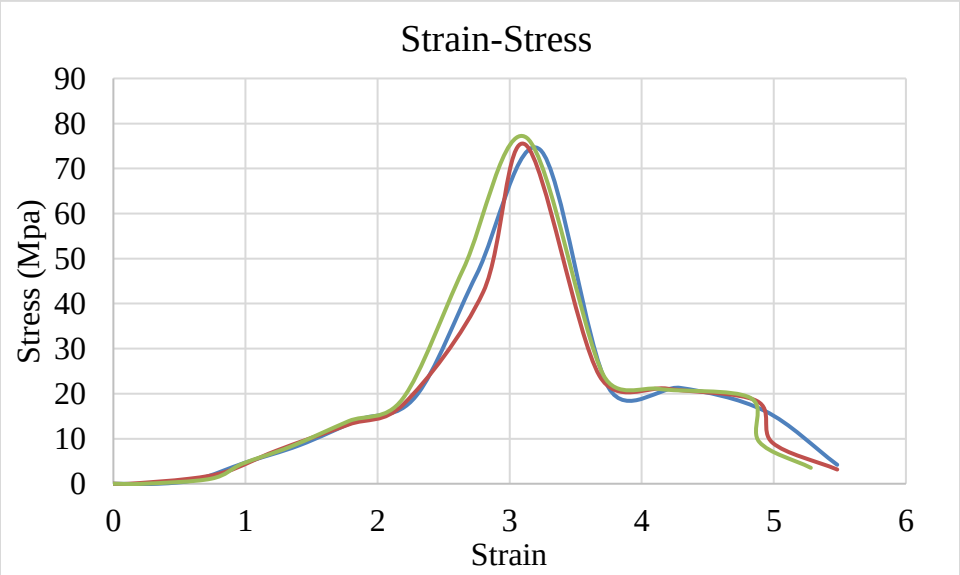

Figure 4.23 Stress-Strain curve for compression test of C3

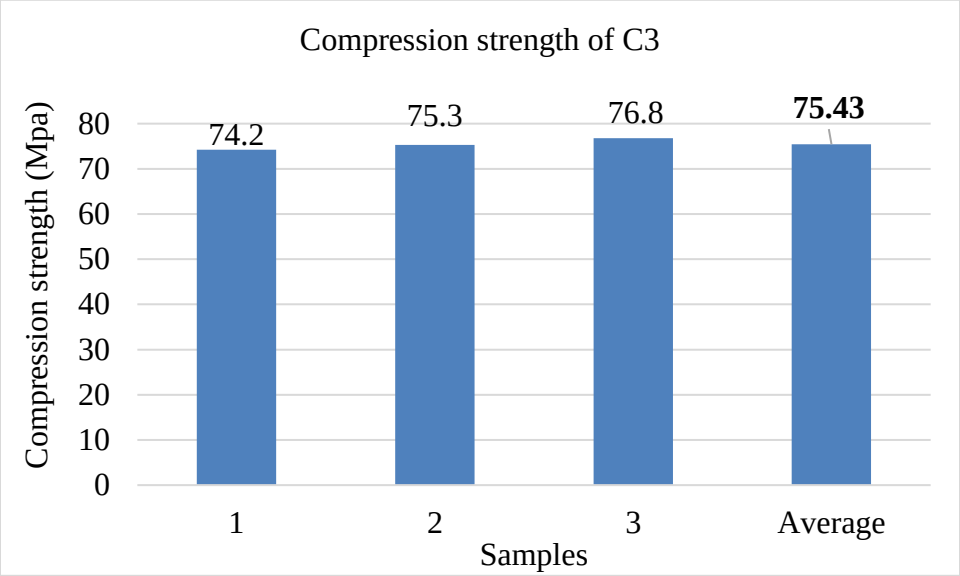

Figure 4.24 Comparison and average compression strength of C3

Composite 4: A sample composite with 6wt% CNC, GF and epoxy resin and three specimens have been tested for compression strength to which three Stress-strain graphs were plotted as shown in figure 4.25 and an average value was taken as illustrated in figure 4.26.

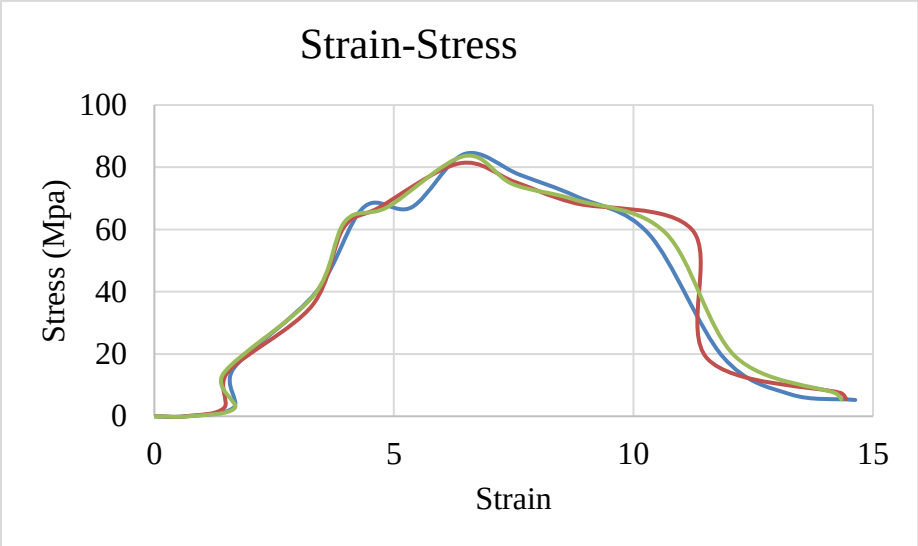

Figure 4.25 Stress-Strain curve for compression test of C4

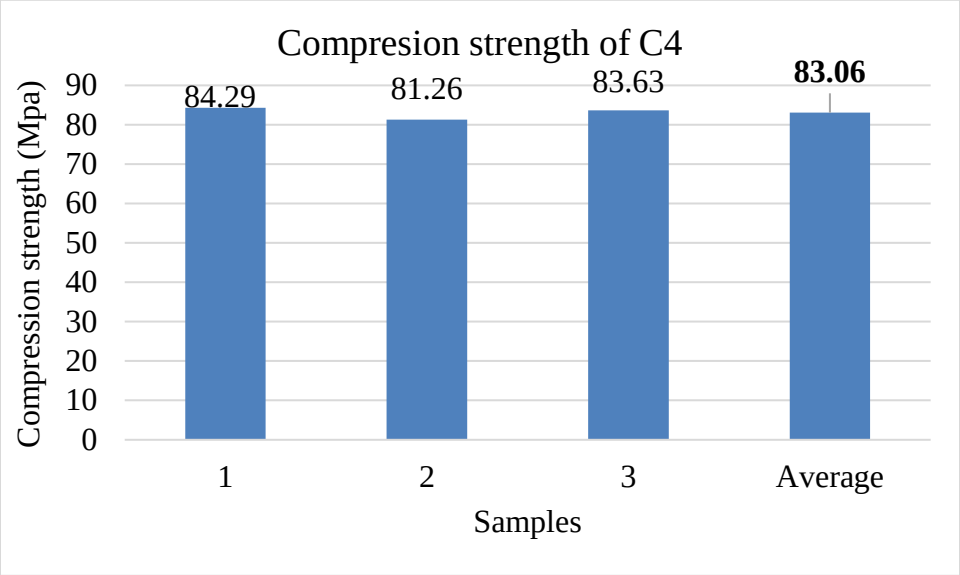

Figure 4.26 Comparison and average compression strength of C4

Composite 5: A sample composite with 8wt% CNC, GF and epoxy resin and three specimens have been tested for compression strength to which three Stress-strain graphs were plotted as shown in figure 4.27 and an average value was taken as illustrated in figure 4.28.

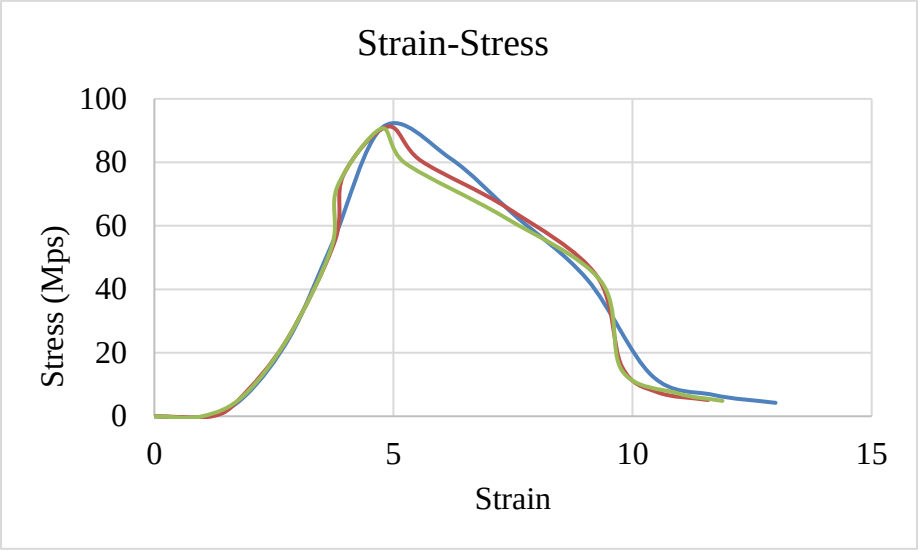

Figure 4.27 Stress-strain curve for compression test of C5

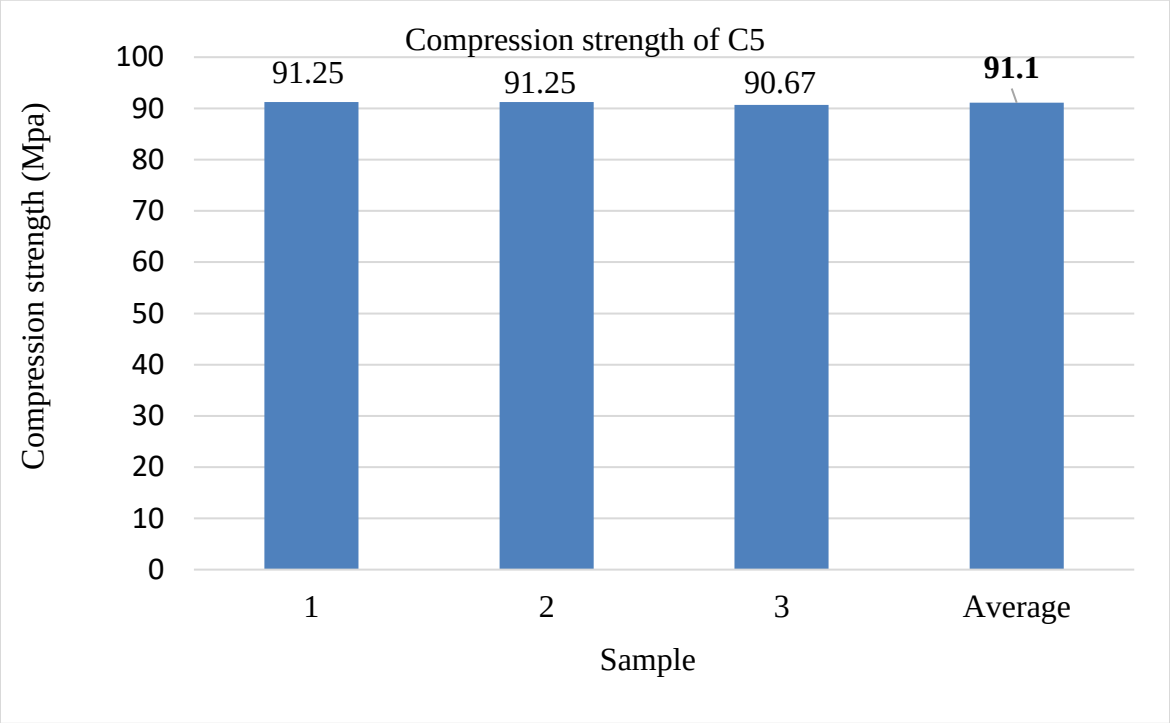

Figure 4.28 Comparison and average compression strength of C5

The overall tensile strength comparison of the composite materials with varying weight percentage of CNC and without CNC is described in the graph plotted as shown in figure 4.29.

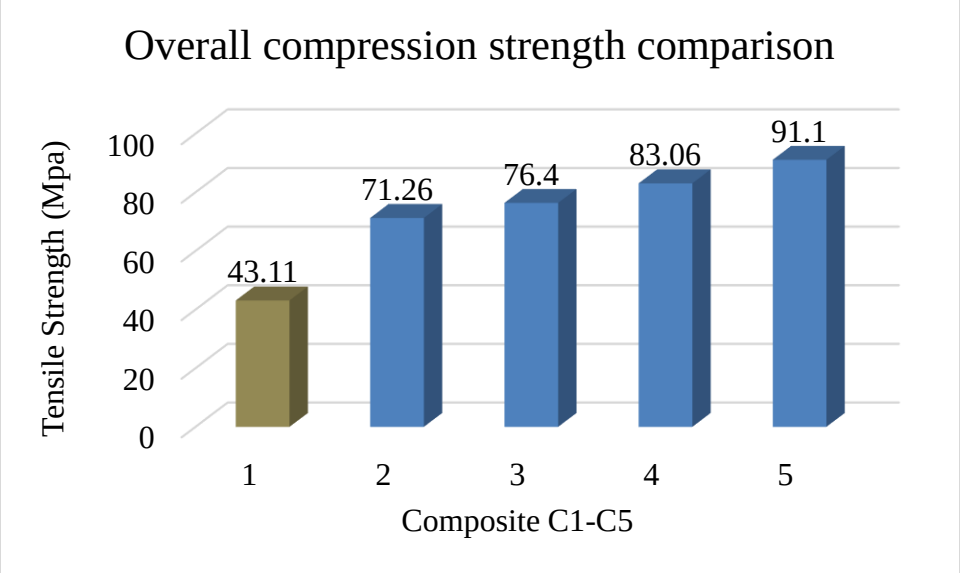

Figure 4.29 Overall compression strength comparison

4.1.2.4 Compression Strength discussion

Figure 4.29 shows the compression strength of the composite materials with different CNC wt%, thus the composite sample with 8wt% CNC has the highest compressive strength of 91.1Mpa. The composite sample with 6wt% CNC has the second highest compressive strength with a value of 83.06Mpa. Composite 3 showed compression strength of 76.4Mpa and the control sample showed a compressive strength of 43.11Mpa which is the least value. Composite two showed the least compression strength of all the hybrid composite samples which is 71.26MPa.

4.1.2.5 Flexural Strength results

Test results for flexural strength were obtained from three point bending in which the results were calculated on a computer and three specimen results were analyzed for each composite material. Thus, the following formulas were employed to obtain the flexural strength as per the testing machine specifications. Figure 4.30 shows a sample test result displayed on the testing computer:

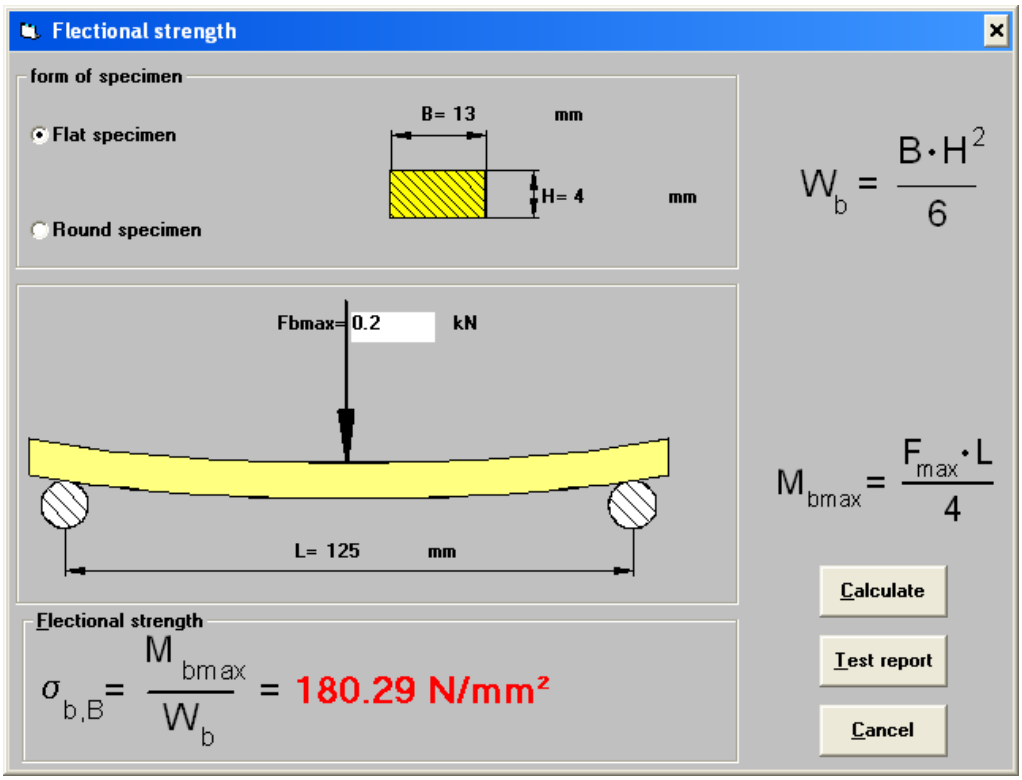

Figure 4.30 Schematic of testing set up and formulas to interpret results on testing machine output

Where:

M_{bmax}: Maximum bending moment F_{max} = Maximum applied force

W_b = Section modulus H =Thickness of specimen

σ_{bmax} = Flexural strength L = Span Length

B = Width of Specimen

Composite 1

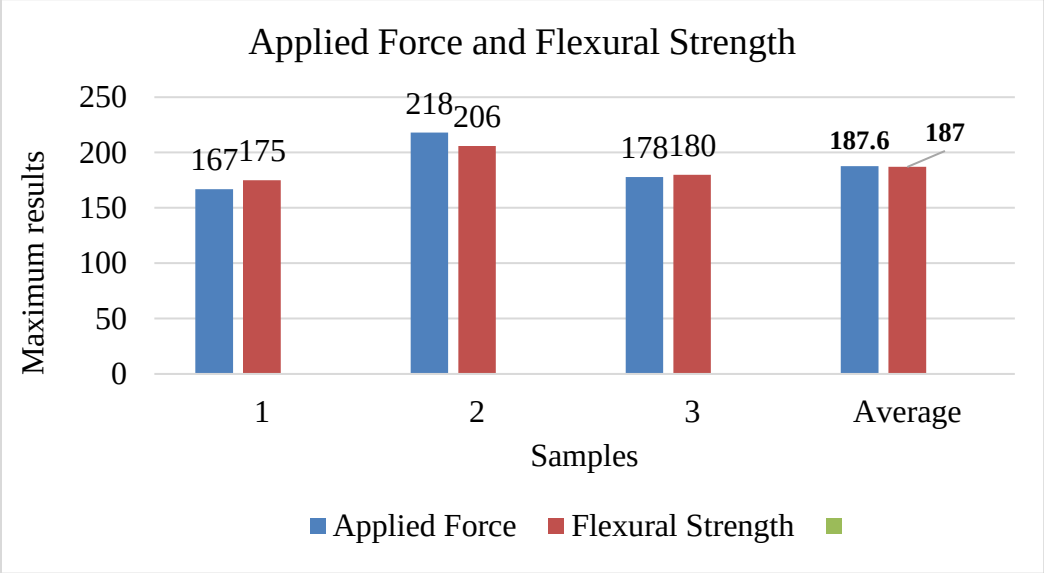

Figure 4.31 Applied force and flexural strength of C1

Composite 2

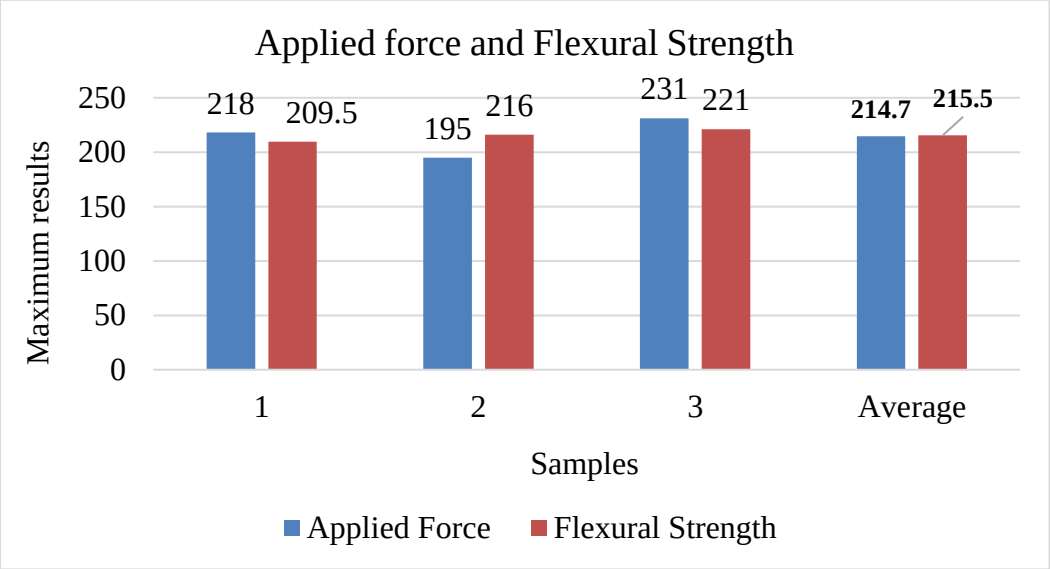

Figure 4.32 Applied force and flexural strength of C2

Composite 3

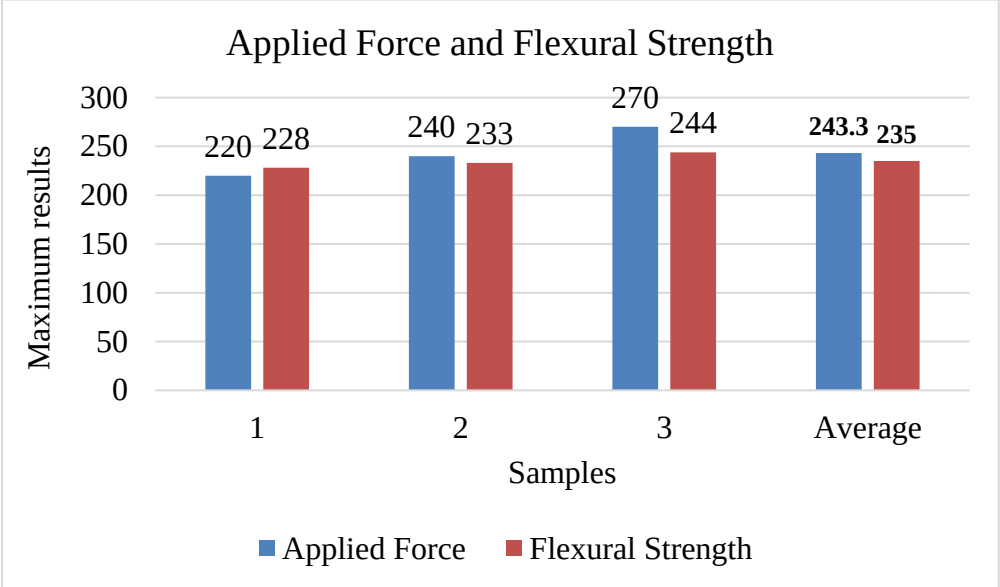

Figure 4.33 Applied force and flexural strength of C3

Composite 4

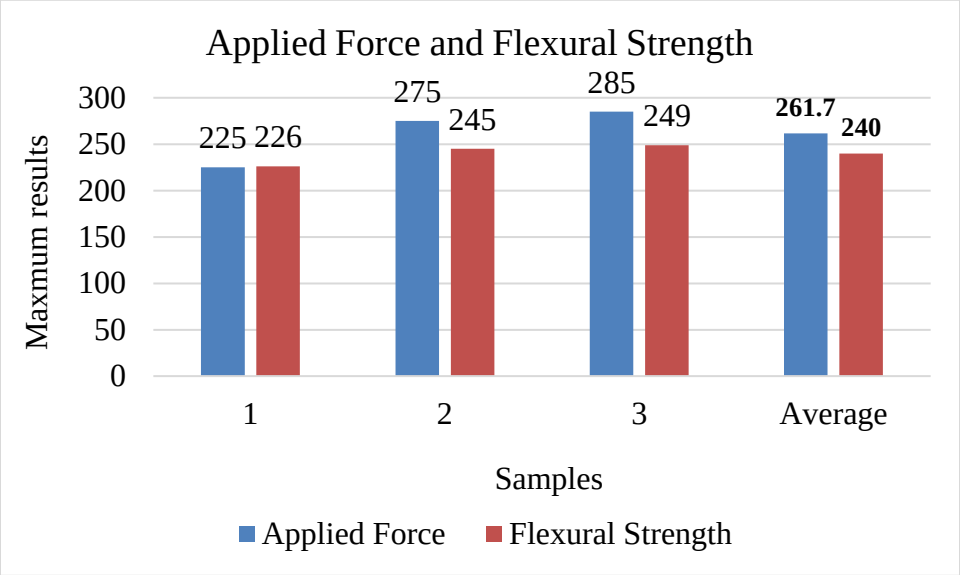

Figure 4.34 Applied force and flexural strength of C4

Composite 5

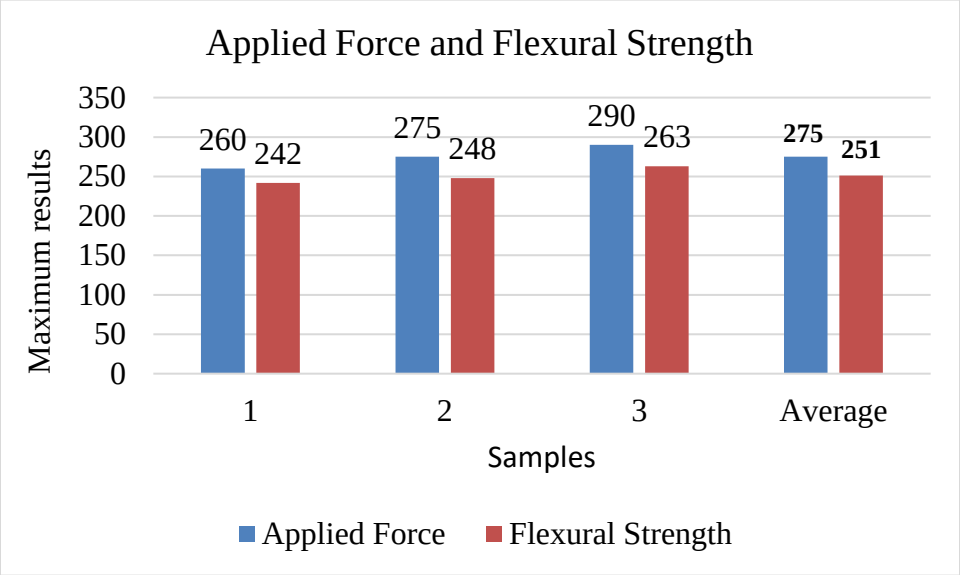

Figure 4.35 Applied force and flexural strength of C5

The overall maximum applied force and flexural strength obtained is describes as follows.

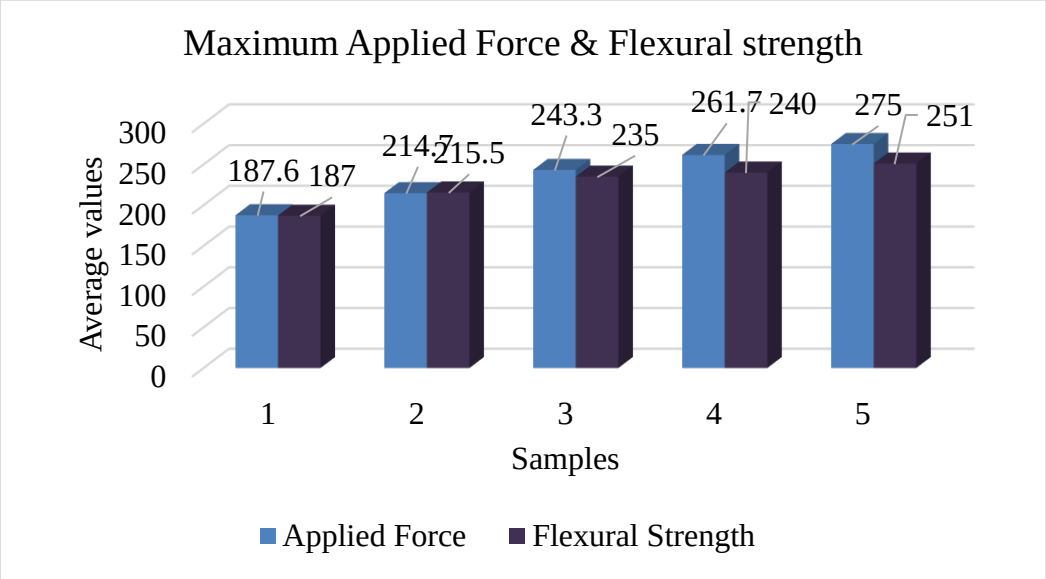

Figure 4.36 Overall maximum applied force and average flexural strength of composites

4.1.2.6 Flexural Strength discussion

As obtained from the UTM composite 5 that is with a composition of CNC 8wt % exhibits superior flexural strength of 251Mpa having maximum applied force of 275N. The second highest flexural strength composition is C4 that is with CNC weight percentage of 6 exhibiting 240Mpa at a maximum force 261.7N. C3 having 4wt % of CNC shows the third highest of all which is 223Mpa at 243.3N, and that of C2 with 2wt % CNC showed the least flexural strength of all the hybrid samples which was found to be 215.5Mpa. The control sample showed a flexural strength of 187MPa at a load of 187.6N. The improvement in flexural strength with increasing wt% of CNC was most likely due to the gradient interphase layer between glass fibers and epoxy matrix retarding interlaminar and intralaminar microcracks [88]. According to Romanov et al. an interphase gradient containing carbon nanotubes connected to carbon fibers proved successful in lowering stress concentration at the fiber-epoxy matrix interface and then delaying fracture propagation from the epoxy matrix to the carbon nanotube interface [97].

4.1.2.7 Impact strength results

Test results for impact test results were obtained from Charpy testing technique by manually reading the pointer as the specimens were under impact load for each composite material as it is shown in table 4.5.

Table 4.5 Impact energy results

No.	Composition of composite	Sample	Impact Energy (J)	Swing Angle (°)
1	Neat	1	4.5	140
		2	5	139
		3	4.5	140
		Average	**4.7**	
2	CNC 2%	1	4.5	140
		2	4.5	140
		3	5	139
		Average	**4.7**	
3	CNC 4%	1	5	138
		2	5.5	138
		3	6	136
		Average	**5.5**	
4	CNC 6%	1	6	136
		2	5.5	138
		3	6	136
		Average	**5.83**	
5	CNC 8%	1	6.5	133
		2	7	132
		3	7	132
		Average	**6.83**	

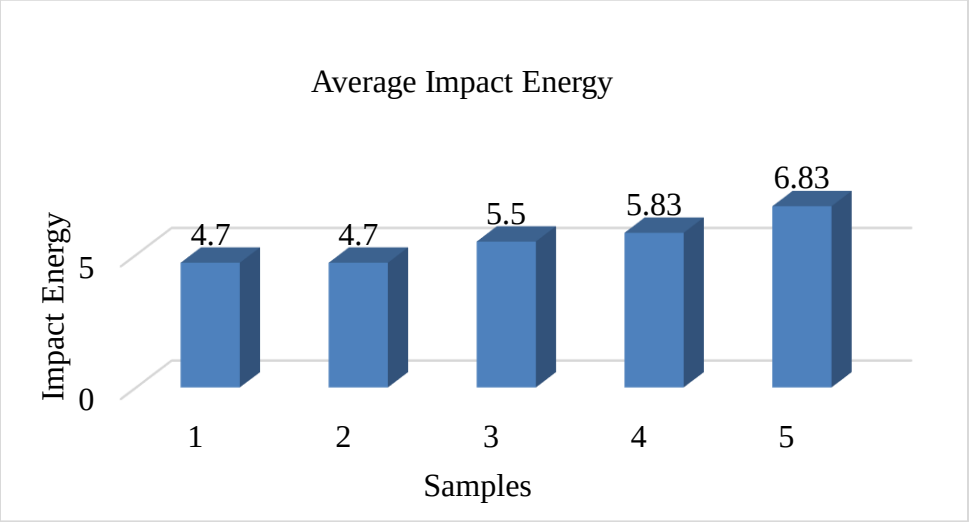

Figure 4.37 Comparison of average Impact results

4.1.2.8 Impact strength discussion

From the Charpy impact strength testing device manual reading it was observed that C5 with CNC weight percentage of 8 have the highest impact energy absorbing capability of 6.83J. C4 a composite material with 6wt % of CNC have shown the second highest impact energy resistance which is 5.83J. the composite material with a composition of 4wt % CNC shown the third highest impact strength which is 5.5J. C2 which have 2wt % CNC exhibits an equivalent impact strength with that of the control sample which is 4.7J. The result obtained was found to be similar with the findings of Parveen et al., who found that adding 1 wt percent cellulose microcrystals (CMCs) to GRFP composites enhanced the impact energy by 9.4%, but that adding 3 wt percent CMC reduced the impact energy due to CNF agglomeration [98]. The reduction in impact toughness may be as a result of weak interfacial adhesion and inadequate CMC dispersion [99]. The improved compatibility of the dispersed CMCs/CNC with the polymer, according to various prior research, could increase the polymer's impact strength [100]. As a result, the dispersion of the particles in the polymer matrix, the characteristics of individual fibers, and interlaminar and interfacial adhesion between the fibers and the polymer matrix all had a significant impact on the impact strength of micro and nanoparticles reinforced GFRPs [101]. Thus, the impact test results have shown an increase in impact strength with increasing the weight percentage of CNC.

4.1.3 Comparison of results with literatures

As nanotechnology is a recently developing technology at its infant stage there are few numbers of researches related to CNC/ E-glass fiber hybrid epoxy composite. But of those few numbers of research works this study was compared with the following selected papers to validate what has been done so far.

The experimental physical and mechanical test results of the composite material with 8 wt% CNC/E-glass fiber and epoxy resin were compared with literatures.

Tensile strength = 127.8Mpa Water absorption = 0.5%

Flexural strength = 201.32Mpa Density = 1.3633 g/cm^3

Compression strength = 91.1Mpa

Impact strength = 6.83 J

4.1.3.1 Researches on hybrid E-glass/CNC fiber epoxy composite

Taufik Azhary et al. studied the mechanical, morphological and thermal characteristics of epoxy/glass fiber/ cellulose nanofiber hybrid composites.

Table 4.6 Results obtained by Taufik Azhary et al.

Composite	CNC wt%	Tensile Strength (Mpa)	Flexural Strength (Mpa)	Density (g/cm^3)
GF/Epoxy	0wt%	69.76	103.78	1.19
GF/CNC/Epoxy	1wt%	75.2	120	1.24
GF/CNC/Epoxy	2wt%	69.25	120.33	1.22

Sandeep Kumar et al studied on high performance multiscale glass fiber epoxy composite integrated with cellulose nanocrystals for advanced structural applications.

Table 4.7 Result obtained by Sandeep Kumar et al.

Composite	CNC wt%	Tensile (%)	Flexural (%)
GF/CNC/Epoxy	2wt%	24	55

From table 4.6 and 4.7 its observed that the addition of CNC resulted in an improved mechanical and physical properties of the composite material. From the results its proved that addition of CNC

has significant enhancement in flexural strength than that of tensile strength, as discussed in previous section it is because of the effect of CNC on interfacial adhesion and crack tip bridging. Density of the composite material also decreased as the wt% of CNC increased providing a lighter material.

4.2 Simulation of prosthetic pylon

4.2.1 Finite element modeling and analysis

A sample composite material with E-glass fiber/ 8wt % CNC and epoxy resin was selected for the analysis of the composite material to be employed as a prosthetic pylon. The analysis was conducted using ANSYS 2022 software package. Static analysis was executed to show the deformation and equivalent stress of the prosthetic shank. The analysis was performed with steps of modeling, meshing, applying boundary conditions and loads then analyzing the model. Figure 4.38 shows the overall steps.

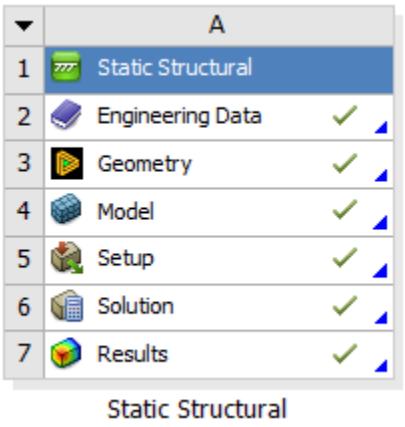

Figure 4.38 Steps in ANSYS

4.2.1.1 Defining engineering data for the pylon material

The material to be simulated was predefined by inserting the type and name of the material on engineering tab of the ANSYS working space as indicated in figure 4.39. E-glass / 8wt % CNC fiber reinforced epoxy composite was inserted as the material name. Prior to data entry of the selected composite material assumptions were made. As hand lay-up was employed as a fabrication technique the following assumptions were taken into consideration:

- ✓ Perfect bind and uniform distribution of fiber and matrix

- ✓ Homogenous dispersion of CNC and
- ✓ Free of void material

Properties of the selected composite material were inserted:

Density = 1.3633g/cm3 Young's Modulus = 4765.4Mpa

Tensile strength = 127.8Mpa Poisson's Ratio = 0.19

Compression strength = 91.1Mpa

Properties of Outline Row 3: BTM

	A	B	C	D	E
1	Property	Value	Unit		
2	Material Field Variables	Table			
3	Density	13633	kg m^-3		
4	Isotropic Elasticity				
5	Derive from	Young's Modulus and Poisson...			
6	Young's Modulus	4765.4	MPa		
7	Poisson's Ratio	0.19			
8	Bulk Modulus	2.562E+09	Pa		
9	Shear Modulus	2.0022E+09	Pa		
10	Tensile Yield Strength	127.8	MPa		
11	Compressive Yield Strength	91.124	MPa		

Figure 4.39 Material engineering data of E-glass fiber/CNC reinforced epoxy composite

4.2.1.2 Modeling of prosthetic pylon in ANSYS workbench

The prosthetic pylon was modeled to be a hollow cylinder with outer diameter of 45mm and inner diameter 35mm, on a design modeler which is integrated on ANSYS workbench software considering a literature [57] [102] as shown in figure 4.40.

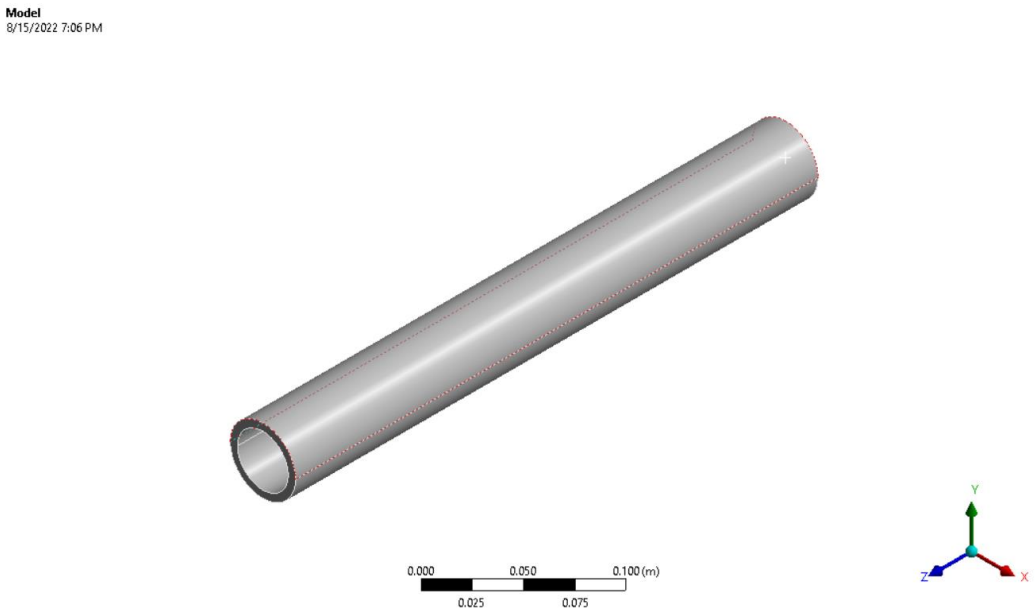

Figure 4.40 3D model of prosthetic pylon

4.2.1.3 Mesh generation

Discrete and topological cells were formed by subdividing a continuous geometric space, fine meshing was employed for sizing and default mesh controls were set as shown in figure 4.41.

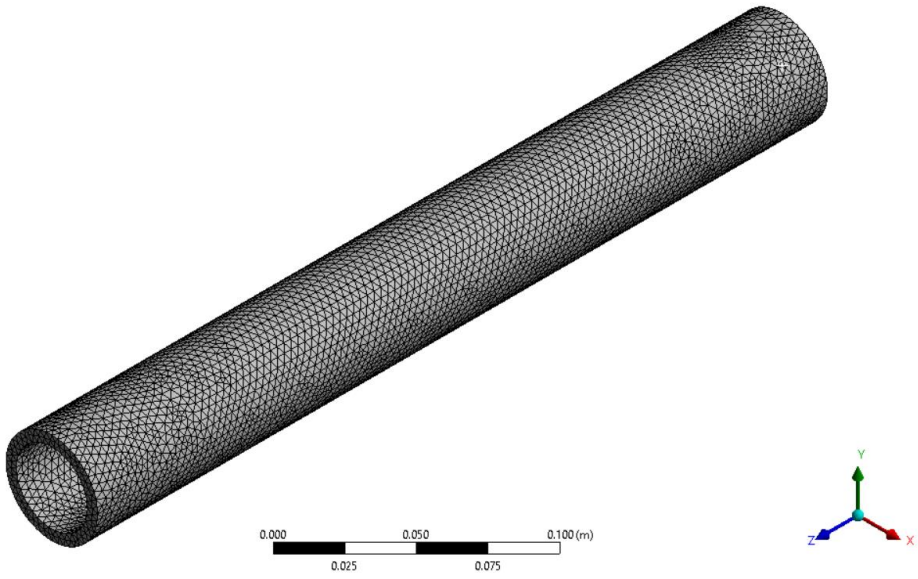

(a)

Details of "Mesh"

Display	
Display Style	Use Geometry Setting
Defaults	
Physics Preference	Mechanical
Element Order	Program Controlled
Element Size	Default
Sizing	
Use Adaptive Sizi...	Yes
Resolution	Default (2)
Mesh Defeaturing	Yes
Defeature Size	Default
Transition	Fast
Span Angle Center	Fine
Initial Size Seed	Assembly
Bounding Box Di...	0.36558 m
Average Surface ...	1.5269e-002 m²
Minimum Edge L...	5.4978e-002 m
Quality	
Inflation	
Advanced	
Statistics	
Nodes	111882
Elements	68150

(b)

Figure 4.41 Meshed prosthetic shank model (a) and meshing details (b)

4.2.1.4 Applying boundary conditions and loading

As shown in figure 4.42 one fixed support at the upper end of the prosthetic shank which fitted to the socket part and a movable lower end was applied [57]. From a literature with a case study involving a 17 years old and 39kg weighing male with a height of 160cm was considered [103]. Thus, the patient considered will generate ground reaction force of 450N according to ISO 10328 standards [104].

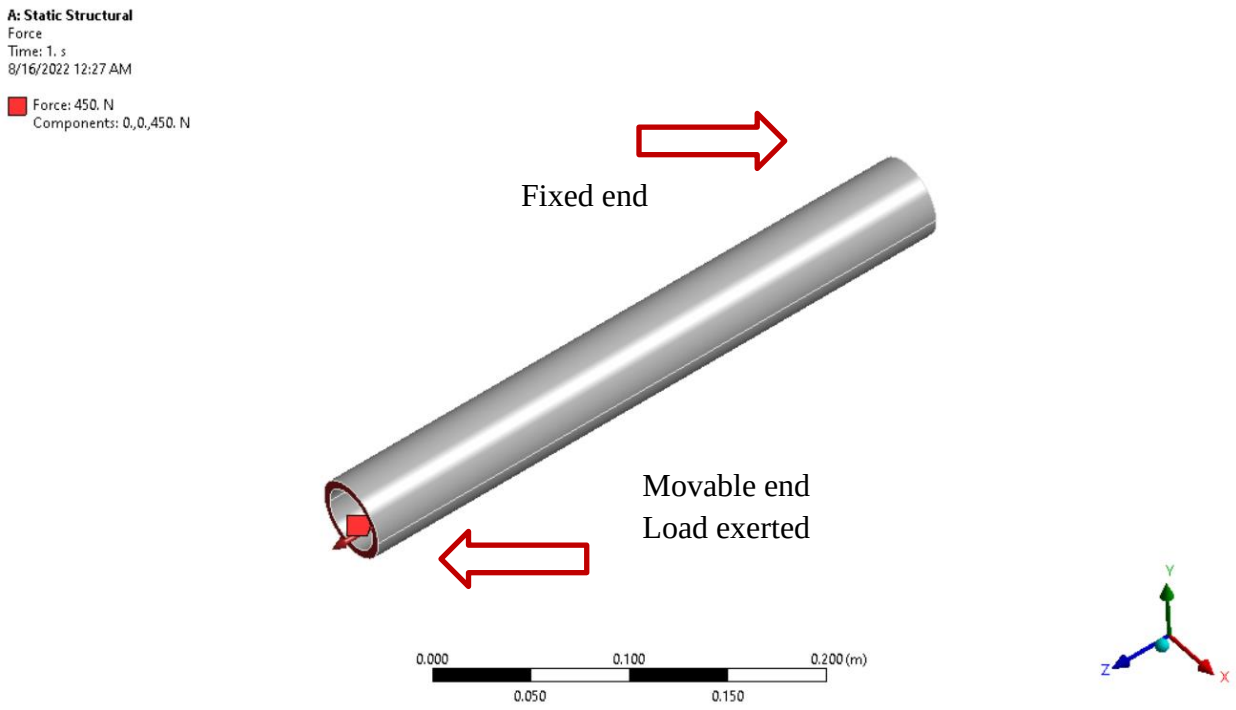

Figure 4.42 Applied load and boundary conditions

4.2.1.4 Generating solution

Based on the input parameters equivalent von mises stress and total deformation were generated and the results are presented as follows.

4.2.2 Result

4.2.2.1 Equivalent von mises stress

The equivalent von misses stress vales obtained from the software for the prosthetic shank material of hybrid E-glass fiber/ 8wt% CNC epoxy composite has maximum value of 0.82598Mpa and a minimum value of 0.43917Mpa as shown in figure 4.43.

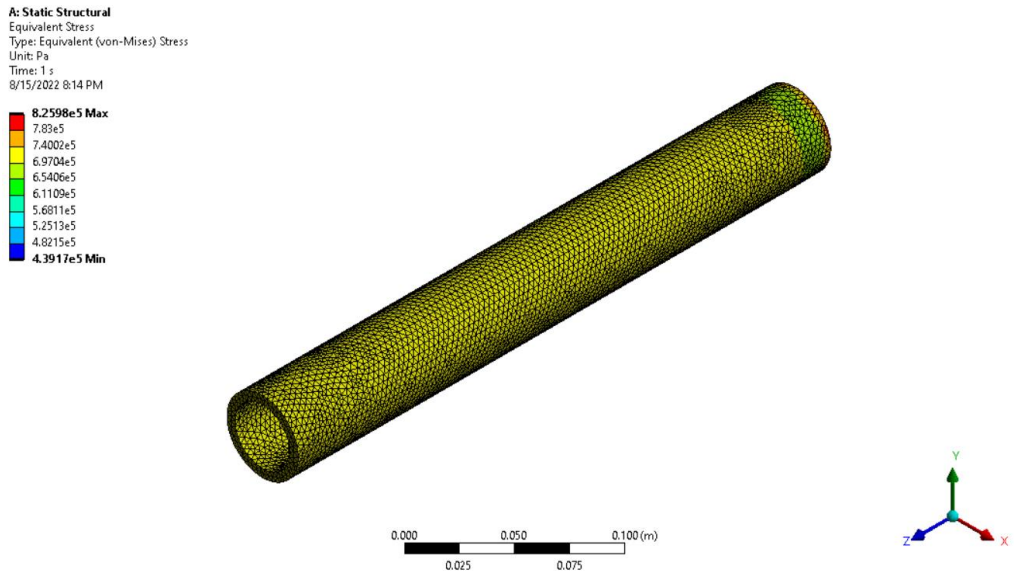

Figure 4.43 Results of equivalent von mises stress

4.2.2.2 Deformation

The deformation for prosthetic pylon material of hybrid E-glass fiber/ 8wt% CNC epoxy composite has the maximum value of 0.054065mm and minimum value of 0mm as shown in figure 4.44.

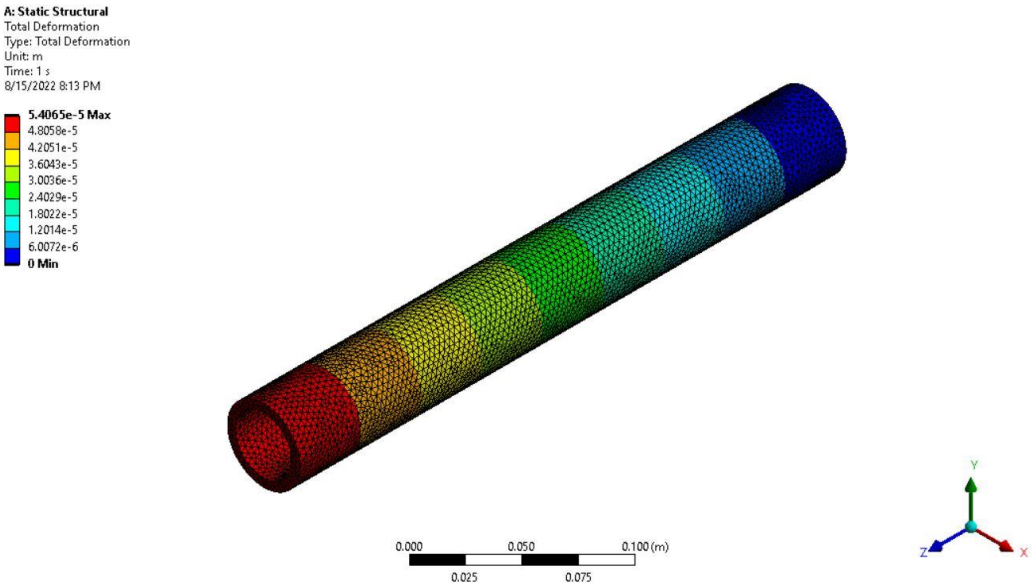

Figure 4.44 Result of deformation

4.2.3 Discussion

4.2.3.1 Equivalent von mises stress

The numerical result of FEA from ANSYS shows the maximum stress occurs at the bottom of the prosthetic pylon. However, comparing this value with yield strength of the fabricated composite material of hybrid E-glass fiber/CNC epoxy composite can be a suitable substitute for the existing material in the prosthetic limb fabrication industry.

4.2.3.2 Deformation

The value obtained from the ANSYS software revealed that the suggested composition of the composite material exhibits very low deformation while subjected to a certain specified load. This result showed that the newly developed material can be a suitable replacement for the conventional one.

CHAPTER FIVE

5. CONCLUSION AND RECOMMENDATION

5.1 Conclusion

Due to war and other health issues, the demand for prostheses is rising today. The demand has been rising rapidly, especially in developing countries. Most widely prosthetics are fabricated with synthetic fibers like carbon and glass fibers. Due to its low-cost glass fiber is used most widely but with lower mechanical properties as compared to other synthetic fibers like carbon. Thus, this study focused on fabrication and characterization of hybrid E-glass fiber/CNC reinforced epoxy composite for prosthetic pylon/shank. The study involved chemical extraction and characterization of CNC from sugarcane bagasse, determining its morphological properties, thermal behavior, particle size and crystallinity of the particles. Further it has been presented flexural, tensile, compressive, impact, density, void content and water absorption capacity of the hybrid composite material with different wt% of CNC. The study recommended hybrid E-glass fiber/8wt%CNC epoxy composite for the prosthetic pylon application as it behaved in better mechanical and physical properties compared to other compositions tried in this study.

As performed and presented on this research different weight percentage of CNC were hybridized with glass fiber to observe its effect on the composite material performance. Thus, the composite materials have exhibited an alternating mechanical and physical property improvements. Overall, of this research some optimization on extraction of CNC have been performed and the following points can best conclude what has been done throughout the research work.

Crystalline nanocellulose extraction method was optimized with three trials of the acid hydrolysis process, which was tried with three different concentrations of sulphuric acid (H_2SO_4) solution that is 50% w/v, 55% w/v, and 60% w/v. Found out that 60% w/v can best give the crystalline nanocellulose which showed more jelly like end product of CNC. as it's known having a jelly product at the end of acid hydrolysis is an indication for a crystalline nanocellulose formation.

It was also found that 1:12 of the bleached pulp to H_2SO_4 solution is the best ratio to form the jelly like product of CNC having tried that of 1:9 and 1:10 ratios.

Again, on acid hydrolysis process keeping the pulp and H_2SO_4 mixture on a hot plate at room temperature stirring with a magnetic stirrer for 15 minutes was found to be optimal. This conclusion was reached comparing to a process of keeping the pulp and acid mixture in a water bath at 45^oC with a mechanical blender. Surface morphology of CNC was evaluated with SEM thus, deagglomerated cellulose crystals were observed which enhance a uniform dispersion of the particles in the matrix material. According to the data obtained from XRD analysis crystalline nanocellulose was formed at 2theta values of 19.89, 44.04, 64.344 and 77.51 degrees with respective crystallite sizes of 13nm, 37.6nm, 85.3nm and 53.4nm.

Fabrication of hybrid Glass fiber/CNC epoxy resin composite was performed using hand layup fabrication process followed by compression. The effect of CNC addition (2,4,6, and 8wt%) on the physical and mechanical properties was evaluated.

Thermal property of the hybrid composite was slightly affected by the addition of CNC as observed with the evaluation of TGA analysis. A slight increase in density of the hybrid composite was observed due to the incorporation of CNC in a cavity formed in between the epoxy and E-glass fiber while the fabrication process. The void content of the composite material was decreased with increasing wt% of CNC.

The highest tensile and compression strength which is 127.8Mpa and 91.1Mpa respectively was exhibited by C5 which have 8wt % of CNC. The composite material with CNC weight percent of 8% have shown the highest flexural strength that is 251Mpa. According to the result found from the Charpy impact strength test C5 having 8wt % of CNC shown best impact energy absorption of 6.83J. C3, with a composition of 4wt % CNC was found to be less water absorbent with water absorption of 0.483%.

C5 with the highest tensile and compression strength of 127.8Mpa and 91.1Mpa respectively, highest impact load absorption of 6.83J, flexural strength of 251Mpa and the second least water absorbent which exhibits 0.5% water absorption and density of 1.36g/cm^3 can be selected as a convenient composition of all. In FEA of the prosthesis shank using ANSYS the selected composition of the composite material the maximum von mises stress and deformation obtained

are 0.82598Mpa and 0.054065mm respectively. Thus, hybrid E-glass fiber/CNC epoxy composite can be selected as an alternative material for prosthetic pylon/shank.

5.2 Recommendation

This study has conducted various experimental and numerical analysis, thus on extraction of CNC further treatment of the fiber with different parameters can result in a better output. Different weight percentage of CNC can result in different mechanical and physical properties of the hybrid composite, thus various composition trials are recommended. Advanced technique of fabrication like vacuum assisted resin transfer molding is also recommended since uniform distribution of resin material is a key point for a better composite material.

5.3 Future work

- Developing a prototype and investigate the effect of flexibility of shanks on gait mechanics and on users' subjective experience with the prosthesis.
- More research is needed to understand the role of shank flexibility in the prosthesis' overall operation, to define what constitutes optimal flexibility, and to provide feedback for the design of improved components.

REFERENCE

[1] I. I. M. Priya and B. J. A. i. M. E. Vinayagam, "Enhancement of bi-axial glass fibre reinforced polymer composite with graphene platelet nanopowder modifies epoxy resin," vol. 10, no. 8, p. 1687814018793261, 2018.

[2] J. Gordon and D. C. Mattis, "The New Science of Strong Materials, or, Why You Don't Fall Through the Floor," ed: American Association of Physics Teachers, 1985.

[3] D. A. J. O. Berry and Prosthetics, "COMPOSITE-MATERIALS FOR ORTHOTICS AND PROSTHETICS," vol. 40, no. 4, pp. 35-43, 1987.

[4] R. C. Me, R. Ibrahim, P. M. J. A. C. Tahir, International Journal of Sustainable Tropical Design Research, and Practice, "Natural based biocomposite material for prosthetic socket fabrication," vol. 5, no. 1, 2012.

[5] C. Quintero-Quiroz and V. Z. J. R. d. l. F. d. M. Pérez, "Materiales en interfaces y encajes ortoprotésicos de miembro inferior: Evolución y problemas dermatológicos asociados/materials for lower limb prosthetic and orthotic interfaces and sockets: Evolution and associated skin problems," vol. 67, no. 1, p. 117, 2019.

[6] M. Z. Khan, S. K. Srivastava, M. J. J. o. R. P. Gupta, and Composites, "Tensile and flexural properties of natural fiber reinforced polymer composites: A review," vol. 37, no. 24, pp. 1435-1455, 2018.

[7] T. Sathishkumar, J. a. Naveen, S. J. J. o. R. P. Satheeshkumar, and Composites, "Hybrid fiber reinforced polymer composites–a review," vol. 33, no. 5, pp. 454-471, 2014.

[8] M. Nurhanisah, N. Saba, M. Jawaid, and M. J. G. B. Paridah, "Design of prosthetic leg socket from kenaf fibre based composites," pp. 127-141, 2017.

[9] S. Sapuan, *Composite materials: Concurrent engineering approach*. Butterworth-Heinemann, 2017.

[10] W. D. Callister and D. G. Rethwisch, *Materials science and engineering*. John wiley & sons New York, 2011.

[11] K. Senthilkumar *et al.*, "Mechanical properties evaluation of sisal fibre reinforced polymer composites: a review," vol. 174, pp. 713-729, 2018.

[12] T.-D. J. C. Ngo and N. M. F. K. t. I. Applications, "Introduction to composite materials," 2020.

[13] A. Riccio, F. Caputo, G. Di Felice, S. Saputo, C. Toscano, and V. J. A. C. M. Lopresto, "A joint numerical-experimental study on impact induced intra-laminar and inter-laminar damage in laminated composites," vol. 23, no. 3, pp. 219-237, 2016.

[14] S. Heimbs, J. Cichosz, M. Klaus, S. Kilchert, and A. J. C. s. Johnson, "Sandwich structures with textile-reinforced composite foldcores under impact loads," vol. 92, no. 6, pp. 1485-1497, 2010.

[15] D. R. Askeland, P. P. Phulé, W. J. Wright, and D. Bhattacharya, "The science and engineering of materials," 2003.

[16] K. Friedrich and A. A. J. A. C. M. Almajid, "Manufacturing aspects of advanced polymer composites for automotive applications," vol. 20, no. 2, pp. 107-128, 2013.

[17] M. A. Masuelli, "Introduction of fibre-reinforced polymers− polymers and composites: concepts, properties and processes," in *Fiber reinforced polymers-the technology applied for concrete repair*: IntechOpen, 2013.
[18] B. E. Tawfik, H. Leheta, A. Elhewy, T. J. I. J. o. N. A. Elsayed, and O. Engineering, "Weight reduction and strengthening of marine hatch covers by using composite materials," vol. 9, no. 2, pp. 185-198, 2017.
[19] A. K. Sharma, R. Bhandari, A. Aherwar, and R. J. M. T. P. Rimašauskienė, "Matrix materials used in composites: A comprehensive study," vol. 21, pp. 1559-1562, 2020.
[20] Y. G. Thyavihalli Girijappa, S. Mavinkere Rangappa, J. Parameswaranpillai, and S. J. F. i. M. Siengchin, "Natural fibers as sustainable and renewable resource for development of eco-friendly composites: a comprehensive review," vol. 6, p. 226, 2019.
[21] R. J. Moon, A. Martini, J. Nairn, J. Simonsen, and J. J. C. S. R. Youngblood, "Cellulose nanomaterials review: structure, properties and nanocomposites," vol. 40, no. 7, pp. 3941-3994, 2011.
[22] E. J. P. D. Suttie and Stability, "Wood and Cellulosic Chemistry-DN-S. Hon and N. Shiraishi, editors, revised and expanded. Marcel Dekker, Inc. New York, Basel. ISBN 0-8247-0024-4. 928 pp., Price US $250," vol. 3, no. 73, pp. 567-569, 2001.
[23] D. Bondeson, A. Mathew, and K. J. C. Oksman, "Optimization of the isolation of nanocrystals from microcrystalline cellulose by acid hydrolysis," vol. 13, no. 2, pp. 171-180, 2006.
[24] I. Siró and D. J. C. Plackett, "Microfibrillated cellulose and new nanocomposite materials: a review," vol. 17, no. 3, pp. 459-494, 2010.
[25] A. Balaji, B. Karthikeyan, and C. S. J. I. J. o. C. R. Raj, "Bagasse fiber–the future biocomposite material: a review," vol. 7, no. 1, pp. 223-233, 2014.
[26] I. Šimkovic, J. Mlynár, J. Alföldi, and M. Micko, "New aspects in cationization of lignocellulose materials. XI. Modification of bagasse with quarternary ammonium groups," 1990.
[27] A. Pandey, C. R. Soccol, P. Nigam, and V. T. J. B. t. Soccol, "Biotechnological potential of agro-industrial residues. I: sugarcane bagasse," vol. 74, no. 1, pp. 69-80, 2000.
[28] S. E. Jacobsen, C. E. J. I. Wyman, and e. c. research, "Xylose monomer and oligomer yields for uncatalyzed hydrolysis of sugarcane bagasse hemicellulose at varying solids concentration," vol. 41, no. 6, pp. 1454-1461, 2002.
[29] M. M. Mekonnen and A. Y. Hoekstra, "The green, blue and grey water footprint of farm animals and animal products. Volume 2: Appendices," 2010.
[30] A. Moslemi, T. Behzad, A. J. I. j. o. a. Pizzi, and adhesives, "Addition of cellulose nanofibers extracted from rice straw to urea formaldehyde resin; effect on the adhesive characteristics and medium density fiberboard properties," vol. 99, p. 102582, 2020.
[31] N. Lavoine, I. Desloges, A. Dufresne, and J. J. C. p. Bras, "Microfibrillated cellulose–Its barrier properties and applications in cellulosic materials: A review," vol. 90, no. 2, pp. 735-764, 2012.
[32] S. Erden, K. Sever, Y. Seki, M. J. F. Sarikanat, and polymers, "Enhancement of the mechanical properties of glass/polyester composites via matrix modification glass/polyester composite siloxane matrix modification," vol. 11, no. 5, pp. 732-737, 2010.

[33] M. J. C. P. B. E. Sayer, "Elastic properties and buckling load evaluation of ceramic particles filled glass/epoxy composites," vol. 59, pp. 12-20, 2014.
[34] D. J. R. P. Fecko, "High strength glass reinforcements still being discovered," vol. 50, no. 4, pp. 40-44, 2006.
[35] M. R. Ismail, Y. Y. Kahtan, and S. M. Abbas, "A modified shank for below knee prosthesis," in *IOP Conference Series: Materials Science and Engineering*, 2020, vol. 671, no. 1, p. 012061: IOP Publishing.
[36] D. B. Popovic and T. Sinkjaer, *Control of movement for the physically disabled: control for rehabilitation technology*. Springer, 2000.
[37] D. Christine Miller, A. Finn, and E. Delzell, "Battlefield injuries: Saving lives and limbs throughout history."
[38] A. KUMAR and P. J. M. J. KUMAR, Armed Forces India, "Endoskeletal prosthesis: A new era for amputee," vol. 57, no. 2, p. 93, 2001.
[39] B. O'Keeffe and S. J. I. J. o. P. S. Rout, "Prosthetic rehabilitation in the lower limb," vol. 52, no. 01, pp. 134-143, 2019.
[40] S. Mehanny *et al.*, "Extraction and characterization of nanocellulose from three types of palm residues," vol. 10, pp. 526-537, 2021.
[41] A. Mandal and D. J. C. P. Chakrabarty, "Isolation of nanocellulose from waste sugarcane bagasse (SCB) and its characterization," vol. 86, no. 3, pp. 1291-1299, 2011.
[42] S. Rashid, H. J. I. C. Dutta, and Products, "Characterization of nanocellulose extracted from short, medium and long grain rice husks," vol. 154, p. 112627, 2020.
[43] M. Boopalan, M. Umapathy, and P. J. S. Jenyfer, "A comparative study on the mechanical properties of jute and sisal fiber reinforced polymer composites," vol. 4, no. 3, pp. 145-149, 2012.
[44] R. Badrinath and T. J. P. m. s. Senthilvelan, "Comparative investigation on mechanical properties of banana and sisal reinforced polymer based composites," vol. 5, pp. 2263-2272, 2014.
[45] S. Boufi, H. Kaddami, A. J. M. M. Dufresne, and Engineering, "Mechanical performance and transparency of nanocellulose reinforced polymer nanocomposites," vol. 299, no. 5, pp. 560-568, 2014.
[46] K. Srivastava *et al.*, "Effect of nanocellulose on mechanical and barrier properties of PVA–banana pseudostem fiber composite films," vol. 21, p. 101312, 2021.
[47] G. K. Rai and V. J. M. T. P. Singh, "Study of fabrication and analysis of nanocellulose reinforced polymer matrix composites," vol. 38, pp. 85-88, 2021.
[48] A. Khan, A. M. Asiri, M. Jawaid, and N. J. C. P. Saba, "Effect of cellulose nano fibers and nano clays on the mechanical, morphological, thermal and dynamic mechanical performance of kenaf/epoxy composites," vol. 239, p. 116248, 2020.
[49] M. F. Miller, "Nanocellulose reinforced sheet molding compound for automotive composite manufacturing," Georgia Institute of Technology, 2016.
[50] K. Ansal Muhammed, C. Ramesh Kannan, B. Stalin, and M. J. M. T. P. Ravichandran, "Experimental investigation on AW 106 Epoxy/E-Glass fiber/Nano clay composite for wind turbine blade",," vol. 21, pp. 202-205, 2020.

[51] V. A. Prakash and A. J. A. S. S. Rajadurai, "Thermo-mechanical characterization of siliconized E-glass fiber/hematite particles reinforced epoxy resin hybrid composite," vol. 384, pp. 99-106, 2016.
[52] B. S. Halemani, K. Chandrasekhar, Y. Ravitej, T. H. Raju, and S. J. M. T. P. Udayshankar, "Investigation and analysis for mechanical properties of banana and E glass fiber reinforced hybrid epoxy composites," vol. 47, pp. 2509-2515, 2021.
[53] M. Abhishek, P. Suresh, and H. S. J. M. T. P. Murthy, "Evaluation of mechanical properties of Jute/E-Glass epoxy hybrid composites by varying fibre loading with and without shear thickening fluid," vol. 4, no. 10, pp. 10858-10862, 2017.
[54] S. Sivasaravanan and V. B. J. P. E. Raja, "Impact characterization of epoxy LY556/E-glass fibre/nano clay hybrid nano composite materials," vol. 97, pp. 968-974, 2014.
[55] M. M. Nadeem, S. Chethan, K. Srinivasa, M. K. Kumar, and N. J. M. T. P. Yathisha, "Effect of glass fibers and multi walled carbon nano tubes (MWCNT's) on mechanical properties of epoxy hybrid composites at elevated temperature," vol. 44, pp. 2013-2018, 2021.
[56] M. S. A.-D. Tahir and F. M. Kadhim, "Design and Manufacturing of New Low (Weight and Cost) 3D Printed Pylon Prosthesis for Amputee," in *IOP Conference Series: Materials Science and Engineering*, 2021, vol. 1094, no. 1, p. 012144: IOP Publishing.
[57] J. K. Oleiwi, S. J. J. E. Ahmed, and T. Journal, "Tensile and buckling of prosthetic pylon made from hybrid composite materials," vol. 34, no. 14 Part (A) Engineering, 2016.
[58] E. Stenvall *et al.*, "Additive manufacturing of prostheses using forest-based composites," vol. 7, no. 3, p. 103, 2020.
[59] M. S. Hasnain, S. A. Ahmad, M. A. Minhaj, T. J. Ara, and A. K. Nayak, "Nanocomposite materials for prosthetic devices," in *Applications of Nanocomposite Materials in Orthopedics*: Elsevier, 2019, pp. 127-144.
[60] H. J. S. Sidhu, T. Garg, and B. Singh, "Design Of E-Glass Epoxy Prosthetic Leg."
[61] N. A. Jebur, F. A. Abdulla, and A. F. J. I. J. M. E. T. Hussein, "Experimental and numerical analysis of below knee prosthetic socket," vol. 9, no. 8, pp. 1-8, 2018.
[62] H. N. Shasmin, N. A. Osman, L. A. Latif, J. Usman, and W. A. B. J. J. o. B. Wan Abas, "A new pylon materials in transtibial prosthesis: a preliminary study," vol. 40, no. 2, p. S297, 2007.
[63] S. Hanie Nadia, "Development of a new pylon material in transtibial prosthesis/Hanie Nadia Shasmin," University of Malaya, 2012.
[64] A. A. Kadhim, E. A. Abbod, A. K. Muhammad, K. K. Resan, and M. J. J. M. E. R. D. Al-Waily, "Manufacturing and analyzing of a new prosthetic shank with adapters by 3D printer," vol. 44, no. 3, pp. 383-391, 2021.
[65] S. Z. Naqvi, J. Ramkumar, and K. K. J. J. H. o. F. A. Kar, "Fly ash/glass fiber/carbon fiber-reinforced thermoset composites," pp. 373-400, 2022.
[66] S.-J. Park and M.-K. Seo, *Interface science and composites*. Academic Press, 2011.
[67] L. Santaella, *Linguagens líquidas na era da mobilidade*. Paulus, 2007.
[68] A. Singels *et al.*, "Review of South African sugarcane production in the 2018/19 season: too much of a good thing?," in *Proceedings of the Annual Congress-South African Sugar Technologists' Association*, 2019, no. 92, pp. 1-16: South African Sugar Technologists' Association.

[69] M. Rasul, V. Rudolph, and M. J. F. Carsky, "Physical properties of bagasse," vol. 78, no. 8, pp. 905-910, 1999.
[70] M. A. D. Júnior, C. Borsoi, B. Hansen, and A. L. J. C. p. Catto, "Evaluation of different methods for extraction of nanocellulose from yerba mate residues," vol. 218, pp. 78-86, 2019.
[71] A. Kumar, Y. S. Negi, V. Choudhary, N. K. J. J. o. m. p. Bhardwaj, and chemistry, "Characterization of cellulose nanocrystals produced by acid-hydrolysis from sugarcane bagasse as agro-waste," vol. 2, no. 1, pp. 1-8, 2014.
[72] N. S. Aprilia *et al.*, "Physicochemical characterization of microcrystalline cellulose extracted from kenaf bast," vol. 11, no. 2, pp. 3875-3889, 2016.
[73] I. Y. A. Fatah *et al.*, "Exploration of a chemo-mechanical technique for the isolation of nanofibrillated cellulosic fiber from oil palm empty fruit bunch as a reinforcing agent in composites materials," vol. 6, no. 10, pp. 2611-2624, 2014.
[74] B. Barari *et al.*, "Mechanical characterization of scalable cellulose nano-fiber based composites made using liquid composite molding process," vol. 84, pp. 277-284, 2016.
[75] I. Tharazi *et al.*, "Optimization of hot press parameters on tensile strength for unidirectional long kenaf fiber reinforced polylactic-acid composite," vol. 184, pp. 478-485, 2017.
[76] A. Monshi, M. R. Foroughi, and M. R. J. W. J. N. S. E. Monshi, , 2: 154, "Modified Scherrer equation to estimate more accurately nano-crystallite size using XRD," vol. 160, 2012.
[77] M. R. K. Sofla, R. Brown, T. Tsuzuki, T. J. A. i. N. S. N. Rainey, and Nanotechnology, "A comparison of cellulose nanocrystals and cellulose nanofibres extracted from bagasse using acid and ball milling methods," vol. 7, no. 3, p. 035004, 2016.
[78] M. Sabbaghan and D. S. J. C. p. Argyropoulos, "Synthesis and characterization of nano fibrillated cellulose/Cu2O films; micro and nano particle nucleation effects," vol. 197, pp. 614-622, 2018.
[79] D. V. Mashego, "Preparation, isolation and characterization of nanocellulose from sugarcane bagasse," 2016.
[80] M. Kabir, H. Wang, K. Lau, and F. J. C. P. B. E. Cardona, "Chemical treatments on plant-based natural fibre reinforced polymer composites: An overview," vol. 43, no. 7, pp. 2883-2892, 2012.
[81] A. Asadi, M. Miller, S. Sultana, R. J. Moon, K. J. C. P. A. A. S. Kalaitzidou, and Manufacturing, "Introducing cellulose nanocrystals in sheet molding compounds (SMC)," vol. 88, pp. 206-215, 2016.
[82] A. Asadi, M. Miller, R. Moon, and K. J. E. P. L. Kalaitzidou, Vol. 10 : 11 pages.: 587-597., "Improving the interfacial and mechanical properties of short glass fiber/epoxy composites by coating the glass fibers with cellulose nanocrystals," vol. 10, no. 7, pp. 587-597, 2016.
[83] M. Kim, Y.-B. Park, O. I. Okoli, C. J. C. S. Zhang, and Technology, "Processing, characterization, and modeling of carbon nanotube-reinforced multiscale composites," vol. 69, no. 3-4, pp. 335-342, 2009.
[84] B. A. Patterson, M. H. Malakooti, J. Lin, A. Okorom, H. A. J. C. S. Sodano, and Technology, "Aramid nanofibers for multiscale fiber reinforcement of polymer composites," vol. 161, pp. 92-99, 2018.

[85] W.-H. Liao *et al.*, "Effects of multiwalled carbon nanotubes functionalization on the morphology and mechanical and thermal properties of carbon fiber/vinyl ester composites," vol. 5, no. 9, pp. 3975-3982, 2013.
[86] J. Goswami *et al.*, "The effect of cellulose nanocrystal coatings on the glass fiber–epoxy interphase," vol. 12, no. 12, p. 1951, 2019.
[87] H. Dhakal, Z. Zhang, R. Guthrie, J. MacMullen, and N. J. C. p. Bennett, "Development of flax/carbon fibre hybrid composites for enhanced properties," vol. 96, no. 1, pp. 1-8, 2013.
[88] S. Kumar, G. Graninger, S. C. Hawkins, B. G. J. C. P. A. A. S. Falzon, and Manufacturing, "A nanostructured cellulose-based interphase layer to enhance the mechanical performance of glass fibre-reinforced polymer composites," vol. 148, p. 106475, 2021.
[89] N. Venkateshwaran, V. Santhanam, and A. Alavudeen, "Feasibility study of fly ash as filler in banana fiber-reinforced hybrid composites," in *Processing of green composites*: Springer, 2019, pp. 31-47.
[90] S. S. Chee, M. Jawaid, M. Sultan, O. Y. Alothman, L. C. J. J. o. M. R. Abdullah, and Technology, "Effects of nanoclay on physical and dimensional stability of Bamboo/Kenaf/nanoclay reinforced epoxy hybrid nanocomposites," vol. 9, no. 3, pp. 5871-5880, 2020.
[91] M. Jawaid, H. A. Khalil, A. A. Bakar, P. N. J. M. Khanam, and Design, "Chemical resistance, void content and tensile properties of oil palm/jute fibre reinforced polymer hybrid composites," vol. 32, no. 2, pp. 1014-1019, 2011.
[92] F. H. Latief, A. Chafidz, H. Junaedi, A. Alfozan, and R. J. A. i. P. T. Khan, "Effect of Alumina Contents on the Physicomechanical Properties of Alumina () Reinforced Polyester Composites," vol. 2019, 2019.
[93] I. D. Ibrahim, T. Jamiru, E. R. Sadiku, W. K. Kupolati, and S. C. J. J. o. N. Agwuncha, "Impact of surface modification and nanoparticle on sisal fiber reinforced polypropylene nanocomposites," vol. 2016, 2016.
[94] S. Dehrooyeh, M. Vaseghi, M. Sohrabian, and M. J. M. o. M. Sameezadeh, "Glass fiber/carbon nanotube/epoxy hybrid composites: Achieving superior mechanical properties," vol. 161, p. 104025, 2021.
[95] N. Lachman, H. D. J. C. P. A. A. S. Wagner, and Manufacturing, "Correlation between interfacial molecular structure and mechanics in CNT/epoxy nano-composites," vol. 41, no. 9, pp. 1093-1098, 2010.
[96] K. K. Panchagnula, P. J. J. o. M. R. Kuppan, and Technology, "Improvement in the mechanical properties of neat GFRPs with multi-walled CNTs," vol. 8, no. 1, pp. 366-376, 2019.
[97] V. Romanov, S. V. Lomov, I. Verpoest, L. J. C. S. Gorbatikh, and Technology, "Inter-fiber stresses in composites with carbon nanotube grafted and coated fibers," vol. 114, pp. 79-86, 2015.
[98] S. Parveen, S. Pichandi, P. Goswami, S. J. M. Rana, and Design, "Novel glass fibre reinforced hierarchical composites with improved interfacial, mechanical and dynamic mechanical properties developed using cellulose microcrystals," vol. 188, p. 108448, 2020.
[99] A. Kiziltas, D. J. Gardner, Y. Han, H.-S. J. W. Yang, and f. science, "Determining the mechanical properties of microcrystalline cellulose (MCC)-filled PET-PTT blend composites," vol. 42, no. 2, pp. 165-176, 2010.

[100] Y. A. Mubarak and R. T. J. J. o. T. C. M. Abdulsamad, "Effects of microcrystalline cellulose on the mechanical properties of low-density polyethylene composites," vol. 32, no. 3, pp. 297-311, 2019.
[101] A. Alavudeen, N. Rajini, S. Karthikeyan, M. Thiruchitrambalam, N. J. M. Venkateshwaren, and Design, "Mechanical properties of banana/kenaf fiber-reinforced hybrid polyester composites: Effect of woven fabric and random orientation," vol. 66, pp. 246-257, 2015.
[102] H. Saad, M. Q. Abdullah, H. R. J. I. J. o. C. E. Wasmi, and Technology, "The Modeling and Effect of FEM on Prosthetic limb," vol. 7, no. 3, pp. 892-895, 2017.
[103] A. A. Kadhim, E. A. Abbod, A. K. Muhammad, K. K. Resan, and M. J. J. M. E. R. D. Al-Waily, "Manufacturing and analyzing of a new prosthetic shank with adapters by 3D printer," vol. 44, no. 3, pp. 383-91, 2021.
[104] B. J. B. S. I. L. ISO, UK, "10328: 2006 Prosthetics. Structural testing of lower-limb prostheses. Requirements and test methods," 2016.

APENDICES

APPENDIX A

Tensile test results and stress-strain curves for each sample

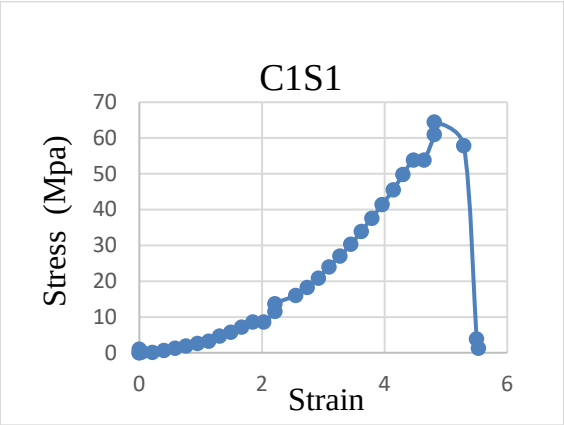

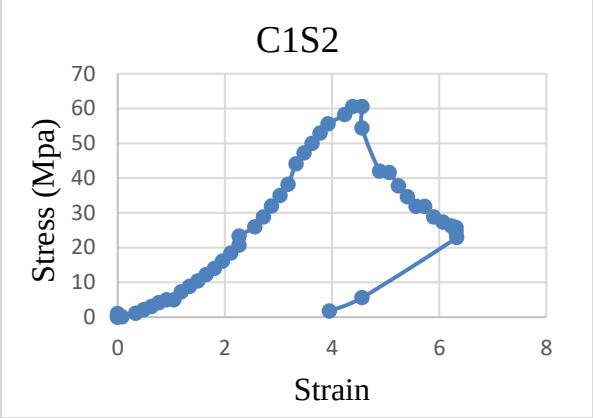

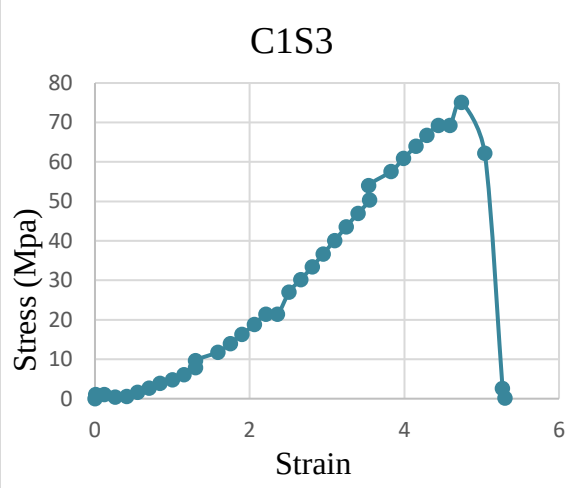

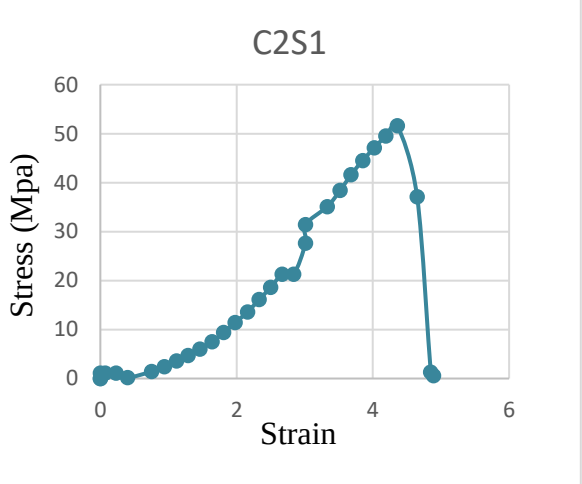

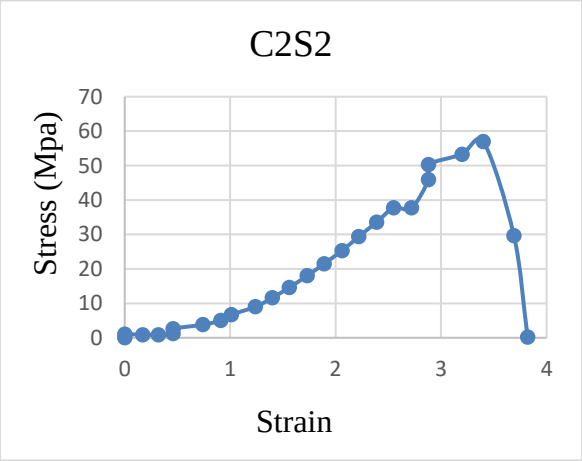

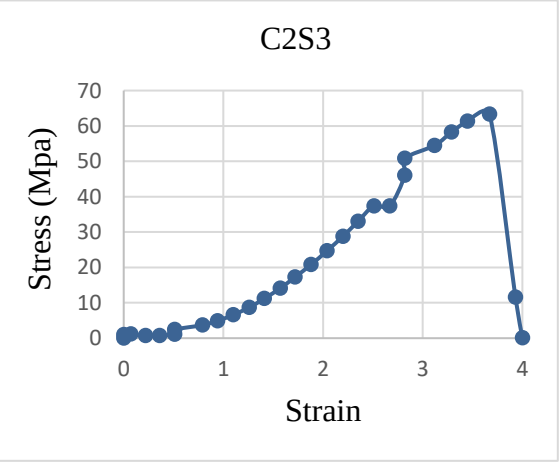

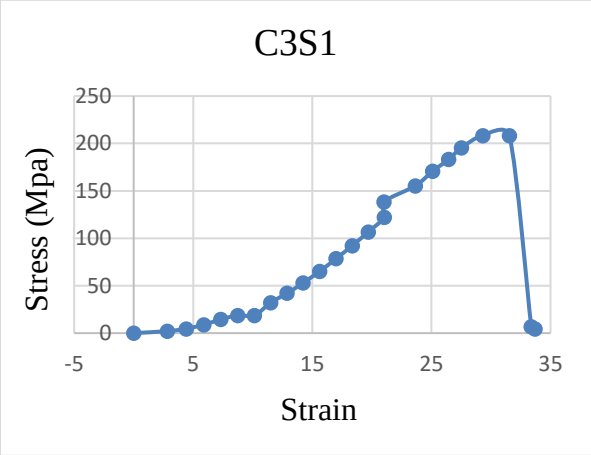
C3S1
Stress (Mpa)
250
200
150
100
50
0
-5
5
15
25
35
Strain

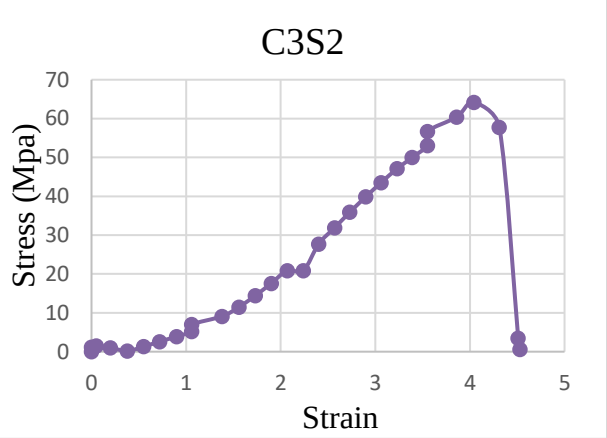
C3S2
Stress (Mpa)
70
60
50
40
30
20
10
0
0
1
2
3
4
5
Strain

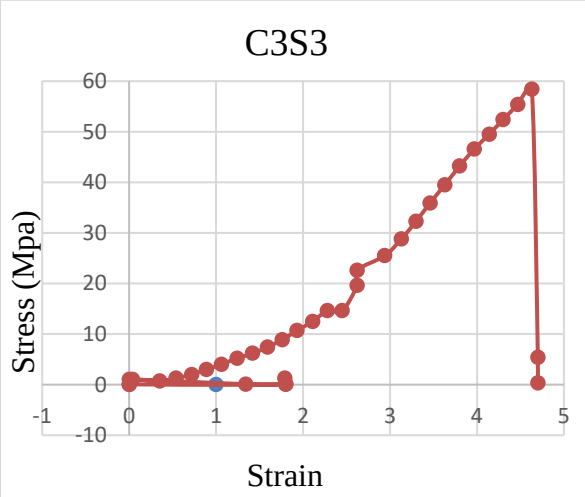
C3S3
Stress (Mpa)
60
50
40
30
20
10
0
-10
-1
0
1
2
3
4
5
Strain

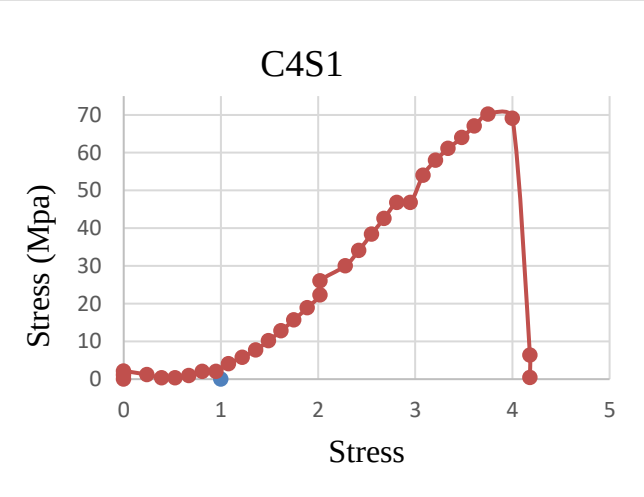
C4S1
Stress (Mpa)
70
60
50
40
30
20
10
0
0
1
2
3
4
5
Stress

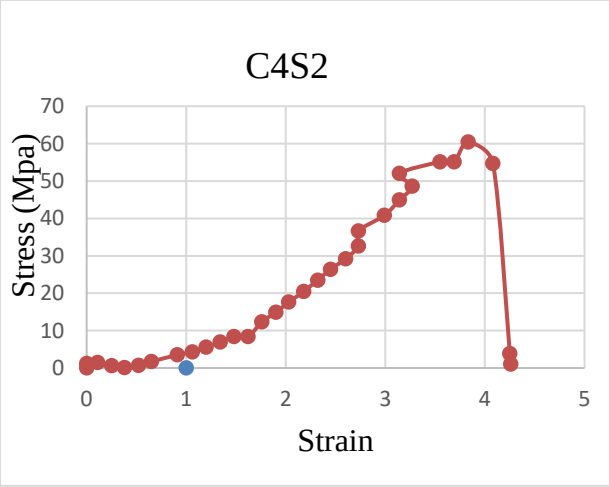
C4S2
Stress (Mpa)
70
60
50
40
30
20
10
0
0
1
2
3
4
5
Strain

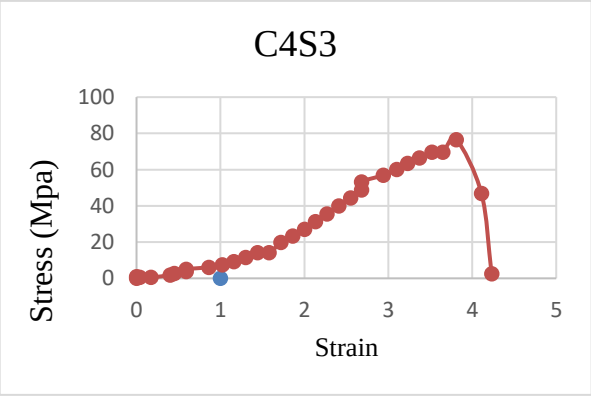
C4S3
Stress (Mpa)
100
80
60
40
20
0
0
1
2
3
4
5
Strain

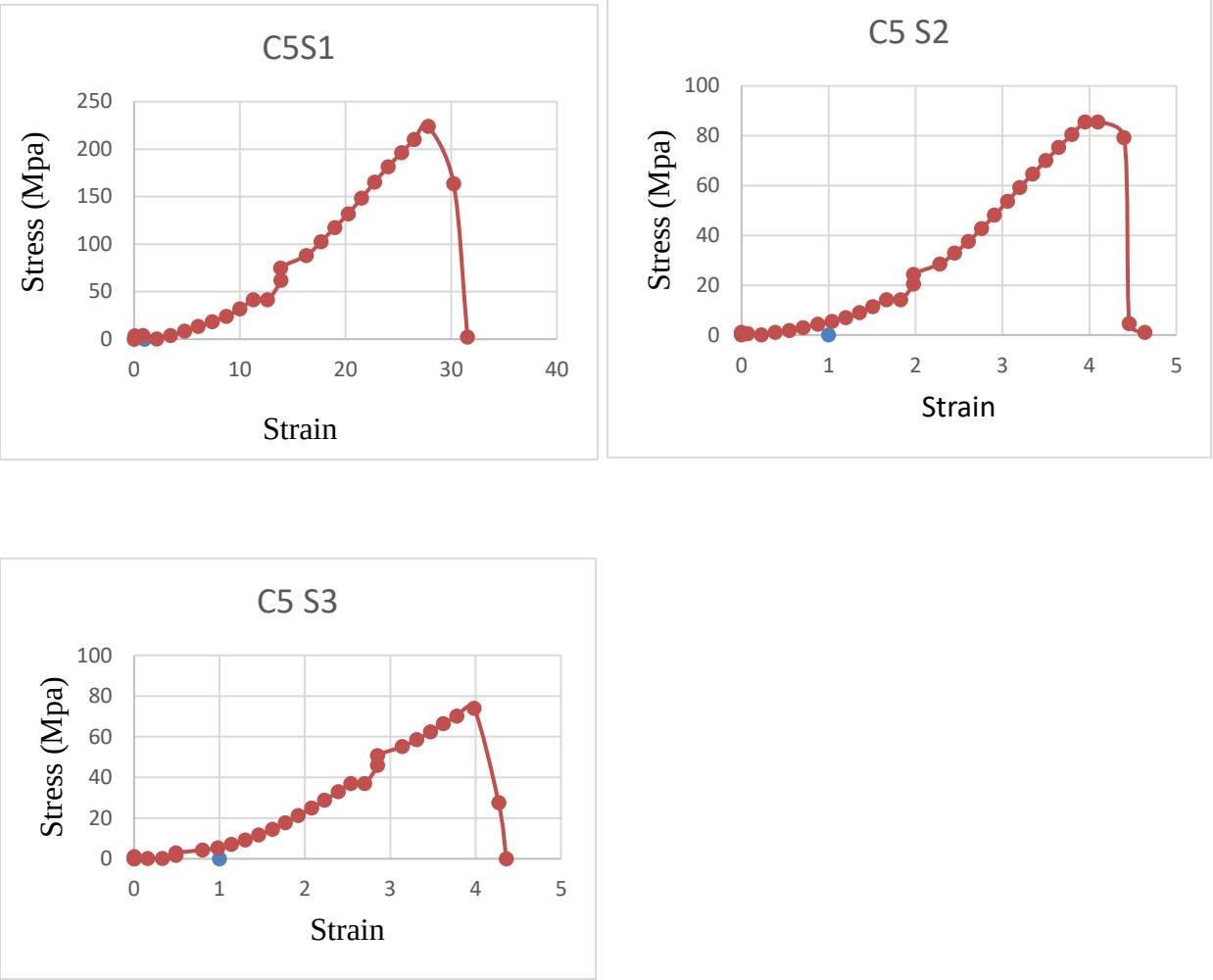

Figure A 1 Tensile test stress-strain curve

Compression test results and stress-strain curves for each sample

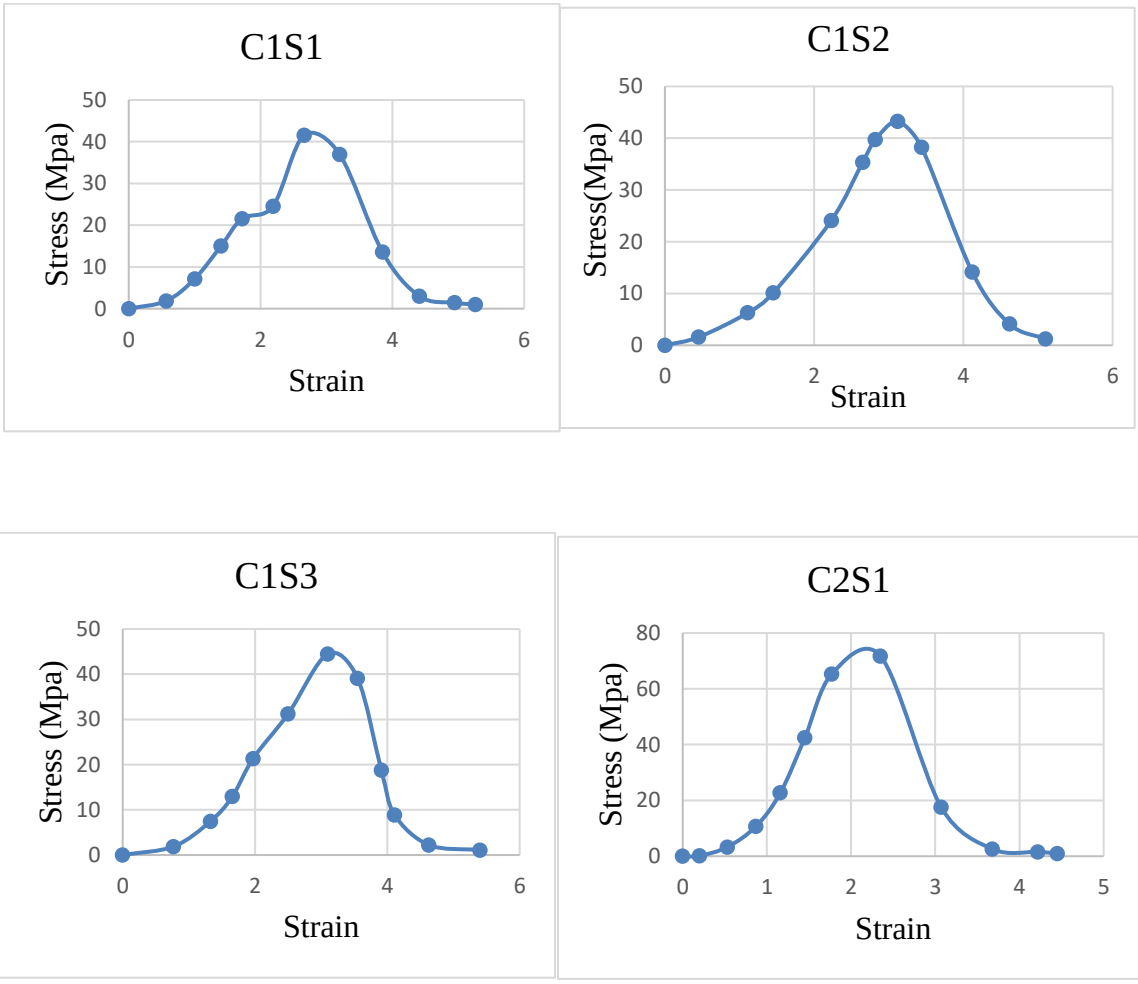

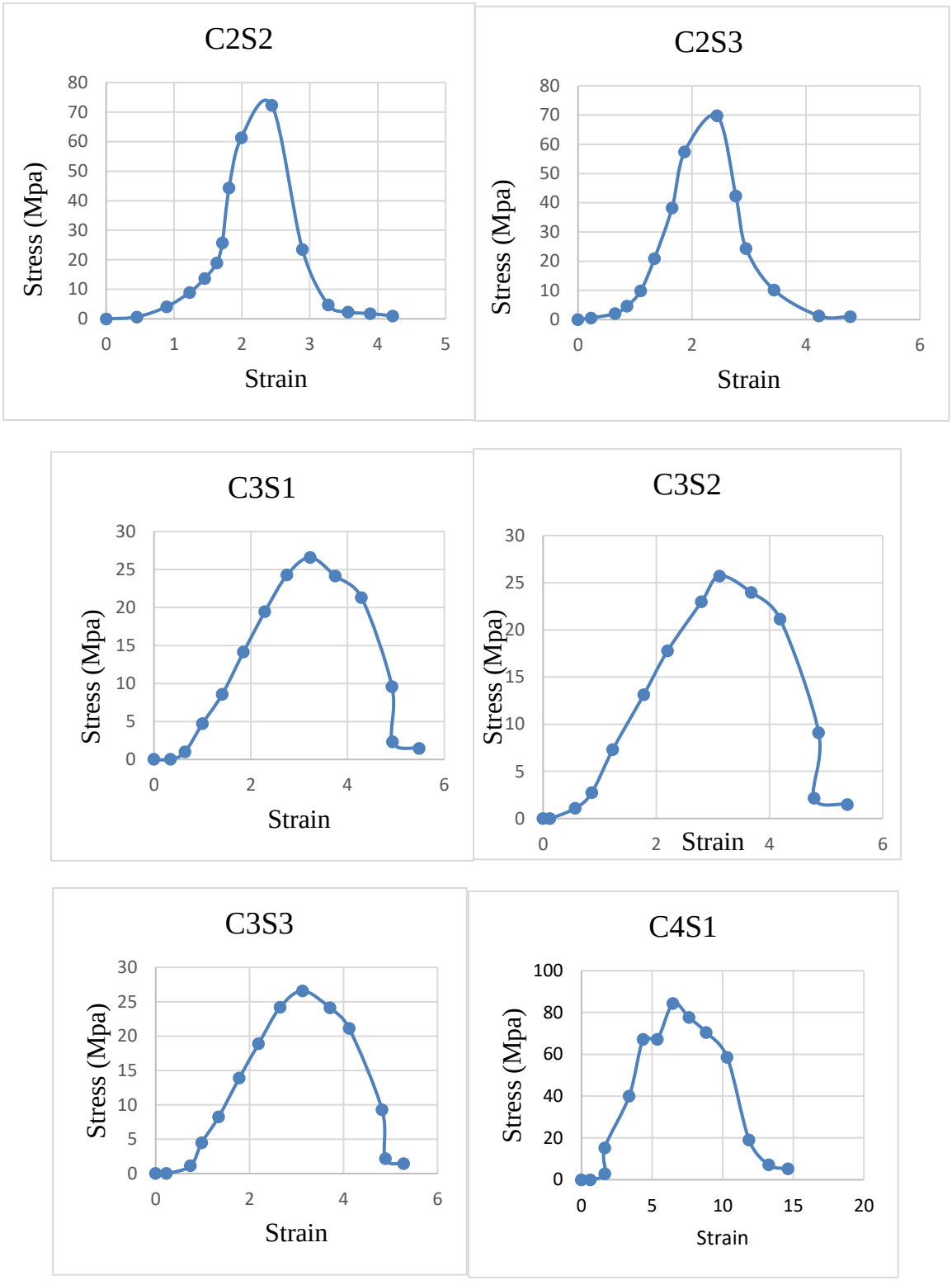
C2S2
Stress (Mpa)
Strain
C2S3
Stress (Mpa)
Strain
C3S1
Stress (Mpa)
Strain
C3S2
Stress (Mpa)
Strain
C3S3
Stress (Mpa)
Strain
C4S1
Stress (Mpa)
Strain

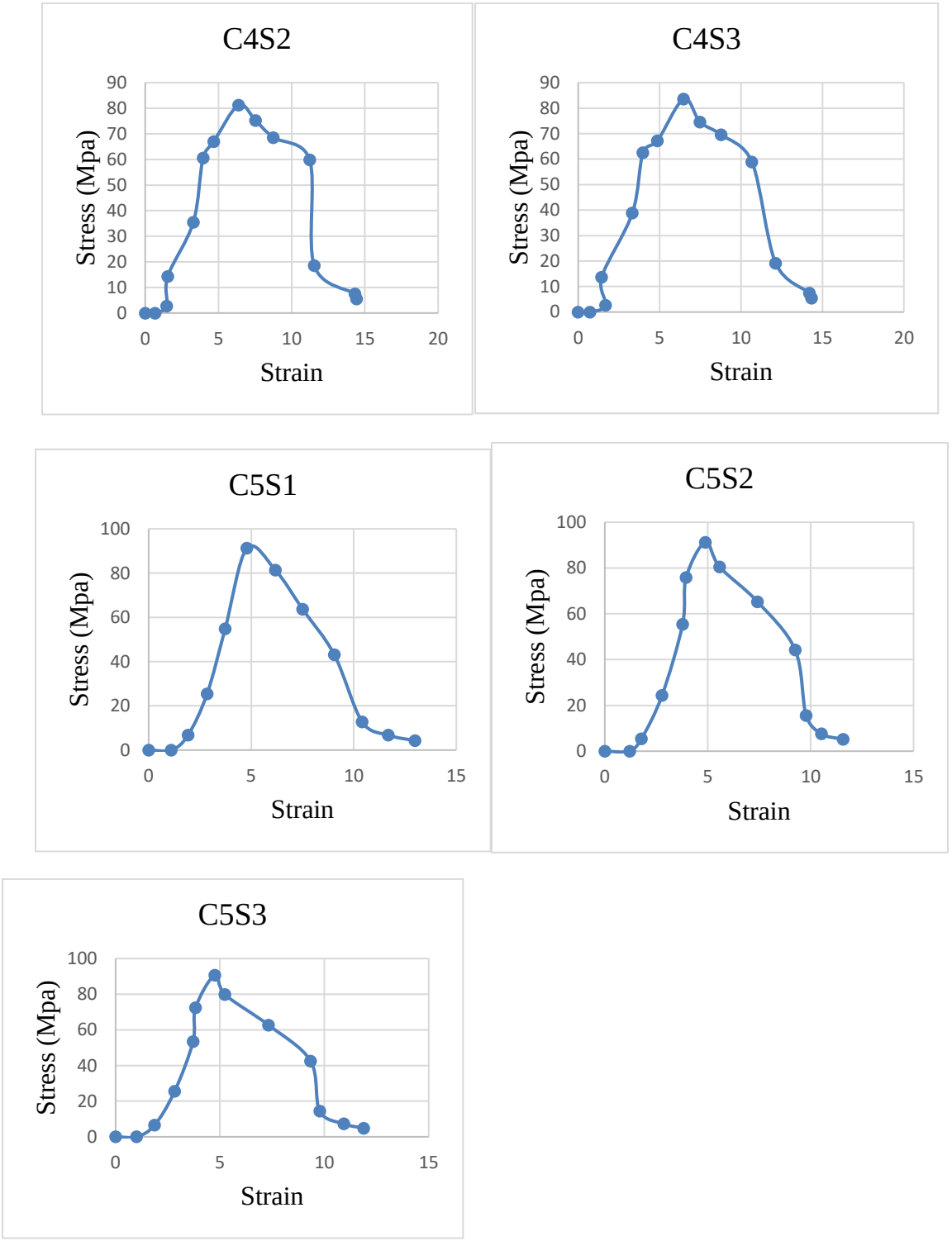

Figure A 2 Compression test stress-strain curve

APENDIX B

Laboratory testing device utilized

Figure B.1 Field Emission Electron Microscope 6500F (FESEM-6500F), JEOL 6500

Figure B.2 STA 409 PC Luxx Simultaneous thermal analyzer